Sodium channel regulatory mechanisms: Current fluctuation analysis on frog skin epithelium

Kuang-Yi Chou

Thesis Presented for the Degree of

DOCTOR OF PHILOSOPHY

in the Department of Anatomy and Cell Biology

Faculty of Medicine

University of Cape Town

Cape Town

October 1994

Dedicated to my parents,

Mrs. Pi-Hsia Liao and Mr. Yang-Lian Chou

CERTIFICATION OF SUPERVISOR

In terms of paragraph 9 of "General regulations for the degree of Ph.D." I as supervisor of the candidate Kuang-Yi Chou, certify that I approve of the incorporation in this thesis of material that has already been published or submitted for publication.

Signed

Professor W. J. Els
Department of Anatomy and Cell Biology
Faculty of Medicine
University of Cape Town

Publications arising from this work

A. International Journals:

1. Els, W. J. and Chou, K.-Y. (1993) Sodium-dependent regulation of epithelial sodium channel densities in frog skin; a role for the cytoskeleton. *Journal of Physiology* **462**: 447-464.

2. Chou, K.-Y. and Els, W. J. (1994) Organisation of the microfilament system in frog skin granular cells. *The Histochemical Journal* (Submitted)

B. Published Proceeding Papers:

1. Chou, K.-Y. and Els, W. J. (1990) Regulation of Na channel densities by mucosal sodium. *Annual Congress of Physiology Society of Southern Africa.* (Abstract).

2. Chou, K.-Y. and Els, W. J. (1991) The localization of microtubules and microfilaments in frog skin epithelial cells: an immunological investigation. *Proceedings of the Electron Microscopy Society of Southern Africa* **21**: 17-18.

3. Els, W. J. and Chou, K.-Y. (1991) Influence of the cytoskeleton on modulation of Na channel densities in a tight epithelium. *Faseb Journal* **5**(4): 1017.

4. Chou, K.-Y. and Els, W. J. (1992) Regulation of membrane permeability by modulating sodium channel densities: towards a mechanistic model. *Annual Congress of Physiology Society of Southern Africa.* (Abstracts). p.93.

5. Els, W. J. and Chou, K.-Y. (1993) Disruption of the actin cytoskeleton does not interfere with the modulation of sodium channels in frog skin epithelium by vasopressin. *Proceedings of the Physiology Society of Southern Africa* **1**(1): 64-65.

6. Chou, K.-Y. and Els, W. J. (1993) Actin filaments in frog skin epithelial cells: a role in sodium transport? *Proceedings of the Electron Microscopy Society of Southern Africa* **23**: 35.

7. Els, W. J., Richards, P. D. G., and Chou, K.-Y. (1993) Cytochemistry of functional facets of the Na-transport model in frog skin. *Proceedings of the Electron Microscopy Society of Southern Africa* **23**: 37.

8. Els, W.J. and Chou, K.-Y. (1994) Role of actin filaments in modulation of sodium channels in frog skin epithelium by vasopressin. *Faseb Journal* **8** (4): 295.

Contents

Abstract
Acknowledgements
Glossary of abbreviations

CHAPTER 1 INTRODUCTION 1

1.1 General introduction 1
1.2 Principal aims of the study 7
1.3 Methodology 8

CHAPTER 2 LITERATURE REVIEW 10

2.1 The cellular basis of renal function 11
2.1.1 Epithelial function and organization 11
2.1.2 Classification of ion transporting epithelia 12
2.1.3 Overview of the cell membrane structure and permeability 13
2.2 Models of sodium transport across tight epithelia 15
2.2.1 Koeffoed-Johnsen and Ussing model 15
2.2.2 The Thévenin equivalent electrical circuit 17
2.2.3 Possible role of sodium transport compartment 19
2.3 Basic electrical methods for studying membrane ionic transport 20
2.3.1 Patch clamp 21
2.3.2 Fluctuation analysis 24
2.3.3 Impedance analysis 28
2.4 Epithelial Na^+ channels 30
2.4.1 Physiological types of epithelial Na^+ channels 32
2.4.1.1 High sodium selective and low conductance channels 32
2.4.1.2 Moderate sodium selective and high conductance channels 35
2.4.1.3 Non sodium selective channels 37
2.4.2 Structure of the epithelial Na^+ channel 38
2.4.3 Immunocytochemical localization of the amiloride-sensitive Na^+ channels 41
2.5 Regulation of amiloride-sensitive Na^+ channel 43
2.5.1 Properties determining transcellular Na^+ permeability 44

2.5.2 Regulation of Na^+ channels by luminal factors 45
2.5.2.1 Inhibition of Na^+ transport by extracellular sodium 45
2.5.2.2 Inhibition of Na^+ transport by intracellular sodium 48
2.5.2.3 Inhibition of sodium transport by luminal proteolysis 49
2.5.2.4 Osmotic effects on sodium channels 50
2.5.3 Regulation of amiloride-sensitive Na^+ channels by hormones 52
2.5.3.1 Regulation of Na^+ channels by aldosterone 52
2.5.3.2 Regulation of Na^+ channels by antidiuretic hormone (ADH) 55
2.5.3.3 Regulation of Na^+ channels by other hormones 60
2.5.4 Modulation of Na^+ channels by interactions with cytoskeleton 60

CHAPTER 3 AIMS 63

CHAPTER 4 MATERIAL AND METHODS 66

4.1 Electrophysiology 66
4.1.1 Tissue preparation 66
4.1.2 Tissue mounting 68
4.1.3 Solutions and chemicals 69
4.1.4 Application of the current fluctuation analysis technique 70
4.1.4.1 Electrodes and electrical connections 71
4.1.4.2 Low-noise equipment 71
4.1.4.3 Data capture and processing 73
4.1.4.4 Blocker-induced fluctuation analysis 74
4.1.4.5 Time course protocol 76
4.1.4.6 Statistical analysis 77
4.2 Cytochemistry 77
4.2.1 Tissue preparation for light microscopy 78
4.2.1.1 Pretreatment of tissue for immunofluorescence microscopy 78
4.2.1.2 Immunostaining for microtubules and microfilaments 79
4.2.2 Tissue preparation for transmission electron microscopy (TEM) 82
4.2.2.1 Summary of processing protocols for standard TEM 82
4.2.2.2 Sectioning of tissues for TEM 83
4.2.2.3 Immunogold staining for TEM 84

CHAPTER 5 RESULTS 87

5.1 Electrophysiology 87
5.1.1 Steady-state control data from current fluctuation (noise) analysis 87
5.1.2 Effects of reducing the mucosal Na^+ concentration 92
5.1.2.1 Macroscopic current kinetics 92
5.1.2.2 Reduction in mucosal Na^+ concentration increased channel densities 92
5.1.2.3 Reduction in mucosal Na^+ concentration causes rapid changes in N_O 97
5.1.3 Effects of depolymerizing the cytoskeleton on autoregulatory mechanism of Na^+ channel densities 98
5.1.3.1 Disrupting microtubules by colchicine did not alter the effects of reduced mucosal Na^+ concentration 98
5.1.3.2 Disrupting microfilaments by cytochalasin B blocks the increase in open channel density 101
5.1.4 Disrupting actin filaments did not interfere with the regulation of Na^+ channels by AVP 105
5.1.4.1 Steady-state experiments 106
5.1.4.2 Macroscopic changes of I_{Na} 106
5.1.4.3 Results from noise analysis 108
5.2 Immunocytochemical localization of the cytoskeletal network in frog skin granular cells 113
5.2.1 General morphology of isolated frog skin epithelium 113
5.2.2 Demonstration of the cytoskeleton 115
5.2.2.1 Demonstration of microtubules 115
5.2.2.2 Demonstration of microfilaments 118
5.2.2.3 Immunogold labelling of actin filaments 121

CHAPTER 6 DISCUSSION 126

6.1 Modulation of epithelial Na^+ channels by autoregulatory mechanism 126
6.1.1 Regulation of Na^+ channels by luminal Na^+ concentrations 126
6.1.2 Effects of disrupting the cytoskeleton on autoregulation of Na^+ channel densities 130
6.2 Role of the acin in regulation of epithelial Na^+ channels by AVP 133

6.2.1 Regulation of epithelial Na^+ channels by AVP 134
6.2.2 The effect of disrupting actin filaments on the modulation of Na^+ channels by AVP 137
6.3 Immunocytochemical evidence for a possible interaction between the actin network and the Na^+ channel regulatory mechanisms 139

CHAPTER 7 CONCLUSION 143

CHAPTER 8 REFERENCES 146

APPENDIX 169

Abstract

This project examined the role of the cytoskeleton in regulatory mechanisms of the amiloride-sensitive Na^+ channels in isolated frog skin epithelium. The epithelium from ventral frog skin is a model tissue which has proved significant in our understanding of the basic principles involved in water and Na^+ homeostasis. In particular, this project examines ways in which local (non-hormonal) and hormonal regulatory mechanisms adjust the Na^+ permeability of apical membranes of frog skin epithelium. Both mechanisms contain factors that are known to increase the apical membrane Na^+ permeability mainly by increases in the number of open channels. The origin of these new open channels is unknown but, it is postulated that they could arise either by activation of quiescent channels already present in the apical membrane, or by recruitment of channels from cytoplasmic stores. Regarding the latter hypothesis, we also examined the idea that the cytoskeleton might somehow be involved in the insertion of Na^+ channels within vesicles, into the apical membrane. This is based on the fact that the cytoskeleton is involved in a similar mechanism whereby, in the toad urinary bladder, anti-diuretic hormone (ADH) causes the insertion of aggregates with water channels. Much current interest focuses on the role of the cytoskeleton in the regulation of epithelial Na^+ channels. To test this hypothesis, we used noise analysis to examine the effects of disrupting the cytoskeleton, on two different mechanisms which bring about changes in open channel densities. The mechanisms are: (1) lowering mucosal Na^+ concentration (non-hormonal), and (2) addition of arginine-vasopressin (AVP) (hormonal).

Non-hormonal, autoregulatory changes in apical membrane Na^+ conductance were examined by investigating the effects of reducing the mucosal Na^+ concentration. Our results showed that lowering the mucosal Na^+ concentration induced large increases in the open channel density in order to stabilise the transport rate. In addition, we observed an average 55-60% increase in the open channel probability, which implies

that in epithelium from *Rana fuscigula*, changes of channel open probability are also an important mechanism in the autoregulation of channel densities in response to a reduction in mucosal Na^+.

The hormonal control of Na^+ channels by AVP has been intensively studied by noise analysis and the patch clamp. Our results confirmed previous reports that AVP increases the Na^+ transport rate by increasing the number of open Na^+ channels, primarily through large changes in the total number of channels, without a significant change in open probability.

Regarding the role of the cytoskeleton in regulation of Na^+ channels and/or its possible role in control of inserting putative vesicles with Na^+ channels, we studied the effects of disrupting the cytoskeleton on the two regulatory mechanisms. Disrupting microtubules with colchicine had no, or very little effect on either of the regulatory mechanisms. On the other hand, the integrity of the microfilaments was very important for the autoregulatory changes in the number of open channels. After cytochalasin B treatment, lowering the mucosal Na^+ concentration did not result in the usual compensatory changes in channel densities.

There was no prior evidence that cytochalasin B had any actual effect on the F-actin network in the frog skin epithelium. Accordingly, modified cytochemical techniques were designed to demonstrate and localise F-actin in the epithelial granular cells. The direct immunofluorescent method proved useful, but did not allow sufficient resolution to examine the changes to different populations of actin in the cells. We then modified an immunogold method to suit our conditions, and the results demonstrated the localisation of different pools of F-actin and showed the effects of the cytochalasin B and vasopressin.

Acknowledgements

This thesis could not have been completed without help from others.

First, I would like to thank Dr. Cheng-Yi Huang, former supervisor from the Department of Chemical Pathology Chinese Air Force General Hospital, who convinced me to come to South Africa to study.

In particular, I wish to thank Professor R. P. Millar for introducing me to this field of study, for advice and moral support. The same gratitude extends to Professor B. B. Rawdon for giving me the opportunity to work in this department.

I am greatly indebted to my supervisor, Professor W. J. Els, for his continued enthusiastic guidance and patient support. Even when things were not going that well, he was always so helpful and available to give assistance. He has taught me the principles of electrophysiology as well as his philosophical estimation of life. I also wish to extent my appreciation to Mrs. Annatjie Els for her warm hospitality that made me feel at home. Prof. Els and Annatjie, I thank you from the bottom of my heart.

Many thanks would give to Professor L. C. Isaacson for encouragement and advice during the long hours of research, and Professor W. Van Driessche for his helpful discussions. Special thanks to Professor F. X. Omlin for expert and reliable electron microscopic technical advice, and Dr. Linda Stannard for editorial comment of this thesis.

I greatly appreciate the technical assistance given to me by Mr. B. Dando, Mrs. S. Marshall, Mr. J. Pepler, Mrs. E. Fuller, and Mr. H. Fortuin.

I sincerely wish to express my gratitude to Miss Celia Walter for her invaluable support during my study and for assistance in editing the text of the thesis, also Mr. Johnson Lin for generously providing me with a good computer during the final stages of the project.

A very deep thanks goes to my parents, and Mr. Y-R Yen for their understanding, patience and constant encouragement, especially during the lengthy process of my study. I must also express my greatest gratitude to my parents for their financial assistance throughout my academic career.

Finally, I would like to thank Mr. Hugh Anger for the love he expressed in his letters and phone calls, spiritually keeping me company during the long and lonely days of writing, and fellow student Kieron Baldwin for his limitless help and advice.

I am grateful for the financial assistance of the University of Cape Town for the award of a bursary, and the Foundation for Research Development (FRD) for its South Africa-Republic of China Bilateral Exchange Programme which covered my subsistence expenses during this work. In part, this study was also funded by grants to Prof. W. J. Els by the Medical Research Council of South Africa (MRC), and the South African Kidney Foundation.

Glossary of abbreviations

I_{SC}	short-circuit current; μA/cm²
I_{Na}	Amiloride inhibitable macroscopic sodium current; μA/cm²
[B]	blocker concentration in apical solution; μM
S_O	low frequency plateau value of power density spectrum of blocker induced Lorentzian
i_{Na}	single channel sodium current; pA
k_{ob}	open to blocked state rate coefficient; radians/s·μM
k_{bo}	blocked to open state rate coefficient; radians/s
K_B	equilibrium blocker coefficient of open channels ≡ k_{bo}/k_{ob}; μM
β	closed to open state rate coefficient; s^{-1}
α	open to closed state rate coefficient; s^{-1}
β'	open probability in the absence of blocker ≡ $\beta/(\beta + \alpha)$
N_O	open channel density in the absence of blocker
$N_{O,B}$	open channel density in the presence of blocker
N_b	density of blocked open channels
N_{ob}	sum of open and blocked open channel densities; $N_{ob} = N_{O,B} + N_b$
N_c	density of closed channels in the absence of blocker
N_T	total channel density in the absence of blocker
f_c	corner frequency of current noise power density spectrum; Hz
$2\pi f_c$	corner frequency of Lorentzian; radians/sec
PDS	power density spectra
G_m	membrane conductance
R	resistance
V	volts
Ω	ohms
pA	picoamperes

S	siemens
M	molars
I.U.	international unit
min	minutes
s	seconds
°C	temperature in degree Celsius
kD	kilo-daltons
µF	micro-Farad
IgG	immunoglobulin G
AVP	arginine-vasopressin
CDPC	6-chloro-3,5-diamino-pyrazine-2-carboxamide
CB	cytochalasin B
CCD	cortical collecting duct
FITC	fluorescein isothiocyanate
PKA	protein kinase A
PKC	protein kinase C
P.O.	propylene oxide
PBS	phosphate buffer saline

Chapter 1

Introduction

1.1 General Introduction

The concentration of extracellular Na^+ is of essential significance for an organism's body solute and water balance, and abnormal variations in Na^+ concentration will have serious effects on a wide variety of physiological processes. Homeostatic mechanisms, responsible for the delicate regulation of body Na^+, have evolved in epithelial membranes separating distinct body compartments. In humans, and most other vertebrates, the kidney is primarily responsible for Na^+ homeostasis. While the bulk of Na^+ reabsorption occurs in the proximal nephron segments, distal segments, including the cortical collecting duct (CCD), allow fine regulation of the amount of body Na^+ by controlling the rate of Na^+ reabsorption. In a similar fashion, the rate of Na^+ transport is strictly regulated in "tight epithelia" that are responsible for Na^+ reabsorption against steep transepithelial electrochemical potential differences[1]. Classic tight epithelia include the mammalian CCD, the descending colon, the trachea, and the amphibian urinary bladder and skin. Strikingly, much of the fundamental information in renal physiology about the regulation of Na^+ transport has been gathered from studies of amphibian epithelia.

In the CCD and other tight epithelia, electrogenic transepithelial Na^+ transport is a two step process. Firstly, Na^+ moves passively down an electrochemical gradient

[1] An epithelium offers two transport routes to ion flow: the paracellular path and the transcellular path. "Tight epithelia" are generally characterized by a large transepithelial electrical potential difference and resistance (in the order of $k\Omega \cdot cm^2$). The latter resides primarily in the tight junction encircling the cells near their apical surfaces, thus determining the resistance to ion flow in the paracellular pathway. In tight epithelia the transcellular pathway is the most significant, and allows regulated Na^+ reabsorption against steep electrochemical gradients.

(approximately -120 mV) through an amiloride-sensitive, Na^+-specific channel allowing the passage of ~10^6 ions/s (Lindemann and Van Driessche, 1977). This is also the rate limiting step in the transport process. The second step involves the active extrusion of Na^+ across the basolateral membrane by the Na^+/K^+ -ATPase pump.

An important feature of the transcellular Na^+ pathway is the fact that the rate of transport is regulated. The regulation of Na^+ reabsorption is by homocellular processes[2], factors in the external environment of the cell, physical factors such as swelling, and by several circulating hormones. Regarding the distal nephron, environmental or luminal factors would include substances released into tubular fluid, i.e. kallikrein, epidermal growth factor and urokinase-type plasminogen activator. Amongst these factors, the concentration of Na^+ in the extracellular fluid is an important regulator of Na^+ reabsorption. It is well documented that in many tight epithelia Na^+ reabsorption shows self-inhibition of the transport rate with an inverse relationship to the luminal Na^+ concentration. The mechanism of self-inhibition has also been referred to as "autoregulation" of Na^+ reabsorption (Abramcheck *et al.*, 1985).

While aldosterone is considered to be the primary hormone responsible for regulating the reabsorption of Na^+ in the distal nephron, vasopressin is known to be a powerful and fast-acting stimulator of Na^+ transport in many tight epithelia. Recently it was shown that in the rat CCD and in cultured A6 cells, arginine vasopressin (AVP) stimulates Na^+ reabsorption and acts synergistically with mineralocorticoids in the control of the transport rate (Bindels *et al.*, 1988; Chen *et al.*, 1990). In amphibian epithelia, the natriferic actions of AVP acting via cAMP are particularly well

[2] We use the word "homocellular" to infer processes intrinsic to the cell as proposed by Schultz (1985). These would include processes that regulate Na^+ transport via changes to, e.g. intracellular Na^+, Ca^{++} and pH. In contrast there are a number of "extrinsic" regulatory mechanisms involving factors released into the extracellular fluid and hormones.

documented. In fact, the idea that cAMP is the second messenger for vasopressin action was first established in studies on the toad bladder (Orloff and Handler, 1962), and later, confirmed on frog skin (Els and Mahlangu, 1987).

Results from the early electrophysiological studies with vasopressin defined, primarily, the "macroscopic" characteristics of Na^+ transport. These studies provided the basis of our concept of the mechanism of the action of vasopressin and other natriferic hormones such as aldosterone. It was shown that regulation occurs mainly by changing the conductance of the apical membrane to Na^+ entry. The advent of new electrophysiological techniques was responsible for major advances in our understanding of especially the molecular mechanisms of the renal handling of Na^+ reabsorption. In this regard, current fluctuation analysis has demonstrated that the apical membrane conductive pathway resides in Na^+-selective channels (Lindemann and Van Driessche, 1977). These earlier studies have since been extended by the use of the patch-voltage clamp technique (c.f. Helman *et al.*, 1985; Marunaka and Eaton, 1991) and the reconstitution of channels into planar lipid bilayers (Sariban-Sohraby *et al.* 1984b). These and other new techniques have contributed significantly to our understanding of the properties of the Na^+ channel (Reviewed by, Helman and Van Driessche, 1990; Smith and Benos, 1991).

Results have shown that the Na^+ channel, found in the apical membranes of tight epithelia, usually has a relatively low conductance of about 4 to 6 pS, with a much higher selectivity for Na^+ than K^+, and can be blocked by the diuretic drug amiloride. However, several types of amiloride-sensitive Na^+ channels have been distinguished in epithelial cell membranes. These differ in their conductance, their ionic selectivity and their sensitivity to amiloride. These features have been reviewed by Hamilton and Eaton (1986) and Palmer (1992). The Na^+ channel protein has now been isolated, purified and reconstituted into other membrane systems (Benos *et al.*, 1987).

Significantly, molecular studies have revealed that the channel may have multiple regulatory subunits, substantiating the idea that the channel is the target for regulation by hormones and other factors. Unlike the Na^+ channel in nerve cells, the epithelial channel is relatively voltage insensitive. The highly selective, low conductance Na^+ channel found in the rat CCD, the toad urinary bladder and A6 cells has characteristics consistent with the general macroscopic Na^+ conductance of the apical membrane in Na^+ reabsorbing epithelia. The gating characteristics of this type of Na^+ channel are slow, with open and closed times being long (in the order of seconds). Single channel kinetics vary with spontaneous rates of transport but, generally, noise analysis shows that open probability averages around 0.5 in frog skin, but varies widely amongst different tissues and experimental conditions. The Na^+ channel density is surprisingly low compared to that of other channel types, with amphibian epithelia ranging between 10 and 50 million channels/cm^2 under steady-state control conditions (Reviewed by Helman and Kizer, 1990).

The rate of transport through the Na^+ channel may be regulated by modifying either the single channel conductance, the open probability (P_o) or the number of open channels. Fluctuation ("noise") analysis has been most useful in the study of the molecular mechanisms whereby AVP and mineralocorticoids stimulate Na^+ transport in amphibian epithelia. Results with fluctuation analysis have clearly indicated that AVP increases the number of open channels, without modifying the channel unit conductance (c.f. Li, *et al.*, 1982; Helman *et al.*, 1983; Els and Helman, 1991). This effect of AVP has been verified with the patch clamp by Marunaka and Eaton (1991) who reported that in A6 cells, AVP increased the average number of channels from about 2 to 6 per patch. Regarding the mechanisms of action of the aldosterone, the picture is somewhat less clearly defined. Palmer *et al.* (1982) showed that aldosterone increased the number of open channels in toad bladder, while Kemendy *et al.* (1992)

demonstrated that aldosterone increased channel activity in A6 cell patches. However, statistically the latter effect was attributed to a large increase in the open probability and not to a change in the channel density. This conclusion was also consistent with earlier observations with labeling studies on A6 cells (Kleyman *et al.*,1989) where no evidence was found to support the idea that the mineralocorticoid increases channel densities. The current evidence, therefore, is somewhat ambiguous but seems to suggest that both AVP and aldosterone increase apical membrane Na^+ conductance, but by different mechanisms. AVP increases Na^+ conductance mainly by changes in channel densities, while aldosterone acts by increasing the open probability and/or channel density.

Using fluctuation analysis, Els and Helman (1991) argued that since AVP did not increase P_o, the increase in open channel density was elicited mainly through changes in the total number of open and closed channels. Whether an increase in the number of open channels is due to activation of existing channels in the membrane, or to "recruitment" from other cellular pools, remains a vexing question. Many investigators have supported the hypothesis for the insertion of new Na^+ channels into membranes, as occurs in the case of water channels insertion under the influence of ADH. Garty and Edelman (1983) found that apparent inactivation of membrane Na^+ channels in the toad bladder by trypsin did not alter the stimulation of Na^+ transport by AVP but did prevent the response to aldosterone. This observation was offered to support the idea for a recruitment mechanism by AVP, but not for aldosterone. It was suggested that the latter hormone operates by activating channels already present in the membrane. Patch clamp studies have provided some support for the insertion theory (see e.g., review by Schafer and Hawk, 1992), however, not all results are consistent. Frings *et al.* (1988) showed, with patch clamp on toad urinary bladder cells, that the addition of protein kinase A (PKA), cAMP and ATP to an excised patch activated a previously

quiescent channel. Unfortunately, this effect was not observed consistently during the experiments. Immunohistochemical studies similarly have not provided consistent evidence either for or against the insertion theory (c.f. Sorscher *et al.*, 1988; Kleyman *et al.*, 1991). A problem with many immunocytochemical studies is that the methods cannot accurately resolve the occurrence of specific binding to small vesicles directly beneath the cell membrane. On the other hand, biochemical studies on isolated and purified Na^+ channels have provided compelling evidence that the channel may be phosphorylated directly by the action of AVP, thus arguing against the insertion theory (Oh *et al.*, 1993).

Recently, there has been a marked interest in the role of the cytoskeleton in the regulation of Na^+ channels. Results by Benos and his collaborators have shown that in A6 cells the channel was linked to the cytoskeleton, probably by ankyrin and fodrin (Smith *et al.*, 1991). Furthermore, depolymerization of actin filaments increased Na^+ channel activity in A6 cells (Cantiello *et al.*, 1991). Nevertheless, a regulatory role for the cytoskeleton on Na^+ channel activity has not been demonstrated unequivocally. It has been postulated that the cytoskeleton may regulate the insertion of Na^+ channels into the membrane by a mechanism analogous to the manner in which water channels are inserted into the collecting duct membranes by AVP. According to the scheme, the actin framework provides a barrier that holds aggregates or aggrephores of water channels in place in the unstimulated cell. Under the influence of AVP, the barrier breaks down and the aggrephores are able to fuse with the apical membrane, thus increasing the water conductance of the cell. In this regard, studies from the laboratory of Hays have shown that in the toad bladder and rat medullary duct, AVP rapidly depolymerises F-actin with a concurrent increase in the water permeability (Gao *et al.*, 1992; Simon *et al.*, 1993). Whether cytoskeletal elements play an essential

role in the insertion of new Na^+ channels into apical membranes from cytoplasmic pools, has not been resolved.

1.2 Principal Aims of the Study

The main aim of this study was to investigate possible roles of the cytoskeleton in the regulation of Na^+ channels. The intention was to establish, firstly, whether the intact cytoskeleton is necessary for the regulatory processes, and secondly; whether any additional evidence could be uncovered to support the insertion theory as an explanation for changes in channel densities. With this in mind, we investigated two separate regulatory processes of topical interest: viz. regulation by changes in the ionic environment of the cell (non-hormonal), and by a hormonal process. It was assumed that these two processes would modulate the Na^+ channel activity by distinct mechanisms.

We first studied the effects of changing the external Na^+ concentration in the mucosal solution. Autoregulatory modulation of Na^+ channels is a non-hormonal mechanism that is still poorly understood, and it is not known whether intracellular messengers are involved or not. The effects of mucosal Na^+ on membrane conductance have been described in terms of alterations to Na^+ channel saturation and channel densities, but the results have often been at variance. For example, in tight epithelia, fluctuation analysis and patch clamp results have shown that without affecting channel conductance, changes in the mucosal Na^+ modify apical membrane permeability primarily by regulating the number of active Na^+ channels (Van Driessche and Lindemann, 1979; Lewis, *et al.*, 1984; Ling and Eaton, 1989). On the other hand, using the patch clamp on rat CCD, Palmer and Frindt (1988) failed to observe any change in the number of active channels by altering the external Na^+ concentrations.

Various factors including differences in species, methods and conditions have been advanced to explain the contradictions.

Mineralocorticoids are considered to be the major regulators of Na^+ reabsorption in the distal nephron. However, for two important reasons, we selected to study the effects of vasopressin as an example of a hormonal control mechanism. Firstly, AVP is a potent stimulator of Na^+ transport in frog skin; it is known to exert its primary effect on the short-circuit current (I_{SC}) by increasing the number of open channels without raising the channel open probability. Secondly, it exerts its effects within minutes rather than in hours.

1.3 Methodology

Electrophysiological studies were performed by analysing the fluctuations in membrane currents arising, in part, from opening and closing Na^+ channels in the apical membrane. While direct recording from single channels with the patch clamp is a popular and powerful method for studying single channel properties, fluctuation analysis is still a widely used method for monitoring channel events. In fact, for a number of reasons, fluctuation analysis proved particularly significant in our studies. It was not practical to record the data from Na^+ channels in frog skin epithelial cells with the patch clamp, in part, because of the cornified layer covering the granulosum cells. Moreover, fluctuation analysis provided a rapid assessment of the actions of channel modulators without the intricacies of the patch clamp technique. Despite the possibility of errors associated with the method (Gardner *et al.*, 1984), many comparisons with data obtained from single channel recordings have established the validity of fluctuation analysis (c.f. Lux and Brown, 1984; Robinson *et al.*, 1991), and, most importantly, it is still a method of choice to study changes in channel densities.

To our knowledge, interactions between Na^+ channels and the cytoskeleton in frog skin epithelial cells have not been described elsewhere and, we were therefore keen to demonstrate the effects of the respective regulatory treatments on the arrangement of the cytoskeletal fibres. Initial results with standard histochemical techniques provided important information in this regard. Because of the improved resolution of the methods, we subsequently used a modification of the immunogold cytochemical method to study the actin cytoskeleton, using the electron microscopy.

Chapter 2

Literature Review

Maintenance of body solute and water balance requires stringent control of the extracellular Na^+ concentration. This is mainly achieved by the regulated transport of Na^+ and Cl^- across various epithelial tissues. In humans, this important homeostatic function is primarily performed by the epithelium of segments of the distal nephron such as the cortical collecting duct (CCD). The class of epithelia involved in the transport of Na^+ is generally referred to as tight epithelia, because of their high electrical resistance ($\geq 1\ k\Omega \cdot cm^2$). Aside from the epithelial lining of the mammalian CCD, tight epithelia implicated in Na^+ transport are found, amongst others, in the urinary bladders of mammals and amphibians, the colon of mammals, reptiles and birds, and the amphibian skin. Because of inherent problems associated with using mammalian CCD (e.g. the small size of tubule, the maintenance of the temperature at 37 °C, etc.), the other epithelia mentioned above often serve as experimental models for the analysis of epithelial ion transport. In this regard, frog skin is an osmoregulatory organ, and it is used extensively in the study of ionic transport mechanisms. Initially, Krogh (1937) determined that salt-depleted frogs may absorb NaCl across their skin from very hypo-osmolar pond water. Thereafter, the use of isolated frog skin for studies on ion transport gained prominence as a result of the significant work on transepithelial tissue and Na^+ transport mechanisms by Ussing (1949), and Ussing and Zerahn (1951). In part, its wide use can be attributed to the fact that it is ideally suited for electrophysiological studies of Na^+ transport across cell membranes. It is relatively easy to care for the animals in the laboratory, isolated frog skin can be prepared as extensive epithelial sheets and it is not necessary to heat or aerate the preparation during the experiment.

2.1 The Cellular Basis of Renal Function

2.1.1 Epithelial function and organization

Differentiated cells in vertebrates perform specific functions in addition to those constitutive functions that are common to almost all cell types. Epithelia are examples of such specialised cells. They are sheets of cells that cover all the free surfaces and line both internal and external compartments of the body. Epithelial interfaces are involved in a wide variety of activities such as absorption, secretion and protection. Apart from protecting underlying internal tissues from mechanical and chemical stress, epithelia are essential in regulating the internal environment of the body which is necessary for the optimal functioning of physiological processes. Amongst the important homeostatic functions carried out by these cells are the absorption and secretion of various products in the digestive tract, gaseous exchange in the lung, and water and electrolyte transfer in the kidney.

Sodium is often regarded as the most important cation in the body. The extracellular Na^+ concentration is strictly controlled within very narrow limits. The capability of Na^+-transporting epithelia is enhanced by their structural organisation as is exquisitely evident in the kidneys of higher vertebrates. To perform this important function, Na^+-transporting epithelia have developed distinct features. Firstly, they are composed of one or more layers of cells which are separated from each other by very small intercellular spaces (~ 20 μm) (Krause and Cutts, 1986). The spaces between the cells allow for the passage of various small molecules. Access to this paracellular route is controlled by specialised intercellular junctions between the cells at the apical surfaces. These are called tight junctions. The structure and function of the outward-facing (mucosal) cell membranes are very different from those of the basolateral (serosal) membranes. Renal epithelial cells are an excellent example of this as they

have a surface membrane that is polarised into apical and basolateral components, separated by an occluding junction (McNeil and Nelson, 1992). In addition, these two surface membrane components are known to be functionally different with respect to transport processes, hormone receptors, enzymes, electrical resistance, and membrane lipid composition (Els and Helman, 1989; Granitzer *et al.*, 1991; Simons and Fuller, 1985).

2.1.2 Classification of ion transporting epithelia

Ion-transporting epithelia are functionally classified according to the quantity and quality of tight junctions on which the nature of transport is dependent. Renal epithelia, which provide and regulate the vectorial transport of selected compounds, comprise one type of transporting epithelia, specifically they are important sodium-transporting epithelia.

On the basis of the permeability of the paracellular pathway, ion-transporting epithelia may be classed as tight or leaky epithelia. Tight junctions (zona occludens) are composed of interacting strands of lipoprotein that encircle the apex of epithelial cells. They function to seal the epithelial cells into a continuous sheet and act as a selectively permeable barrier to ion transport between the cells (paracellular transport), and they may also function as a "fence" to limit the diffusion of membrane constituents between apical and basolateral membranes (Van Meer and Simons, 1986; Simons, 1987; Gumbiner, 1987). The tight junctions of leaky epithelia such as the small intestine, gallbladder, choroid plexus and renal proximal tubule have fewer strands than tight epithelia. Often, they consist of only a single continuous strand of protein that offers little transepithelial resistance (~5 $\Omega \cdot cm^2$) (Gumbiner, 1987). Consequently, small ions and molecules are able to easily cross the epithelial layers via the paracellular pathway between the cells.

Tight epithelia with large electrical resistance (~several thousand $\Omega \cdot cm^2$) and low diffusion permeability, such as the mammalian and amphibian urinary bladders, frog skin, the mammalian renal cortical collecting tubule, and the colon in mammals, amphibians, reptiles, and birds, can have more than eight protein strands lying in parallel across the tight junction from the apical to the basolateral membrane (Gumbiner, 1987). In this type of epithelium, where the permeability of the paracellular pathway is low, the main route of transport is via the transcellular pathway, crossing the apical and basolateral membranes. This allows for more selective absorption of molecules and, more importantly, the permeability of the pathway is usually regulated.

While tight epithelia usually govern much smaller transport loads than leaky epithelia, they have a greater discriminative capacity and therefore, an important regulatory role in water and solute balance. This is particularly clear when comparing the structure and functions of the mammalian proximal and distal renal tubules.

2.1.3 Overview of the cell membrane structure and permeability

Intracellular components are separated from the external environment by a barrier known as the cell or plasma membrane. In addition to acting as a barrier, the plasma membrane must act as a mediator because it forms the interface between the cell and its environment. Most plasma membranes serve as highly selective filters that maintain a different concentration of ions on either side of them. The basic structure of the plasma membrane is a phospholipid bilayer which accounts for the impermeability of the membrane to most water soluble molecules. All phospholipids are amphipathic molecules which have both hydrophobic and hydrophilic portions. Hydrophobic interactions between the fatty acyl chains of phospholipid molecules result in the formation of the bilayer, in such a way that the hydrophilic head groups

face outwards to the aqueous media and the hydrophobic tails are sandwiched between them. Any molecule transported across the lipid bilayer has to pass through the hydrophobic core, which is impermeable to all charged molecules (ions), regardless of the size of the charge. The high degree of hydration of ions further prevents them from entering the hydrophobic region of the bilayer (Alberts *et al.*, 1989).

Membranes vary in behaviour between cell types because of the variation in their complement of membrane proteins. These proteins serve an extensive range of functions, including for example, facilitating the transport of specific molecules into and out of the cell, and acting as receptors for receiving and transducing chemical signals to the cell interior. Two main types of proteins are found associated with membranes: integral or intrinsic proteins, and peripheral or extrinsic proteins. Integral proteins are anchored in the membrane by means of one or more segments that interact directly with the hydrophobic core of the phospholipid bilayer and, in most cases, they have polar regions that are exposed on either side of the membrane. Such proteins span the membrane and are known as transmembrane proteins. Certain of these transmembrane proteins have become highly specialized to serve as channels for the movement of substances across the membrane. Peripheral membrane proteins on the other hand are not able to interact with the hydrophobic core, and are usually bound to the membrane surface either directly, by interactions with lipid polar head groups, or indirectly by interactions with integral membrane proteins.

The manner in which ions or hydrophobic molecules are able to traverse the cell membrane has been a highly significant field of research in modern cell biology during the last decade. Studies of the mechanisms whereby ions cross the membrane and how these processes might be regulated, have supplied substantial information, thus improving our basic knowledge of cell biology and its clinical applications. The latter

are especially important in the field of nephrology as many diseases can be related to impairments in the membrane transporting system.

2.2 Models of Sodium Transport Across Tight Epithelia

The kidney is mainly responsible for sodium homeostasis, with the distal nephron, being the major site of regulation of Na^+ reabsorption. The transport of Na^+ across epithelia is important since this is the most considerable extracellular cation in the body. The frog skin epithelium is universally regarded as a typical tight epithelium which shares many transport features with the distal renal tubule, and for this reason frog skin has proven to be a most valuable experimental model for studies on Na^+ transport. Since it is a native, intact epithelium it also has a number of advantages over, e.g. cultured cell-lines. Traditionally, many of the experimental results on mechanisms of Na^+ transport have been analysed in terms of two models for the transport process in frog skin specifically, and also in other epithelia. These models are based on the mechanistic model first proposed by Koeffoed-Johnsen and Ussing (1958) and several electrical equivalent circuits of the transcellular process. Initially, the electrical models provided the basis for analysis of the macroscopic processes involved in Na^+ transport, but are equally applicable in the new single channel electrophysiological experiments.

2.2.1 Koefoed-Johnsen and Ussing model

In frog skin, the distal renal tubule and in other tight epithelia, transepithelial Na^+ reabsorption occurs in a two-step process (Koefoed-Johnsen and Ussing, 1958). The first step is the diffusion of Na^+ into the cell (through the apical membrane) down the ions' electrochemical concentration gradient. The electrochemical gradient is brought about by the electronegativity of the intracellular compartment. The electronegativity is mainly due to the large number of negatively charged proteins, and the low

intracellular Na^+ concentration (10 mM) relative to the extracellular fluid (110 mM) (Helman, 1979). The second step is the active expulsion of Na^+ at the basolateral membrane by the Na^+-K^+-ATPase pumps which also contributes to the electrochemical concentration gradient (Fig. 2.1).

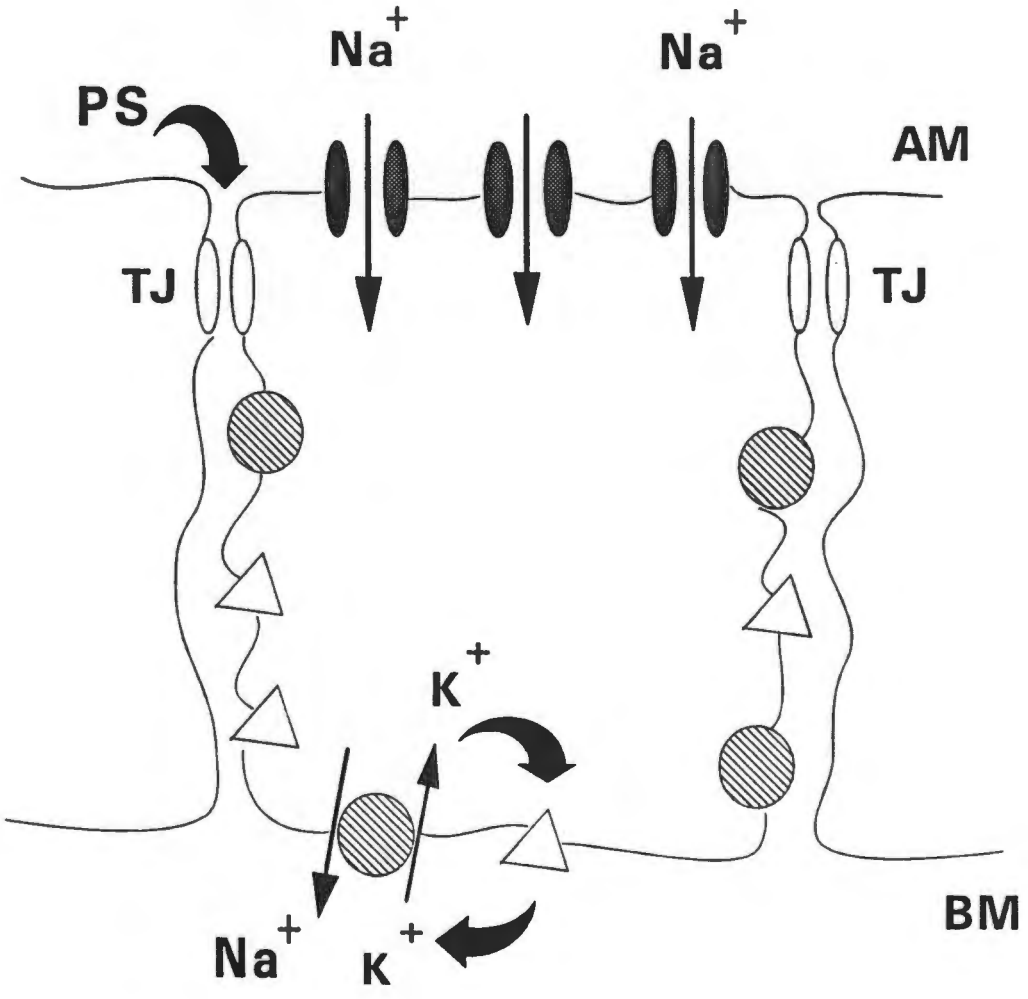

Fig. 2.1 This diagram shows the essential features of the Koefoed-Johnsen and Ussing model (1958). AM: apical membrane; BM: basolateral membrane; PS: paracellular or shunt pathway; TJ: tight junction. Na+ channels are found predominantly in the apical membrane and K^+ channels (Δ) predominantly in the basolateral membrane. The basolateral membrane also contains the Na^+-K^+-ATPase pumps.

As a result of this distribution of transport capacities, net Na^+ movement from the apical solution into the interstitial space becomes possible, while K^+ cycles through the basolateral membrane. The cellular Na^+ concentration remains relatively low and the amount of Na^+ passing through the cell is large. An important feature of the model in frog skin is that the apical membrane is largely permeable to sodium ions alone.

2.2.2 The Thévenin equivalent electrical circuit

Ussing and Zerahn (1951) designed an electrical model of the Na^+ transport process across frog skin that included a Thévenin emf, E_{Na}, and a Thévenin resistance, R_{Na}. Although these investigators recognized that the mechanism of the transport process could not be inferred directly from these parameters, it was understood that any specific mechanism must fall within the thermodynamic constrains imposed by the magnitudes of these parameters. The transepithelial E_{Na} can be characterised further by Thévenin equivalents at both the outer and inner membranes (Helman, 1979). As shown in Figure 2.2, the outer barrier of a Na^+-transporting cell can be modelled with a Thévenin emf, E_o, and resistance R_o. Also, the inner membrane is modelled with the Thévenin E_i and R_i. It is obvious that the E_{Na} and R_{Na} would be defined as follows:

$$E_{Na} = E_o + E_i$$

$$R_{Na} = R_o + R_i$$

The frog skin epithelium consists of a number of different morphologically distinct cell types (Voûte, 1963; Rick *et al.*, 1978). Besides the tight-junctional complexes between the outermost living cells of the stratum granulosum, the transepithelial ions flow and molecules may also pass through the shunt pathways in parallel with the active Na^+ transport pathway (Ussing *et al.*, 1974). The resistance offered by the junctional complexes and the intercellular spaces in the paracellular route is given by

the shunt resistance, R_s (Fig. 2.2). In the presence of a low shunt resistance, current can pass through this circuit both via the transcellular and paracellular route.

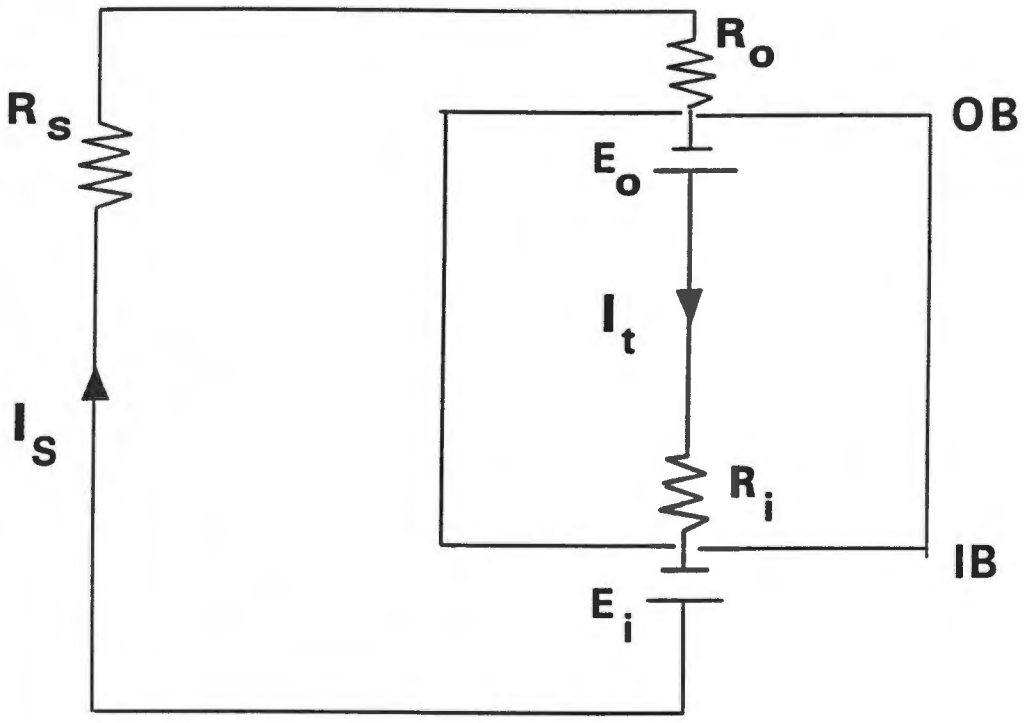

Fig. 2.2 This diagram shows the expanded Thévenin equivalent electrical circuit, as the first described by Helman. **OB**: outer barrier representing the apical membrane; **IB**: inner barrier (basolateral membrane); R_o and R_i: resistance of the apical and basolateral membranes to transcellular Na^+ transport, respectively. The paracellular pathway is parallel to the transcellular pathway and is characterised by the shunt resistance (R_s). E_o represents the potential across the apical membrane while the E_i is the basolateral K^+ diffusion potential plus the electrogenic potential of the Na^+-K^+ pumps. Current flows through the loop with current I_t ($I_t = I_s$) (Adapted from Helman and Fisher, 1977).

According to the circuit shown in Figure 2.2, the outer and inner membranes of the transporting cells are coupled electrically through the parallel shunt pathway assumed to comprise only a resistance, and include no source of electrical potential. The influence of the shunt can be excluded by voltage clamping to zero transepithelial potential, which has the effect of reducing net current through the shunt. In the present studies, skins were short-circuited continuously. Under short-circuit conditions, the net shunt current is zero. The expression for the I_t now is:

$$I_t = (E_o + E_i) / (R_o + R_i)$$

The Thévenin equivalent circuit (Fig. 2.2) allows for the experimental determination of the electrical behaviour of Na^+ transport at the apical and basolateral membrane. Nevertheless, it should be emphasised that the Thévenin behaviour of the barriers, often, but not necessarily, gives a description of the mechanisms of ion transport which provides a basis for analysis by other methods compatible with the Thévenin equivalent (Helman, 1979).

In this regard, the simple Koefoed-Johnsen and Ussing Thévenin equivalent circuit model, or the more complex circuit of Helman, can serve in the design and interpretation of numerous studies of active transepithelial Na^+ transport.

2.2.3 Possible role of sodium transport compartment

As we know now, transepithelial Na^+ transport can be represented by the two step Koefoed-Johnsen and Ussing model which has already been described. In his original experiment with the frog skin epithelium, Ussing assumed that only the basal cell layer was involved in Na^+ transport. Later, he and his co-workers conceded that, either, the whole epithelium is involved in transepithelial Na^+ transport (Ussing and Windhager, 1964), or, that only the outermost living cell layer, the stratum granulosum, is involved

(Voûte and Ussing, 1968). The cornified cell layer appears to be comprised of functionally dead cells which allow the free exchange of fluid . It is not considered to be actively involved in the reabsorption of Na^+, and, therefore, the cornified cell layer is not part of the Na^+ transport compartment. Pursuing this controversy, Rick *et al.* (1978) confirmed that all living epithelial layers share in the transepithelial Na^+ transport with Na^+ entering the outermost living cell layer (stratum granulosum) through channels (in an amiloride-sensitive step). From there, Na^+ diffuses via low-resistance cell-cell pathways into all of the deeper epithelial layers (outer and inner stratum spinosum, and stratum germinativum) and is transported via Na^+-K^+ pumps (in an oubain-sensitive step), into the intercellular spaces of the epithelium (Fig. 5.10A).

Certain cell types in the subepithelial glands do not engage in transepithelial Na^+ transport, rather, they appear to be involved in Cl^- secretion from the epithelium. This secretion can be elicited by the presence, or addition, of norepinephrine or isoproterenol (Mills *et al.*, 1985).

2.3 Basic Electrical Methods For Studying Membrane Ionic Transport

Modern electrophysiological techniques have revolutionised the study of ion transport across epithelia. Early methods provided valuable information on the macroscopic characteristics of ionic transport. These methods included voltage clamp and microelectrode studies which have greatly enhanced our present understanding of the cellular mechanisms of ion transport, but very little was learned regarding the processes at a molecular level. Development of the newer methods have provided us with much more information on ion transport at the microscopic level, allowing us to resolve the molecular mechanisms involved. Insights gained have arisen mainly from studies with patch clamp, impedance analysis, and current fluctuation (or noise)

analysis. These methods were applied to native and cultured tissues as well as to artificial lipid membranes. Both the patch clamp technique and current fluctuation analysis rely on the principle that each time an ion channel opens, it produces a short pulse of the current, of a characteristic amplitude, and duration, related to the open probability. Fluctuations in current flow through membrane channels may be studied by two methods: Power spectral analysis (noise analysis) and single channel analysis with patch clamp methods.

2.3.1 Patch clamp

Much of the current technology is the result of the initial methodology developed by Neher and colleagues (Neher and Sakmann, 1976; Neher *et al.*, 1978; Hamill *et al.*, 1981). Single agonist-activated ion channels can be observed directly with the extracellular patch clamp technique. Many of the initial experiments were carried out on frog muscle fibres and nerves but have since also been applied to a wide variety of ion conducting tissues. Some basic ways in which this technique may be applied are illustrated in figure 2.3.

A specially constructed glass micropipette seals off a small patch on the surface of the cell membrane approximately 1 μm in diameter. The key factor in the application of this technique is the creation of an adequate seal. A development of this technique came about in 1980. Sigworth and Neher (1980) reported that if slight suction was applied to the recording pipette as it was placed on a surface membrane, a very high resistance seal ($>10^9$ Ω) could be created. This seal, referred to as a giga-seal, has enormously improved current resolution and recording bandwidth, and paved the way for numerous studies which provide details of channel characteristics. The high resistance seal reduces noise levels, enabling high resolution recording of single ion channel currents. The giga-seal also allows ion channel current recordings to be made

under a much larger range of voltage clamp conditions. The electrically isolated membrane patch can be pulled off the cell (excised) in such a way that the inside of the plasma membrane faces the bath solution (inside-out) or alternatively, that the inside faces the solution in the micropipette (outside-out). By breaking the patch membrane in the cell-attached configuration, the solution in the pipette gains direct access to the cell interior and whole cell currents can be measured (Peterson and Peterson, 1986).

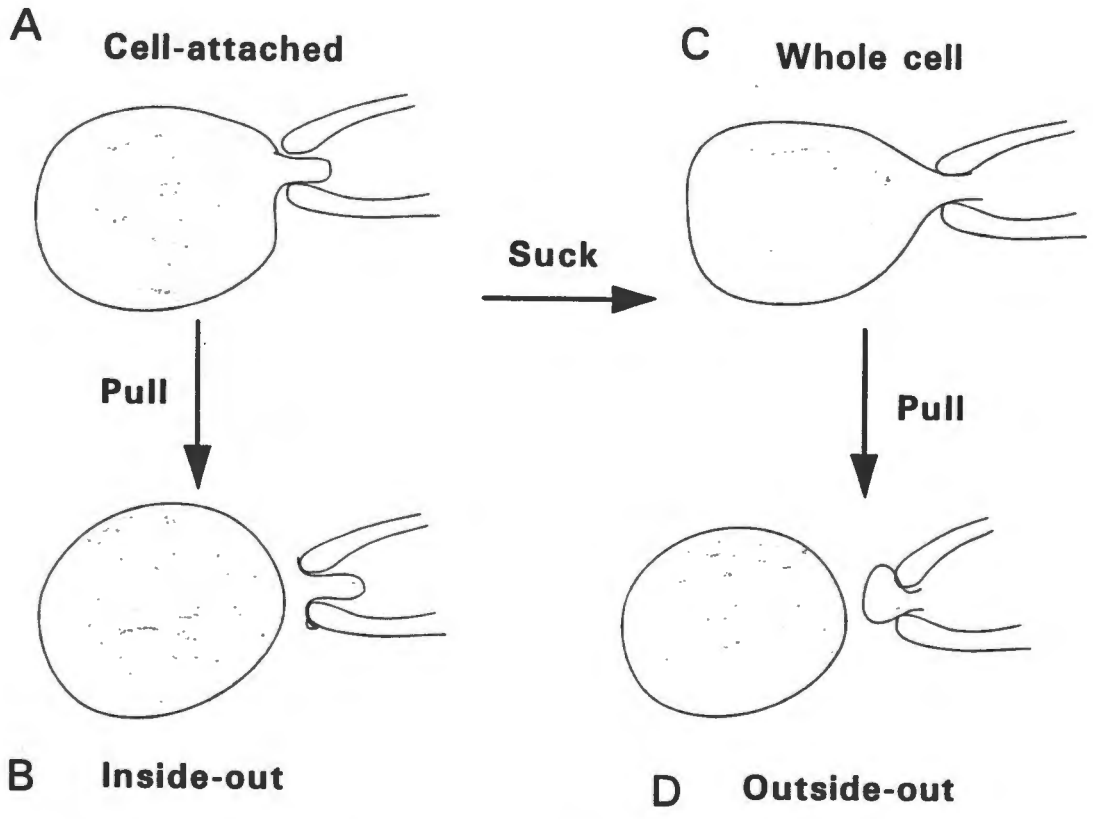

Fig. 2.3 Diagrammatic illustration of the various configurations with the patch clamp technique on an isolated single cell. A: cell-attached patch mode, produced by applying light suction to the patch pipette to produce the gigaseal. B: Isolated inside-out patch. C: Whole cell mode. D: Isolated outside-out patch. In all cases, a gigaseal is produced between the patch pipette and the membrane. (Modified from Sigworth, 1986)

The patch clamp technique has been particularly effective in determining properties of individual ion channels such as relative ion selectivity, single channel conductance, and channel kinetics. These basic parameters constitute the "signature" of the channel and allow the specific channel to be recognised in different cells and tissues. The conductance and selectivity of the channel are perhaps its most basic characteristics, in that they reflect which ions are transported and at what rate. Both characteristics can be determined from a plot of single-channel current (I) vs. voltage (V) across the patch. The kinetics of the channel reveal how frequently the channel opens or closes. By measuring each time interval in which the channel is continuously open or closed, the mean open time and the mean closed time, i.e. the percentage of time that a channel is open or closed, the open probability can be estimated (Colquhoun and Hawkes, 1983).

Consequently, single channel measurements are most valuable for determining kinetic models that describe conformational changes in individual channels. Generally, temporal resolution of patch clamp is extremely good at both high and low frequencies, allowing resolution of different states of the channels. On the other hand, measurements of changes in current flow through epithelial channels are frequently problematic with patch clamp. Since the mean open and closed times of Na^+ channels are several seconds, it is necessary to obtain stable records of many minutes. Sometimes this could be a problem with patch clamp. Further, patches may contain a number of fluctuating channels that makes it difficult to determine the exact number of channels in a patch. It would be difficult to determine whether changes occur in open probability and/or N_T. Eaton and colleagues have developed a procedure to overcome this problem (Marunaka and Eaton, 1991). They use the product of the number of channels and the open probability as a measure of channel activity in a patch according to the relationship:

$$NP_o = \sum_{n=0}^{N} \frac{n \cdot t_n}{T}$$

where **T** is the total recording time, **N** is the maximum number of open channels and **n** is the number of channels open. There is a problem when P_o is very low as when cells have been depleted of aldosterone for some time (Kemendy *et al.*, 1992).

Sometimes, as with frog skin, the nature or dimensions of the epithelium make it impossible to use patch clamp. Recent evidence has shown that patch clamp could be a very invasive technique making it imperative that extreme caution should be exercised when doing these studies on epithelia (Ruknundin *et al.*, 1991). The advantages and disadvantages of single channel measurements compared with power spectral analysis have been discussed in detail (Eaton and Marunaka, 1990).

2.3.2 Current fluctuation ("noise") analysis

The technique of fluctuation (noise) analysis has been a very valuable method for the study of ion channels in epithelia. Originally, the method was used extensively to study ionic channels in excitable tissues (Reviewed by Neher and Stevens, 1977; Lauger, 1980). In these tissues the channels fluctuate between open and closed states in the milliseconds (ms) range making it easy to study the channel characteristics by noise analysis. On the other hand, conformational changes in epithelial channels are much slower (a few seconds in duration) making it virtually impossible to study them with this technique. Lindemann and Van Driessche (1977) introduced the idea of blocker-induced noise analysis of epithelial Na^+ channels by demonstrating that adding amiloride to the apical solution of short-circuited epithelia caused the appearance of a Lorentzian in the power density spectrum (PDS). Since then, this method has been widely used to study the regulation of epithelial Na^+ permeability of the apical

membrane (c.f. Palmer *et al.*, 1982; Helman *et al.*, 1983) and the basolateral K^+ permeability (c.f. Van Driessche, 1986; Dawson *et al.*, 1988).

The concept of fluctuation analysis is based on the idea that each successful activation of an ion channel produces a brief pulse of current of fixed amplitude, and of a duration (or frequency) related to open probability. The length of time each channel stays open, is the time taken for the open channel to gain sufficient energy to exceed the energy barrier for the closing step, according to the kinetic scheme of the channel:

$$\text{open} \underset{\alpha}{\overset{\beta}{\rightleftarrows}} \text{closed}$$

Since the process of acquiring energy depends on interactions between a molecule and its environment and since each individual molecule will not have the same initial energy content (Boltzman's distribution), open times will be random variables drawn from a Poisson (exponential) distribution. The mean of this distribution is the average open time of the ion channel, which is the reciprocal of the rate constant, α, for the closing step in the kinetic scheme outlined above; but a channel may be activated a number of times. Like the channel closing process, the activation process will also be random. In a membrane, however, there are a number of channels which can be activated, and the independent activity of a large number of randomly activated ion channels will sum to produce an overall membrane current response, which fluctuates about a mean current. The mean current can be analysed by converting the amplitude-time relationship via a Fourier Transform to an amplitude-frequency relationship. This produces a power density form which with the use of mathematical analysis yields information on the channel (details in chapter 4).

As outlined above, fluctuation (noise) analysis offers an alternative approach to study epithelial membrane Na^+ channels. It is a non-invasive method allowing us to study membrane Na^+ permeability on extensive sheets of epithelia. It provides information

about the properties of a population of channels, and herein is a major disadvantage of the procedure. One has to assume that the channels have identical properties and contribute in an identical manner to the noise fluctuations. Evidence for the assumptions is based on a knowledge of the kinetics of the system under investigation or on the appearance of Lorentzian components in the PDS (Van Driessche and Zeiske, 1980). Advantages and limitations of the method have been discussed in great detail previously (Eaton and Marunaka, 1990; Van Deynse and Van Driessche, 1992).

In an initial study on frog skin with amiloride-induced fluctuation analysis, Lindemann and Van Driessche (1977) analysed their data in terms of a two-state model where blockage was modelled with pseudo-first-order kinetics (see Lindemann and Van Driessche, 1978). More recently Helman and Baxendale (1990) used a three-state model to analyse data. In part, justification of the three-state model comes from the observation of apparent changes to channel densities with increasing blocker concentration, and that the model is consistent with the Na^+ self-inhibition hypothesis proposed by Lindemann and Van Driessche (1978).

With blocker-induced fluctuation analysis, interaction between the blocker and the Na^+ channel causes the channel to fluctuate between open and blocked states giving rise to a single Lorentzian in the PDS where radian corner frequencies ($2\pi f_c$) are linearly related to the blocker concentration, according to the equation:

$$2\pi f_{c,B} = k_{ob}[B] + k_{bo}$$

where k_{ob} and k_{bo} are the on- and off-rate coefficients. The corner frequencies at the spontaneous fluctuations between closed and open states cannot be observed in the PDS and hence, the rate coefficients α and β were unknown from this method. Recently, Helman and colleagues used 6-chloro-3,5-diamino-pyrazine-2-carboxamide

(CDPC), a weak and electroneutral Na^+ channel blocker, to induce fluctuations, and analysed their data according to a three-state model (see below).

$$\text{closed} \underset{\alpha}{\overset{\beta}{\rightleftarrows}} \text{open} \underset{k_{bo}}{\overset{k_{ob}[B]}{\rightleftarrows}} \text{blocked}$$

From this model, they were able to calculate the channel open probability, referred to as β' (where $\beta' = \frac{\beta}{\alpha+\beta}$) from the following relationship (Helman and Baxendale, 1990):

$$\beta' = \frac{1 - N_{O,B}/N_o}{(N_{O,B}/N_o)\,([B]/K_B)}$$

The mean open probability, determined with this approach, averaged close to 0.5 (Els and Helman, 1989; Helman and Baxendale, 1990). This mean value was remarkably similar to mean open probabilities of Na^+ channels, calculated from open and closed times, that were measured in rat CCD with patch clamp (Palmer and Frindt, 1986b). In Na^+ channels, reconstituted into phospholipid bilayers, the mean open and closed times were much longer and varied between 2 to 10 sec (Sariban-Sohraby *et al.*, 1984b).

In this study, we used CDPC as a fluctuation inducing blocker (as described in chapter 4). The antidiuretic drug amiloride has been widely used for this purpose but certain reservations in using this drug have been raised (Helman and Baxendale, 1990). It has been suggested that amiloride may bind equally well to both the open and closed states of the Na^+ channel. This would necessitate the use of a four-state model to describe the blocker's interactions with the Na^+ channel:

$$\text{closed-blocked} \underset{\gamma}{\overset{\delta}{\rightleftarrows}} \text{closed} \underset{\alpha}{\overset{\beta}{\rightleftarrows}} \text{open} \underset{k_{bo}}{\overset{k_{ob}[B]}{\rightleftarrows}} \text{blocked}$$

In addition, it is known that amiloride may occur in cationic and electroneutral forms and that these two forms may bind to open and/or closed channels at different rates. Furthermore, due to its long association (~1000 ms) with the channels, the likelihood

of finding transitions of blocked channels, in a closed-blocked state, is increased. Hence, the kinetics of amiloride with the Na^+ channel is complicated and involves many uncertainties. This is problematic, since current fluctuation analysis relies on the correct kinetic assumptions. However, in certain tissues and for certain experiments, amiloride is still the blocker of choice. There are certain advantages in using CDPC for our experiments. Firstly, CDPC binds specifically to the channel in the open state, and not the closed state. Secondly, it occurs only in an electroneutral state, hence there is only one state to consider in the Na^+ channel interactions. Thirdly, since it is an electroneutral blocker, the on- and off-rate coefficients of blocker interaction with the channel are voltage insensitive. Fourthly, the off-rate coefficient for CDPC is much larger than for amiloride (about 220 rad/s against <5 rad/s). Therefore, since CDPC is only associated with the channel for a very short time, the macroscopic Na^+ transport rate is only minimally inhibited. Accordingly, experiments could be carried out with tissues close to their physiological transport rates.

2.3.3 Impedance analysis

Membrane capacitance measurement is another of the high resolution electrophysiological techniques used to investigate ion transport across epithelial membranes. Transepithelial ion movements pass through the cellular pathway which is composed of apical and basolateral membranes, and through the paracellular pathway which is formed by the tight junctions and the lateral spaces. Since epithelia are generally highly expandable tissues, it is important to develop techniques which are able to estimate the exposed membrane areas. Impedance analysis allows one to determine specific ionic conductance per unit membrane area, which is an indirect measurement of ionic permeability. Over the last few decades, many of the investigations of the regulation of ionic transport, necessarily involved in endocytotic and exocytotic fusion processes resulting in changes in the exposed area of the apical

and/or basolateral membranes. Recently, the techniques have been use to investigate the Na^+ transport in amphibian urinary bladder (Clausen *et al.*, 1979) and cultured renal cells (Wills *et al.*, 1992; Wills *et al.*, 1993); Na^+ and K^+ transport in mammalian descending colon (Wills and Clausen, 1987), and Cl^- secretion in amphibian cornea (Clausen *et al.*, 1986).

In tight epithelia, in which the paracellular ionic pathway is usually negligible, then impedance analysis produces direct estimates of the apical and basolateral membrane conductances. All biological membranes have a membrane specific capacitance typically averaging at approximately 1 $\mu F/cm^2$ (Cole, 1972). From these observations, the area of the membrane surrounding a single cell may be assayed by measuring the cell membrane capacitance (C_m). A large advance in this technique was made when Neher and Marty (1982) measured C_m changes at femtofarad resolution. With this method C_m changes, representing the fusion of single secretory vesicles in the cell membrane have been observed.

Measurement of membrane capacitance is a non-invasive means of assessing dynamic changes in the membrane area associated with ion transport (Clausen *et al.*, 1979; Warncke and Lindemann, 1981; Lewis and de Moura, 1984; Margineanu and Van Driessche, 1990). Impedance spectra of epithelial membranes generally deviate from idealised behaviour which assumes that membrane resistance and capacitance is frequency-independent. Hence, in Nyquist impedance plots, impedance loci usually exhibit depressed semicircular arc behaviour, as earlier described by Cole and Cole (1941). This behaviour has previously been attributed to the complexity of the epithelium, and has been associated with the lateral intracellular spaces (Clausen *et al.*, 1979). More recently, Helman has recognised that the dielectric properties of tight epithelia are frequency-dependent, thus responsible for the deviation from the ideal behaviour. In their experiments, transepithelial impedance of short circuited frog skin

epithelium was measured under voltage clamp conditions similar to that described by Margineanu and Van Driessche (1990). All experiments were done in the presence of amiloride which isolated apical from basolateral membranes to permit direct assessment of the characteristics of the apical membranes of the epithelial cells. The paracellular shunt was frequency-independent, whereas the apical membrane capacitance was frequency-dependent. Under these conditions, the capacitance spectrum of apical membranes exhibited many relaxation processes which could be classified according to their relaxation frequencies. In their study, the dc capacitance (which avoided measurements at frequencies which could lead to unrelated capacitance changes) averaged 1.85 $\mu F/cm^2$ (Awayda and Helman, 1992). Under conditions which either increased or decreased apical membrane channel densities, they measured concurrent increases and decreases of the dc membrane capacitance, which were consistent with the idea that channels are either inserted or removed from the apical membrane.

It is of interest to note that the relaxation processes of the apical membranes may be associated with different membrane lipid domains. If the properties of the Na^+ channels are influenced by the nature of the lipid in its environment (Awayda and Helman, 1992), then capacitance measurement could provide another important way in which to study the complex mechanism of Na^+ channel regulation. If Na^+ transport can be increased by the recruitment of Na^+ channels from intracellular Na^+ channel-containing vesicles into the apical membrane, this exocytosis can be reported as an increase in C_m. This is currently being investigated.

2.4 Epithelial Na^+ Channels

The entry of sodium and other ions across cell membranes of tight epithelia is accomplished by the employment of specific transport molecules within the apical

plasma membrane. These molecules represent carriers or channels, both of which are transmembrane proteins that allow specific transport of ions via electrochemical gradients. In carrier-mediated transport, the binding of ions to specific carriers facilitates their passage through the lipid phase of the membrane. Carrier- and channel- (or pore-) mediated transport through biological membranes, can be distinguished by the turnover number of individual transport sites (Armstrong, 1975). It has been suggested that carrier-mediated transport is responsible, at maximum rates of transport, for 10^4 ions per second, so, when Lindemann and Van Driessche (1977) demonstrated that in frog skin, more than 10^6 sodium ions are translocated per translocation site per second, this indicated that Na^+ enters the epithelial cells via channels in the apical membrane.

Sodium-transporting epithelia, such as found in the distal and collecting tubules of the kidney, the descending colon, the lung, the trachea and the sweat ducts, contain Na^+ specific channels situated within their apical membranes. The main channel type is referred to as amiloride-sensitive Na^+ channels, for although they are defined by their ability to predominantly conduct Na^+ ions, their high sensitivity to the diuretic amiloride, results in a characteristic inhibition of Na^+ transport.

Several reviews which cover various aspects of epithelial Na^+ channels have been published over the last ten years (Lindemann, 1984; Van Driessche and Zeiske, 1985; Sariban-Sohraby and Benos, 1986a; Wills and Zweifach, 1987; Eaton and Hamilton, 1988; Garty and Benos, 1988; Palmer *et al.*, 1989; Smith and Benos, 1991; Palmer, 1992; Horisberger *et al.*, 1993). This section will focus on both the biochemical and physiological characteristics of the Na^+ channel, and on the mechanisms involved in the regulation of its activity. Information has been obtained by using a variety of macroscopic techniques in which transport across the entire epithelium is measured, as

well as, by microscopic methods (noise or fluctuation analysis, and patch clamp recordings), which indicate the single channel properties.

2.4.1 Physiological types of epithelial Na^+ channels

Under physiological conditions, several types of amiloride-sensitive Na^+ channels have been observed in epithelial cell membranes. They can be characterised by their single-channel conductance, their ionic selectivity and their sensitivity to amiloride.

2.4.1.1 High sodium-selective and low conductance channels

This type represents the most widely distributed and most common Na^+ channel. These channels are highly selective towards Na^+. By means of macroscopic measurement of transepithelial potentials and tracer fluxes, the ion selectivity for Na^+ over K^+ was found to be 670:1 (Na^+:K^+) in a study on the toad urinary bladder (Palmer, 1982a; Palmer, 1987). Another characteristic shared by these channels is their low single-channel conductance (4-5 pS) which has been demonstrated primarily by the studies with patch-clamp technique on the rat cortical collecting tubule (CCT) (Palmer and Frindt, 1986a&b; Palmer and Frindt, 1988), the epithelium of the toad urinary bladder (Frings *et al.*, 1988), and primary cultures of the rabbit cortical collecting tubule (Ling *et al.*, 1991) and the amphibian kidney cell line (A6 cells) (Hamilton and Eaton, 1985; Hamilton and Eaton, 1986; Ling and Eaton, 1989).

This category of Na^+ channel (like all known epithelial Na^+ ion channels) display a gating characteristic of slow spontaneous opening and closing kinetics (opening and closing times are as long as a few seconds). Current fluctuation analysis studies were not able to resolve spontaneous opening and closing times of the channel, but single-channel studies have demonstrated clearly that such a slow transitional state exists. Amongst others, Palmer and Frindt (1986b) demonstrated Na^+ channels with a

mean open time of 3.4 s and mean closed time of 3.9 s in the rat CCT. These slow rates are bordering on the limit of resolution of current fluctuation analysis methods. Similar results were obtained for A6 cells grown on permeable collagen supports which contained channels with mean open and closed times of, 2.2 and 5.1 s, respectively (Hamilton and Eaton, 1986). Frings *et al.* (1988) demonstrated that Na^+ channels from the toad urinary bladder had faster channel kinetics, averaging 0.4 and 1.4 s, respectively. Sariban-Sohraby *et al.* (1984b) and Olans *et al.* (1984) have reported longer spontaneous opening and closing of channels (open time 10 s and closed time 5 s) for reconstituted Na^+ channels from A6 cells incorporated into lipid bilayers. In the rat CCT and A6 cells, the data were consistent with a simple kinetic model having one open and one closed state (Palmer and Frindt, 1986b; Eaton and Marunaka, 1990); however, the probability of the opening of individual channels is often highly variable, even in the same tissue and using the same experimental methods (Palmer and Frindt, 1988), hence the high variability in the reported channel kinetics.

The most widely used inhibitor of epithelial Na^+ transport is the diuretic drug, amiloride (3,5-diamino-6-chloropyrazainoylguanidine). This drug has been used intensively as a tool to study Na^+ transport in epithelia and to characterise the Na^+ channel (Benos, 1982; Garty and Benos, 1988; Kleyman and Cragoe, 1988; Hamill *et al.*, 1992). Amiloride is a pyrazine ring compound possessing amino groups on the 3- and 5-positions, a Cl^- on the 6-position, and an acylguanidium moiety attached to the 2-position (Fig. 2.4).

Due to the presence of the guanidium part, amiloride exists as a positively charged amine or as an undissociated base. These acid-base properties allow amiloride to penetrate both biological and artificial membranes (Benos *et al.*, 1983). For the inhibition of Na^+ transport, amiloride should carry a positive charge. The binding of

amiloride to the Na^+ channel is facilitated by an interaction between the positively charged side chain of the molecule and the channel protein. This complex may then dissociate by an interaction of the Cl^- at the 6-position with another site, and thereby block the channel (Li *et al.*, 1985). In the toad urinary bladder, blocking of Na^+ channels by amiloride is voltage-dependent (Palmer, 1990). The sign of the voltage dependence is consistent with the idea that the amiloride molecule is positively charged at physiological pH, and that the amiloride molecule senses part of the transmembrane electric field at its binding site on the channel.

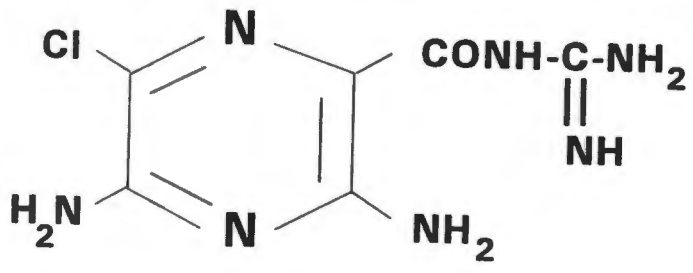

Fig. 2.4 This diagram shows the structure of amiloride.

Recently, Palmer (1990) also presented a combined geometric-kinetic model for the epithelial Na^+ channel which is based on analysis of voltage-dependent blocking of Na^+ channels by impermeant ions. In this model, the outer pore of the channel is large enough to accommodate the guanidinium site of the amiloride molecule, and other similarly sized organic cations. Farther into the channel, the pore subsequently narrows in at least two steps. The impermeant inorganic cations, such as K^+ and Ca^{++}, can penetrate into the electric field, but at some point, the pore is so narrow that it excludes all ions except Na^+, Li^+, and H^+. This model explains both the ion selectivity and the amiloride sensitivity of this channel very well. Transitions between one or more open or closed conformations can be triggered by factors such as chemical and

fluctuation changes (Van Driessche and Zeiske, 1985); however, these Na^+ channels in the apical membrane of tight epithelia are either ligand or chemically gated.

2.4.1.2 Moderate sodium-selective and higher conductance channels

Other types of Na^+ channels have been identified more recently with patch clamp. Amongst them, is a type of Na^+ channel that has been found most extensively in the apical membranes of cultured rabbit CCT (Ling *et al.*, 1991) and A6 cells (Hamilton and Eaton, 1985; Cantiello *et al.*, 1989) when grown under certain conditions and has been studied using the patch-clamp technique. When the A6 cells are grown on plastic culture dishes, the predominant channel type expressed is different from that of the channel type grown on a permeable support such as a collagen-coated filter. The type of channel in A6 cells grown on plastic culture dishes has a lower sodium selectivity (Na^+:K^+ = 3:1), as measured from reversal potentials for single channel currents (Hamilton and Eaton, 1985). Selectivity with respect to other cations has not been widely tested, so it is not known if this represents a qualitative difference in the selectivity sequence. Less selective channels do not always have a higher conductance (Gogelein and Greger, 1986; Verrier *et al.*, 1989), though high Na^+ selectivity is usually associated with low conductance channels (Benos *et al.*, 1980; Palmer, 1982; Lewis *et al.*, 1984; Bremec *et al.*, 1987). For example, channels in cultured thyroid cells have low conductance (2.6 pS) and amiloride sensitivity (1 μM), and do not select for Na^+ over K^+ (Na^+: K^+ = 1.2) (Verrier *et al.*, 1989).

A second property of this type of channel is its single channel conductance. In A6 cells which are grown on plastic dishes, the single channel conductance under physiological conditions is 7-10 pS which is much higher than previously described (Hamilton and Eaton, 1985). However, in primary cultured eccrine sweat duct cells, the single channel conductance is 15 pS. The spontaneous opening and closing

kinetics are faster, with mean open and closed times in the range of 10 ~ 100 mS. As this type of channel is found mostly in cells which are not engaged in transepithelial Na^+ transport, its physiological role is not clear yet (Loris *et al.*, 1989).

Recently, Palmer (1992) has discussed evidence suggesting that these two types of channel (described in sections 2.4.1.1 and 2.4.1.2) are two states of the same protein, and could be interconvertible, perhaps by the processes of proteolytic degradation (Lewis and de Moura, 1982; Lewis and Wills, 1983; Lewis *et al.*, 1984; Lewis and Alles, 1986; Wills and Zweifach, 1987; Zweifach and Lewis, 1988). Sariban-Sohraby and co-workers (1984b) reported that reconstitution of the Na^+ channel into lipid bilayers from the apical membranes of A6 cells grown on permeable supports, resulted in channels with the expected sensitivity to amiloride, but with low selectivity to Na^+. Possibly, the selectivity was lost during the isolation or reconstitution process. Palmer and co-workers (1990) isolated mRNA from A6 cells, grown on impermeable dishes, which induced the expression of high selectivity channels in *Xenopus* oocytes. From these results, we presume that the same message could induce both low selectivity channels in the A6 cells grown on permeable supports and high selectivity channels in the oocyte.

The regulation of these moderately selective, amiloride-sensitive channels has been extensively studied by Cantiello and co-workers (1989 & 1990). In excised membrane patches this type of channel can be activated by the addition of a G protein to the cytoplasmic side of the membrane. In addition, arachidonic acid and its metabolites can also affect channel activity through a mechanism involving the G proteins. Garty *et al.* (1989) reported that G proteins might similarly be involved with high selectivity Na^+ channels. They demonstrated that GTPγS can activate G proteins, and also increase sodium fluxes in apical membrane vesicles from the toad bladder epithelia. However, there is no known evidence to show that the major hormonal regulators of

Na^+ channels, namely aldosterone and antidiuretic hormone (ADH), can affect the activity of moderate sodium-selectivity and higher conductance channels.

2.4.1.3 Non-sodium-selective channels

There is a third type of Na^+-permeable channel that shows a lack of selectivity between Na^+ and K^+, and has a large single channel conductance. This type of channel was found in the apical membrane of the inner medullary collecting duct (IMCD). The ionic selectivity (Na^+: K^+) was about 1.0, and the single channel conductance under physiological conditions was 28 pS (Light *et al.*, 1988). The amiloride sensitivity of this channel also differs from that of other types of Na^+ channels, especially with regard to the voltage dependence of blocking. In the 28 pS Na^+ channels, the sensitivity to voltage was much higher than in other amiloride-sensitive channels. This might be the result of a voltage-dependent conformational change in the protein that alters the affinity for amiloride. Although single channel events were not recorded in this study, recent reports indicate that amiloride can block stretch-activated, non-selective cation channels in the *Xenopus* oocyte (Lane *et al.*, 1990; Lane *et al.*, 1991). These non-sodium-selective channels have various degrees of amiloride sensitivity, and are also present in chick hair cells (Jorgensen and Ohmori, 1988), brain vascular endothelial cells (Vigne *et al.*, 1989), olfactory cells (Frings, and Lindemann, 1988) and many other types of cells (Morris, 1990; French, 1992). In brain vascular endothelial cells, there is a 23 pS non-selective cation channel (Vigne *et al.*, 1989) similar to the 28 pS channels in the inner medullary collecting duct (IMCD) (Light *et al.*, 1988). The sensitivity of the 28 pS channels to amiloride was about 10 μM.

Since 1989, the regulation of non-sodium-selective channels by cGMP-mediated effects has been broadly studied by Stanton and co-workers in rat renal inner

medullary collecting duct cells. They found that in the IMCD cells, channel activity is regulated by the atrial natriuretic peptide (Light *et al.*, 1989a). This hormone leads to a decrease in the open probability of this non-selective channel. The atrial natriuretic peptide hormone also promotes sodium excretion by the kidney through several different mechanisms, including renal vascular effects, which lead to an increase in the glomerular filtration rate, and the inhibition of aldosterone secretion by the adrenal cortex (Maack *et al.*, 1985). All of the biological effects of the atrial natriuretic factor (ANF) are thought to be mediated by increases in cGMP. In this regard, cGMP reduced the channel activity in excised patches, and G protein α_i-3 was shown to activate the channels directly in cell-attached patches (Light *et al.*, 1989b). However, in the toad urinary bladder, ANF did not affect Na^+ transport, but cGMP stimulated the short-circuit current and increased the apical membrane Na^+ permeability (Das *et al.*, 1991). In the rat cortical collecting tubule, ANF decreased Na^+ reabsorption, but this effect was mediated by a NaCl cotransporter in the apical membrane and not the Na^+ channel (Noniguchi *et al.*, 1989). Significantly, the highly selective Na^+ channels are not affected by ANF regulatory system (Palmer, 1992).

2.4.2 Structure of the epithelial Na^+ channel

The following sections will focus only on the highly selective and low conductance Na^+ channels of renal tight epithelial cells. Molecular studies have contributed immensely to the understanding of the actual structure and function of Na^+ channels in tight epithelia. The difficulties in isolating the epithelial Na^+ channel can be understood when it is realised how small an amount of this protein is present in the membrane. Mainly two laboratories have succeeded in purifying and reconstituting the putative amiloride-sensitive Na^+ channels.

Benos and colleagues first purified high amiloride-sensitive Na^+ channels from bovine renal papilla and from an amphibian kidney cell line, the A6 cells (Benos *et al.*, 1986; Sariban-Sohraby and Benos, 1986b; Benos *et al.*, 1987). Consequently, the Na^+ channels derived from the amphibian kidney and the mammalian kidney appear to share similar biochemical structures as well as single-channel characteristics when incorporated into planar lipid bilayers. This implies a conservation of the amiloride-sensitive Na^+ channel among species (Oh and Benos, 1993).

Conventional biochemical purification techniques and size exclusion high pressure liquid chromatography (HPLC) revealed a single peak of molecular mass of 730 kilodaltons (kD). The reduction and denaturation of the native channel by means of sodium-dodecyl sulphate polyacrylamide gel electrophoresis (SDS/PAGE) results in the protein being resolved into five major polypeptides with average molecular mass values of 315, 149, 95, 71, and 55 kD. A few minor polypeptides with molecular weights ranging from 30 to 45 kD were often noted (Benos *et al.*, 1987). Recently, Kleyman *et al.* (1991) developed an antiidiotypic monoclonal antibody that mimics the inhibitory effect of amiloride on Na^+ transport in A6 cells after they have been treated with trypsin, which makes the amiloride-binding site accessible to the antibody. This monoclonal antibody also immunoprecipitated a 700 to 750 kD protein from A6 cells, which seemed to be the same as that identified by Benos *et al.* (1987) and Sorscher *et al.* (1988). Kleyman *et al.* (1991) found four or five subunits with molecular weights of 230 to 260, 180, 110 to 140, 70 and 50 kD, but 50 kD subunit was only occasionally present.

There are several studies which have identified the subunits of the epithelial Na^+ channel protein to which amiloride also binds. Benos *et al.* (1987) demonstrated that the 150 kD subunit distinctively photoincorporated [^{3}H]methylbromoamiloride, a high photoactive amiloride analogue which is thought to include an amiloride binding site.

Thus, Kleyman *et al.* (1986) found that [^{3}H]bromobenzamil, another high affinity analogue of amiloride, convalently incorporates three polypeptides of bovine kidney cortex membrane preparations with molecular masses of 176, 77 and 46 kD. Considering the variation of molecular weight due to various degrees of glycosylation, these subunits could be analogous to the 150-, 70- and 41- kD peptides reported by Benos *et al.* (1987). Kleyman *et al.* (1989) have shown that the amiloride irreversible analogue, 9-2'-methoxy-5'nitrobenzamil (NMBA), binds to the 130 to 150 kD polypeptide. Lately, Kleyman *et al.* (1991) used an antiidiotypic monoclonal antibody to identify the amiloride-binding site of channel subunits. This antibody could recognise the 140 kD subunit, which also corresponds the 150 kD subunit of Benos *et al.* (1987) and Sorscher *et al.* (1988).

Other methods of purification of a [^{3}H]phenamil binding protein from pig kidney outer medulla and cortex were reported by Barbry *et al.* (1987 & 1990). They found that in this tissue the protein had a total molecular mass of 185 kD and consisted of two nearly identical 90 to 105 kD polypeptides crosslinked by disulfide bonds. At present, it is not known whether these two purified putative Na^+ channel proteins are related to each other. This 185 kD protein called amiloride binding protein (ABP), which incorporates [^{3}H]bromobenzamil, mediates an amiloride-sensitive Na^+ channel in the phosphatidylcholine vesicles (Barbry *et al.*, 1990). Recently, it was demonstrated with the patch clamp technique, that the mean single-channel conductance of the 150 kD subunit was 8 pS when reconstituted into liposomes. This is similar to the mean conductance (10 pS) measured for solubilised apical membranes from A6 cultured cells incorporated into liposomes. Accordingly, it is assumed that the 150 kD subunit is capable of conducting Na^+ in the absence of the other subunit components of the channel (Sariban-Sohraby and Fisher, 1992).

In A6 cells that were treated with pertussis toxin, transepithelial Na^+ transport was inhibited (Cantiello *et al.*, 1989). Subunits of 41 and 95 kD isolated from bovine renal papilla and A6 cells have been shown to be ADP-ribosylated by pertussis toxin, a compound which specifically prevents activation of the guanine nucleotide-binding regulatory protein (G protein), thus suggesting that these subunits are actually G protein (Ausiello *et al.*, 1989). To show this, the 41 kD subunit was labelled by an antibody raised against the α-subunit of the G_{i-3} protein. The α_{i-3} subunit was localised by confocal imaging, and was found to be concentrated in a domain in the apical membrane adjacent to the Na^+ channel in A6 cells, also this $G\alpha_{i-3}$ was part of the protein complex purified on an immunoaffinity column using antibodies that recognize the 320-, 150- and 95- kD subunits. The functional significance of this localization is supported by the demonstration that α_{i-3} regulates Na^+ channel activity as assessed by the patch clamp technique, thus indicating that the 41-kD $G\alpha_{i-3}$ can be totally associated with the Na^+ channel regulation in the apical membrane (Ausiello *et al.*, 1992).

It is suggested that aldosterone stimulates effector proteins which activate quiescent channels in the toad urinary bladder (Asher and Garty, 1988). The 70 kD subunit is induced by aldosterone that functions as an effector protein. This aldosterone-induced protein shows cross-reactivity with the 70 kD subunit of the purified bovine Na^+ channel protein in Western blots, and that indicates that the Na^+ channels may also be regulated by aldosterone directly (Szerlip *et al.*, 1989).

2.4.3 Immunocytochemical localization of the amiloride-sensitive Na^+ channels

Most Na^+-reabsorbing epithelia contain amiloride-sensitive Na^+-specific channels situated within their plasma membranes. Antibodies were made from the purified

amiloride-sensitive Na^+ channel isolated from the bovine renal papillary collecting duct (Sorscher *et al.*, 1988). Results from immunocytochemical experiments using this antibody verified that Na^+ channels are predominantly localised in the apical microvilli, with little or no labelling on the basolateral membrane of the renal papillary collecting duct cells (Brown *et al.*, 1989; Tousson *et al.*, 1989) and A6 epithelial cells (Tousson *et al.*, 1989; Kleyman *et al.*, 1991). These studies used anti-amiloride-sensitive Na^+ channel antibodies to identify Na^+ channels with either the light microscopic (L.M.) technique of indirect immunofluorescence, or the electron microscopic (E.M.) method of immunogold labelling. Tousson *et al.* (1989) reported that the Na^+ channel protein is localised in the apical membrane of bovine renal papillary collecting tubules and A6 cells in thick frozen sections, and no appreciable basolateral staining was evident. They further found no evidence for any cytoplasmic pools of Na^+ channel protein when using E.M. or confocal imagine analysis techniques. Therefore, they concluded that the Na^+ channel protein is always present at the cell surface. Kleyman *et al.* (1991) used the antiidiotypic monoclonal antibody (RA6.3), which is directed against the amiloride-binding subunit on the channel protein, to localise the Na^+ channels in semi-thin frozen sections of A6 cells. The results from these experiments showed that the apical membrane is stained by immunofluorescence and it correlates with the physiological data showing the presence of Na^+ channels in the apical membrane domain (Perkins and Handler, 1981). Immunocytochemical localisation also revealed that the RA6.3 antibody bound to the subapical cytoplasmic vesicles (Kleyman *et al.*, 1991). This evidence is consistent with the presence of a cytosolic Na^+ channel pool which possibly is recruited to the apical membrane in a regulatory mechanism (Garty and Edelman, 1983; Asher and Garty, 1988). Kleyman *et al.* (1991) observed imunoreactivity in the deeper regions of the cytoplasm where it was seen at or near the basolateral membrane region of A6 cell

monolayers. These authors could not rule out the presence of immunoreactivity at the basolateral membrane.

Recent work from the laboratory of Benos has shown that the amiloride-sensitive Na^+ channel is linked to the apical cytoskeleton of the microvilli through ankyrin in the A6 cells (Smith *et al.*, 1991). Electron microscopy of A6 cells after treatment with the detergent 0.5% Triton X-100 reveals that the Na^+ channels in the apical membrane are associated with the detergent-insoluble cytoskeleton. Indirect immunofluorescence and confocal microscopy demonstrate that Na^+ channels are predominantly localised to the apical microvillar membrane, and co-localised with ankyrin, fodrin, and actin (Smith *et al.*, 1991). Benos' laboratory also used immunoblot analysis to show that ankyrin, fodrin and actin remain associated with Na^+ channels after isolation and purification from bovine renal papillae. This suggests that the channel may be linked to actin via ankyrin and fodrin; in addition, direct binding of ^{125}I-labelled ankyrin reveals that ankyrin binds to the 150 kD subunit of the Na^+ channel (Smith *et al.*, 1991). Immunocolocalisation of Na^+ channels using specific anti-channel protein to localise the Na^+ channels, and fluorescein isothiocyanate (FITC)-phalloidin to label the F-actin cytoskeleton, indicates that actin is always present in close proximity to apical Na^+ channels in A6 cells (Cantiello *et al.*, 1991).

2.5 Regulation of Amiloride-Sensitive Na^+ Channels

Regulation of the rate of Na^+ entry through Na^+-selective channels in apical membranes of Na^+-reabsorbing epithelia is important in the control of sodium homeostasis. Not surprisingly, apical membrane Na^+ permeability is critically regulated by intrinsic (homocellular or autoregulatory) and extrinsic mechanisms. Extrinsic mechanisms are mediated by factors such as neural and hormonal influences (Reviewed by Wills and Zweifach, 1987; Els and Helman, 1989; Smith and Benos,

1991). Intrinsic or autoregulatory mechanisms are important for primary cell functions like the regulation of intracellular ionic composition (Schultz, 1985). The intrinsic regulation of Na^+ channels is governed, amongst others, by various luminal factors including changes in the composition of the extracellular fluid, in cell volume, in cell metabolism or, in Na^+ transport load (Zeiske and Van Driessche, 1984; Sariban-Sohraby and Benos, 1986; Els and Chou, 1993).

2.5.1 Properties determining transcellular Na^+ permeability

The permeability of the apical membrane to Na^+ is altered by regulating the properties of the Na^+ channels. Regulation of membrane permeability can be achieved in three ways: firstly, by altering the number of Na^+ conducting channels, i.e. open channel density (N_O); secondly, by changing the open probability or the duration that the channel remains open (P_o); or finally, by altering the single channel conductance (g_{Na}). These properties can be represented by the equation: $P_m \equiv N_O \times P_o \times i_{Na}$, where P_m is the apical membrane permeability, and i_{Na} is the single channel current which is related to the single channel conductance by $g_{Na} = i_{Na} (V_m - E_{Na})$. V_m is the potential difference across the membrane, E_{Na} is the equilibrium potential for the Na^+, and $(V_m - E_{Na})$ can be considered as the driving force experienced by the Na^+ ions. In theory, varying any one or a combination of these variables could provide a mechanism for regulating total apical sodium flux. Modern electrophysiological techniques cater for the measurement of all these properties and provide information about the possible molecular mechanisms underlying the regulation of Na^+ transport.

2.5.2 Regulation of Na^+ channels by luminal factors

2.5.2.1 Inhibition of sodium transport by extracellular sodium

The concentration of Na^+ in the extracellular fluid is an important regulator of Na^+ reabsorption. In many tight epithelia, such as frog skin (Fuchs *et al.*, 1977), toad urinary bladder (Palmer *et al.*, 1982), rabbit descending colon (Turnheim *et al.*, 1983), and *Necturus* urinary bladder (Thomas *et al.*, 1983), there is an inverse relationship between the luminal Na^+ concentrations and apical Na^+ permeability. However, increasing the luminal Na^+ concentrations is associated with an increase in the level of Na^+ activity in the cell, but it is still unclear whether the apical membrane Na^+ permeability is decreased by the increasing luminal Na^+ concentrations, or by the increasing of Na^+ activity in the cell. In a study on frog skin, Fuchs *et al.* (1977) showed that there were small changes to the Na^+ activity in the cell after exposure to changes in external Na^+ concentrations ranging from 0 to 60 mM. By using a fast-flow perfusion chamber that permits a very rapid change of the luminal bathing solution, they demonstrated that increasing the luminal Na^+ concentrations caused a fast rise of I_{SC}, followed by a slow decrease to a lower steady-state current. Because the intracellular Na^+ activity remained almost unchanged under the different luminal Na^+ concentrations, it is reasonable, therefore, to conclude that the increasing luminal Na^+ concentrations exert an inhibitory effect on apical membrane Na^+ permeability. This effect was termed "Na^+ self-inhibition".

By using current fluctuation analysis, at various external Na^+ concentrations on frog skin, Van Driessche and Lindemann (1979) have provided evidence that the inhibition of apical membrane Na^+ permeability is due to a decrease in the number of conducting or open Na^+ channels (N_O) per unit of the epithelial surface area, and not to a change in the single-channel current. A similar conclusion was reached in studies of the rabbit

urinary bladder (Lewis *et al.*, 1984), but not all data is consistent with this idea. Patch-clamp studies on vesicles in planar lipid bilayers (Olans *et al.*, 1984) and rat cortical collecting tubules (Palmer and Frindt, 1986b; Palmer and Frindt, 1988) have shown that the conductance of single amiloride-sensitive Na^+ channels saturates with increasing the mucosal Na^+ concentrations. These authors failed to observe any change in the number of active channels in response to an increase in mucosal Na^+ concentrations. This observation was not consistent with the hypothesis that increasing the mucosal Na^+ concentrations decreased the number of conducting Na^+ channels. Furthermore, in patch clamp studies of apical Na^+ channels from rat cortical collecting tubules by increasing Na^+ concentrations, it was found out the open probability (P_o) of the Na^+ channels was independent (Palmer and Frindt, 1988). Recently, Ling and Eaton (1989) demonstrated that a reduction of the external Na^+ concentration results in an increase in the channel activity (open channel probability and the number of open channels) in a single patch on the A6 cells.

The reasons for the different findings in noise analysis and patch clamp studies, are not clear. In a review, Garty and Benos (1988) explained that the apparent lack of evidence of single-channel current saturation in the noise analysis of frog skin, was due to the fact that these experiments were carried out on tissues depolarised by a high-K^+ solution on the serosal side (Van Driessche and Lindemann, 1979). When Hoshiko and Van Driessche (1986) performed noise analysis on non-depolarised frog skin, they found saturation of the single-channel Na^+ current. It is interesting that Lewis *et al.* (1984) showed no evidence of saturation of single-channel Na^+ current in the noise analysis of non-depolarised rabbit urinary bladder. Turnheim (1991) concluded that the differences between the results needed to be clarified, i.e. whether the differences could be attributed to the different species used, the various experimental conditions, or the dissimilar techniques employed.

Abramcheck *et al.* (1985) made use of the current fluctuation analysis technique to study the effects of reducing the rate of Na^+ entry with Na^+ channel blockers. They observed that as Na^+ transport decreased (inhibition of I_{SC}) by addition of amiloride, or its weak amiloride-like Na^+ channel inhibitor CGS 4270, the total number of channels increased in the apical membrane of frog skin. This process was originally referred to as autoregulation by the authors. Initial observations indicated that low concentrations of amiloride or certain amiloride analogues were able to stimulate transepithelial Na^+ transport (Thurman and Higgins, 1982). Subsequently, it was shown that a large increase in the open channel density followed either a reduction in the Na^+ concentration, or an addition of amiloride to the apical (luminal) solution (Helman and Baxendale, 1990; Els and Helman, 1991; Frindt *et al.*, 1993). Ling and Eaton (1989) when examining the same phenomenon with patch clamp, applied 10 μM amiloride to the bathing solution outside the recording pipette on an A6 cell patch, they also found that the open probability of single Na^+ channels increased significantly and functional channel density also increased.

We preferred to use the term autoregulation in this study to indicate regulatory changes in channel densities and open probability in response to any decrease in the rate of Na^+ entry viz. blockers or decrease in Na^+ concentration. It was mainly these discrepancies that motivated us to investigate, with noise analysis, the effects of lowering the mucosal Na^+ concentrations on the autoregulation of Na^+ channels in apical membrane of isolated frog skin epithelium. We performed noise analysis with the relatively weak electroneutral Na^+ channel blocker CDPC which provided excellent noise signals at concentrations in a range well below its equilibrium blocker coefficient K_B (Helman and Baxendale, 1990), allowing analysis on tissues transporting Na^+ near their spontaneous rates. Our results with noise analysis (Els and Chou, 1993) confirmed a recent finding by Ling and Eaton (1989) with patch clamp that a reduction in mucosal

Na^+ causes an increase in channel open probability. Also we resolved that increases in open channel density were brought about by increases in the number of total channels.

2.5.2.2 Inhibition of sodium transport by intracellular sodium

Whether changes in extracellular Na^+ concentrations directly effect apical membrane permeability or via changes in intracellular Na^+ concentrations, is not known. Despite this, it is well-known that strategies which cause changes to the intracellular Na^+ concentration will have major effects on apical membrane Na^+ permeability. Thus, inhibition of the basolateral Na^+ pump might increase the intracellular Na^+ concentration. When the Na^+ concentration in the cell is increased, the amount of apical Na^+ entry will be decreased, mainly because the driving force for sodium entry is reduced. This phenomenon is named "feedback inhibition".

Several methods have been used to express feedback inhibition by preventing basolateral Na^+ extrusion causing a decrease in apical Na^+ entry, viz. using Na^+ tracer fluxes (Stoddard and Helman, 1985), electron-microprobe analysis (Sauer *et al.*, 1989), the constant-field equation (Palmer, 1982b), and Na^+-selective intracellular microelectrodes (Helman *et al.*, 1979; Harvey and Kernan, 1984). Most of these methods deal with either the deletion of K^+ from the serosal solution, or the addition of ouabain (the cardiac glycoside) to block the Na^+-K^+ pumps in the basolateral membrane. An increase of the Na^+ concentration in the cell resulted in a decrease in apical membrane Na^+ conductance (Turnheim *et al.*, 1978), and also a decrease in overall membrane conductance (Helman *et al.*, 1979; Lewis *et al.*, 1976; Palmer *et al.*, 1980).

Regarding the mechanism of action, using current fluctuation analysis on frog skin, Van Driessche and Erlij (1983) have reported that an increase of the Na^+ channel density in the apical membrane was a secondary effect due to the increase of the

intracellular Na^+ concentration caused by ouabain. Although relatively invariant intracellular Na^+ concentration appears advantageous for cell homeostasis, the question arises as to how the basolateral Na^+-K^+ pumps are activated under conditions of increased transepithelial Na^+ transport when intracellular Na^+ concentration remains constant (Schultz, 1981&1989). The membrane coupling between the basolateral Na^+ extrusion and the apical Na^+ entry may also be responsible for the autoregulatory mechanism of Na^+ channels.

2.5.2.3 Inhibition of sodium transport by luminal proteolysis

Serine proteases include trypsin, urokinase, and kallikrein. These enzymes were reported to block the amiloride-sensitive Na^+ flux when added to the luminal solution of an epithelium (Garty and Edelman, 1983; Lewis and Hanrahan, 1985; Lewis and Alles, 1986). Urokinase and kallikrein are released into the urine by nephron segments proximal to the cortical collecting ducts, and can be found in mammalian and amphibian urine. These two enzymes may be responsible for the enzymatic degradation of amiloride-sensitive Na^+ channels to amiloride-insensitive leak pathways, since urokinase and kallikrein were shown to irreversibly inhibit amiloride-sensitive Na^+ transport in the rabbit urinary bladder (Lewis and Alles, 1986). Interestingly, the presence of amiloride will protect the channels from proteolytic cleavage by these enzymes. It is possible that enzymes, urokinase and kallikrein, alter the channel proteins by proteolysis and thus play a role in the physiologic regulation of Na^+ transport. Lewis and Alles (1986) have demonstrated that the loss of Na^+ channels into the urine is dependent on the urinary concentration of kallikrein, which is stimulated by corticoid hormones such as aldosterone. Aldosterone, which increases kallikrein activity in urine, also causes an increase in the number of active channels in the apical membrane (Lewis and Alles, 1986). Kallikrein terminates the

aldosterone-induced increase in the apical membrane Na^+ permeability, under physiological conditions.

2.5.2.4 Osmotic effects on sodium transport

Several investigators have demonstrated that changes in cell volume, produced by anisotonic bathing solutions or by passing an electrical current across the tissue, lead to parallel changes in Na^+ transport in frog skin and in the toad urinary bladder (Lipton, 1972; Ussing, 1982; Zeiske and Van Driessche, 1984). In all studies, a decrease in the osmolarity of the bathing solution increased the short-circuit current (I_{SC}), whereas, hyper-osmotic solutions depressed it. From current fluctuation analysis of the effects of mucosal hypertonicity on Na^+ channels in frog skin, Zeiske and Van Driessche (1984) found that the decline in Na^+ transport when cell volume decreased, caused a decrease in both apical membrane Na^+ channel density and in single-channel current. Although the mechanisms of how cell swelling increases apical Na^+ transport, and how cell shrinkage affects the membrane permeability, are not totally clarified, the possible mechanisms in modulating Na^+ transport was proposed by Lewis and de Moura (1982). These authors found that reducing the mucosal osmolarity of the rabbit urinary bladder increases the epithelial membrane capacitance. Probably the stretch process leads to expansion of the apical cell membrane by fusion of cytoplasmic vesicles that contain Na^+ channels. This process causes a reversible increase in the apical membrane area and apparently requires intact microfilaments, since the membrane expansion process was completely blocked by a microfilament disrupting drug cytochalasin B. "Punching", the exposure of an isolated rabbit urinary bladder to rapid and repeated changes of apical hydrostatic pressure by filling and emptying the luminal compartment, stimulated amiloride-sensitive Na^+ transport without changes in membrane capacitance, and was blocked by cytochalasin B (Lewis and de Moura, 1982). This process produced a more than ten fold increase in amiloride-sensitive Na^+

channel density (Loo *et al.*, 1983). This finding supports the postulation that during the pressure pulses, Na^+ channels are stored in cytoplasmic vesicles underneath the apical membrane. In a study on a rabbit urinary bladder done by current fluctuation analysis, Lewis *et al.* (1984) showed that the punching process similarly increased the density of amiloride-sensitive Na^+ channels but not the single-channel current. These authors also showed that after the punching process there was a big decrease in the amiloride-insensitive current (leak pathway) across the rabbit urinary bladder epithelium. This amiloride-insensitive current was also reduced by the repeated washing of the apical surface of the bladder epithelium with Ringer solution. It is likely that washing removed the leak protein itself. It has been suggested that the leak pathway may arise by degradation of the amiloride-sensitive Na^+ channels.

The study of the effects of osmolarity on Na^+ transport seems very relevant particularly in the field of cultured cells. Wills *et al.* (1991) showed that Na^+ channels are highly sensitive to small osmolarity changes in the serosal solution on A6 cells. These investigators performed experiments on A6 cells which were perfused with hypo-, iso-, and hyper-osmotic solutions. The I_{SC} was 25 ± 2.9, 2.3 ± 0.4, and 0.6 ± 0.5 $\mu A/cm^2$ for the respective solutions. From these results, we can see the I_{SC} of those cells in the hypo-osmotic solutions are 10 times greater than those in iso-osmotic solutions. The number of open channels was 3 times larger in the hypo-osmotic solutions than in the iso-osmotic solutions. They also reported no changes in the blocker binding kinetics, which ruled out the possibility that two channels being involved. These results are very important beacuse during conditions of plasma hypo-osmolarity, salt absorption should increase; and during plasma hyper-osmolarity (dehydration), salt absorption should decrease (Wills *et al.*, 1991).

2.5.3 Regulation of amiloride-sensitive Na^+ channels by hormones

Sodium transport across tight epithelia is controlled by several hormones, the major ones being the anti-diuretic hormone (ADH) or vasopressin, and the mineralocorticoid aldosterone. Hormonal regulation of Na^+ permeability is of great significance to physiology and is of special interest to our studies. The pathways through which the hormones act to regulate the channels are complicated and involve complex kinetics. The interactions between the different regulatory and signalling pathways are not understood and makes the analysis of data difficult and is often speculative. Much more biochemical information, consistent with physiological studies are needed.

2.5.3.1 Regulation of sodium channels by aldosterone

Aldosterone is a mineralocorticosteroid hormone which has been regarded as the primary hormone regulating cation transport in the CCD, the colon, frog skin, toad urinary bladder and A6 cells (Schwartz and Burg, 1978; Garty, 1986; Garty and Benos, 1988; Kemendy *et al.*, 1992) and in tight epithelia in general. In the mammalian kidney aldosterone acts primarily on the CCD; it increases Na^+ reabsorption and K^+ secretion (Schwartz and Burg, 1978). Aldosterone, being a steroidal hormone, is lipophilic and, therefore, able to diffuse through the cell membrane and bind with cytoplasmic receptors. These receptor-steroidal hormone complexes then migrate to the nucleus where they bind to nuclear receptors on genomic DNA and promote the transcription of specific mRNA that is translated into proteins (Edelman, 1981; Darnell *et al.*, 1990). These aldosterone induced proteins (AIPs) can increase the apical membrane permeability, or basolateral membrane Na^+-K^+ ATPase activity eliciting a rise in Na^+ transport (Verrey *et al.*, 1987). Although the rate-limiting step in Na^+ transport is the apical membrane's Na^+ permeability, the increase in the I_{SC}, with additional exogenous aldosterone, is

generally accompanied by a surprisingly small elevation in Na^+ concentration in the cell (Eaton, 1981). This indicates that Na^+ permeability changes might directly increase Na^+-K^+ pump activity (Handler *et al.*, 1972; Rick *et al.*, 1988).

The time course of the transport events, when aldosterone is added to the toad urinary bladder, consists of three stages: (a) a latent period of ~ 45 min after the aldosterone is added but before the I_{SC} begins to increase; (b) an early response of 3-6 hr in which there is a two - fourfold increase in I_{SC} after the aldosterone is added, the increase in I_{SC} being accompanied by a decrease in transepithelial resistance which raises Na^+ permeability of the apical membrane (Spooner and Edelman, 1975); and (c) a longer response (> 6 hr up to 24 hr) in which there is a continuous increase in I_{SC}, probably because of the synthesis of Na^+-K^+-ATPase. The initial event in Na^+ transport is an increase in the amiloride-sensitive Na^+ conductance of the apical membrane, which allows increased Na^+ entry to the cell down its electrochemical potential gradient; and then there is an increase in both the α and β subunits of the Na^+-K^+-ATPase synthesis resulting in increased pump activity in the basolateral membrane (Verrey *et al.*, 1987; Rossier *et al.*, 1989), and hence an elevated Na^+ transport rate.

Several studies have shown that the initial effect of aldosterone in the toad urinary bladder is fully accounted for by an increase in the apical membrane Na^+ permeability. Using current fluctuation analysis of the toad bladder, Palmer *et al.* (1982) showed that aldosterone increases the density of open channels, while the single-channel current is unchanged. Garty and Edelman (1983) reported that the aldosterone-related increase in density of the open channels is not due to the insertion of new channels in the apical membrane, but rather to an activation of quiescent channels already present in the apical membrane. This was shown by experiments in which the effect of aldosterone on membranes pre-treated by trypsinization was monitored. However, by using a photoactive, high affinity ligand and anti-ligand antibodies to identify polypeptide

subunits of the epithelial Na^+ channel and using these tools to examine the cellular pool of Na^+ channels in A6 cells, Kleyman *et al.* (1989) found that activation of Na^+ transport by aldosterone was not accompanied by a change in the biochemical pool of channels and no change in the distribution of immunoreactive proteins was observed with the aid of immunofluorescent microscopy. Later findings were consistent with this conclusion. Kemendy *et al.* (1992) used the patch clamp technique to demonstrate that aldosterone increases the open probability of Na^+ channels in A6 cells and does not cause a change in the channel density. The mechanism by which aldosterone activates Na^+ channels remains unknown. The current evidence seems to suggest that aldosterone acts by increasing open probability and/or channel density. There is evidence to suggest that the activation may be associated with methylation of specific proteins within inactive channels in the apical membrane. Sariban-Sohraby *et al.* (1984a) have shown that incubation of membrane vesicles from A6 cells with a methyl donor, results in augmentation of Na^+ transport associated with an increased incorporation of methyl groups into membrane proteins. Wiesmann *et al.* (1985) reported that aldosterone might induce a specific methyltransferase by acting on cytoplasmic enzymes, since blockers of methylation (such as the methyltransferase blocker, 3-deaza-adenosine), block the increase in I_{SC} produced by aldosterone. Of late, a two step model for the mechanisms involved in the stimulation of Na^+ transport by aldosterone has become popular. The two steps are separated into an short-term and a late response. The short-term response is that seen after exposure of tissue to aldosterone for less than 4 hours; the late response is categorised as the response after 24 hours exposure to the aldosterone. It is suggested that the short-term response involves the stimulation of channels already residing in the membrane by AIPs , through methylation, phosphorylation or glycosylation. It is proposed that the late response involves the insertion of newly synthesised channels into the membrane

thereby increasing its conductance to Na^+ ions (Garty, 1986; Minuth *et al.*, 1987; Wills *et al.*, 1991; reviews by Schafer and Hawk, 1992; Bastl and Hayslett, 1992).

2.5.3.2 Regulation of sodium channels by the antidiuretic hormone (ADH)

In many epithelia, Na^+ channels are also regulated by the antidiuretic hormone (ADH) [arginine vasopressin (AVP)]. AVP is a water soluble hormone, and thus interacts with cell surface receptors. AVP receptors have been localised in the basolateral surface of the collecting tubule and collecting duct, in man and rat (Cort *et al.*, 1975). AVP is known to bind to two types of receptors (type I and type II) which are involved with the mechanisms which induce changes in water permeability, and sodium uptake respectively (Ausiello *et al.*, 1987; Els and Helman, 1989). Once the binding of AVP to its receptor has occurred, the subsequent steps include (1) the activation of adenylate cyclase, (2) the adenylate cyclase-induced formation of cyclic adenosine monophosphate (cAMP), and (3) the cAMP-induced activation of protein kinase A (PKA). Earlier Els and Mahlangu (1987) demonstrated that cAMP is a major second messenger in control of Na^+ reabsorption in frog skin.

The mechanism by which AVP brings about the activation of the adenylate cyclase system involves several steps. Firstly, AVP binds to the receptors on the cell membrane which then undergo a conformational change. This conformational change allows coupling of the receptor to an α guanine nucleotide-binding regulatory protein (G protein). The G protein is a peripheral membrane protein comprising 3 subunits, α, β and γ, in close proximity to the hormone receptor. The G protein in the resting stage has guanosine-diphosphate (GDP) bound to the α-subunit. The activated receptor causes the G protein to release GDP and bind guanosine triphosphate (GTP). The G protein α-subunit ($G\alpha$-GTP) then dissociates from the G protein $\beta\gamma$ subunit complex ($G\beta\gamma$) and binds to adenylate cyclase thus activating it. Activated adenylate cyclase

then catalyses the conversion of cAMP from adenosine triphosphate (ATP). This step may cause a conformational change in Gα-GTP that results in its dissociation from adenylate cyclase. Hydrolysis of GTP to GDP prevents further activation of adenylate cyclase (probably catalysed by Gα itself), and Gα and Gβγ reassociate. The net result is an increase in the intracellular second messenger, cAMP, which has been correlated with an increase in Na^+ transport in the toad bladder (Orloff and Handler, 1962; Omachi *et al.*, 1974) and frog skin (Els and Helman, 1991).

All G proteins are known as signal-coupling proteins. G proteins that stimulate a second messenger-generating enzyme, such as adenylate cyclase, are called stimulatory G proteins (G_s); G proteins that inhibit a second messenger-generating enzyme are called inhibitory G proteins (G_i). The role of G protein in the regulation of epithelial Na^+ channels was first suggested by Mohrmann *et al.* (1987). Pertussis toxin, a compound that prevents receptor-dependent activation of G_i and G_s was shown to reduce Na^+ transport in LLC-PK_1 and A6 cells. Subsequently, using membrane vesicles derived from toad bladder cells, Garty *et al.* (1989) demonstrated that GTPγs can stimulate amiloride-blocked Na^+ transport across the vesicles, whereas GDPβs can reverse the effect, thereby providing further evidence for the role of G proteins in regulating amiloride-sensitive Na^+ channels. More recently, it has been demonstrated that Gαi directly activates an amiloride-sensitive, non-selective cation channel in renal medullary collecting duct cells, and an amiloride-sensitive Na^+ selective channel in A6 cells. Further evidence supporting the role of G proteins in the regulation of epithelial Na^+ channels reveals that 40 and 95 kD subunits of the Na^+ channel may be G proteins. A recent proposal suggests that ion channels are direct G protein effectors (Brown, 1991).

Using fluctuation analysis, various authors have consistently shown that AVP, or any procedure which increases intracellular cAMP levels, increases Na^+ permeability by

increasing the Na^+ channel density (N_T), with little or no change in single-channel conductance and in channel open probability (Li *et al.*, 1982; Helman *et al.*, 1983; Krattenmacher *et al.*, 1988; Els and Helman, 1991). Similarly, using the patch clamp technique on A6 cells, Marunaka and Eaton (1991) confirmed that AVP causes an increase in the number of active Na^+ channels in patches of the apical membrane (increasing from 2 to 6 channels in each patch after AVP treatment), without changing the open probability of individual channels (~0.4). Els and Helman (1991) also reported that AVP increases apical conductance by inducing large increases in open channel density which could be referred to a significant increase in the Na^+ channel density in the apical membrane of frog skin epithelium, and not to changes of open channel probability. Although its effect on the I_{SC} is often transitory, exogenous AVP, cAMP and other cAMP activators induce the maximum natriuretic effect within 5 to 20 min after stimulation, thereby indicating that these changes in channel density do not arise as a result of protein synthesis. We now know that the response of AVP on the tissues is quite complicated and important, since AVP causes large changes in N_O and N_T. This was the reason for investigating AVP effects in our study.

The origin of these channels has frustrated researchers for many years. Two main theories have been put forward to explain the mechanism whereby hormones may induce an increase in the Na^+ channel density. On stimulation, quiescent channels already present in the membrane may be activated or alternatively, channels may be recruited from subapical stores and inserted into apical membranes of epithelial cells (Li *et al.*, 1982; Garty and Edelman, 1983; Lewis and de Moura, 1984).

Regarding the activation of quiescent channels already present in the membrane, Frings *et al.* (1988) demonstrated with patch clamp on toad urinary bladder luminal membrane that the addition of protein kinase A, cAMP and ATP to an excised patch could activate quiescent channels, but this effect was observed in only three of nine

experiments. Lester *et al.* (1988) showed that reconstituted Na^+ channel-containing vesicles could not be activated directly by cAMP or cAMP-dependent protein kinase. These observations indicate that neither cAMP nor cAMP-dependent protein kinase appear to have a direct effect on the kinetics of Na^+ uptake. Therefore, they suggested that cAMP may phosphorylate a mediator protein, that will activate channels in the membrane, or cause the insertion of new channels. Sariban-Sohraby *et al.* (1988) reported that a cAMP-dependent kinase A directly phosphorylated the 315 kD subunit of the Na^+ channel both *in vivo* and *in vitro*. This observation implies that one action of AVP is to stimulate PKA to phosphorylate Na^+ channels. Ordinarily, the phosphorylation of membrane channel proteins is associated with altered channel kinetics, but the results available indicate that AVP has no significant effect on the open probability of individual Na^+ channels. This suggests that even if AVP does phosphorylate the channel protein, the site that is phosphorylated by the cAMP-dependent protein kinase A is not related to the kinetics of channel opening or closing. Using immunocytochemical techniques, Sorscher *et al.* (1988) developed a polyclonal antibody which acts against the purified amiloride-sensitive Na^+ channel protein. Binding of the antibody was specific to the apical membrane and not to any cytoplasmic elements on AVP-induced A6 cells, or to rat or bovine renal medullary collecting ducts (Sorscher *et al.*, 1988; Brown *et al.*, 1989; Tousson *et al.*, 1989). The results gained from these experiments have provided evidence against the presence of a pool of Na^+ channels in the cytoplasm of other AVP responsive epithelia. In contrast to these results, Kleyman *et al.* (1991) used a monoclonal antibody which acts against the purified Na^+ channel protein, to label the frozen sections of A6 cells. These authors found the antibody bound to the subapical regions and also to the apical membrane. Recently, several biochemical investigations of purified Na^+ channels from A6 cells have provided evidence that AVP increases the apical Na^+ permeability by activating Na^+ channels already resident in the apical membrane by a direct

phosphorylation mechanism rather than by an insertion of Na^+ channels. Oh *et al.*, (1993) used a biotinylation/immunoprecipitation protocol to examine the expression of Na^+ channel proteins within the apical membrane of ADH-treated A6 cells, also tested the functional consequences of PKA phosphorylation of highly purified renal Na^+ channel reconstituted into planar lipid bilayers. These investigators found that AVP did not induce the apical insertion of new channel proteins in A6 cells. They concluded that AVP increases the apical Na^+ permeability by activating Na^+ channels already resident in the apical membrane by a direct phosphorylation mechanism rather than by cytoplasmic recruitment of latent Na^+ channels.

On the other hand, several lines of evidence are consistent with the recruitment theory. Garty and Edelman (1983) provided convincing evidence for an insertion mechanism by using trypsin to inactivate channels that were accessible to the extracellularly applied enzyme. They found that treatment with trypsin did not reduce the stimulatory response to AVP, indicating that AVP elicits its response despite the proteolysis of the existing channels in the apical membrane. This suggests that AVP may cause the insertion of Na^+ channels, probably in much the same way that it causes the insertion of water channels in toad bladder. In amphibian urinary bladder, AVP causes the insertion of water channels by the fusion of aggregates, in the subapical membrane region, with the apical membrane (Wade, 1989; Verkman, 1989). Under the stimulation of AVP, the aggregate-containing vesicles are located towards the apical surface prior to their exocytotic incorporation into the apical plasma membrane (Muller *et al.*, 1980). The aggregates (putative water channels) are thus transferred from cytoplasmic vesicles to the apical membrane, increasing the water permeability. Following hormonal stimulation, using the freeze-fracture electron microscopic technique, Coleman *et al.*, (1987) observed that the aggregates are retrieved by endocytosis and, may be recycled (Wade, 1989). A similar exocytosis and endocytosis

is thought to be involved in the water permeability response to AVP in the mammalian collecting tubule (Brown, 1989). By analogy with the situation in frog skin epithelium, an AVP-stimulated increase in the number of Na^+ channels in the apical membrane may occur due to insertion by an exocytosis of Na^+ channels preformed in cytoplasmic vesicles of the epithelial granular cells.

2.5.3.3 Regulation of sodium channels by other hormones

Very little has been done on the modulation of Na^+ channels by transmitters or other hormones, besides AVP and aldosterone. Recently, Cantiello and Ausiello (1986) reported that the atrial natriuretic factor (ANF) inhibits Na^+ transport in LLC-PK_1 cells. Light *et al.* (1989a) also reported that atrial natriuretic peptide (ANP) inhibits amiloride-sensitive Na^+ transport in rat inner medullary collecting duct cells, decreasing the open probability of individual channels; however, not all studies have shown this inhibition mechanism. Thus, ANP did not affect Na^+ transport in the toad urinary bladder (Das *et al.*, 1991). ANP inhibits aldosterone secretion and reduces adenylate cyclase activity in various renal tubules (Anand-Srivastava *et al.*, 1986), therefore, ANP might indirectly down-regulate Na^+ channels.

2.5.4 Modulation of Na^+ channels by interactions with the cytoskeleton

Elements of the cytoskeleton, in addition to providing support structure in cells, play a major role in the transport of substances. In this regard, the axons of nerves contain actin filaments, microtubules and neurofilaments, that are found to be instrumental in the movement of neurotransmitter products from their origin in the soma of the neuron to the terminal button. Similarly, there is substantial evidence indicating that interactions between the actin cytoskeleton and the plasma membrane are important for regulating the vectorial movement of water and solutes in ion-transporting epithelia.

In toad bladder granular cells, depolymerization of microtubules and microfilaments decreases AVP-stimulated water permeability (Pearl and Taylor, 1985; Holmgren *et al.*, 1992). Freeze fracture electron microscopic investigations of the apical membrane of frog epidermis and toad bladder cells, have identified membrane particle aggregates that have been implicated in AVP increased water permeability (Muller *et al.*, 1980; Brown *et al.*, 1983). Similar results were shown by Kubat *et al.* (1989) on rabbit renal cortical collecting duct cells, who reported that AVP gives rise to an increase in transepithelial water flow and a significant increase in the size and number of aggregates containing tubules. In renal epithelial cells, the actin network is also involved in a process whereby AVP induces the insertion of aggregates containing water channels into the apical membrane to stimulate water transport (Verkman, 1989). Since AVP causes large increases in water permeability in the apical membrane of certain tight epithelia, like toad bladder (Harris and Handler, 1988), it is reasonable to suggest that the hormone AVP might increase Na^+ permeability along similar lines and that the insertion of Na^+ channels may similarly be controlled by the cytoskeleton..

Of current interest is evidence suggesting that regulation of Na^+ channel activity may occur by interactions with the actin network. Kellerman *et al.* (1990) and Linshaw *et al.* (1991) demonstrated that an intact actin network is essential for sustaining the rate of Na^+ reabsorption in the rat renal proximal tubules, and for cell volume regulation in the rabbit renal proximal tubules. On the other hand, much less is known about the role of actin in the mechanism of transepithelial Na^+ reabsorption. Nevertheless, the functional role of the cytoskeleton in Na^+-transporting epithelial cells is not clearly defined. In A6 cells, it has been shown that the Na^+ channel is structurally linked to the cytoskeleton by regulating proteins (Smith *et al.*, 1991), but the significance of this is not understood. Recently, there has been much interest in the role of the actin network in the control of the functioning of Na^+ channels. With reference to this,

experiments performed using patch clamp have suggested a possible regulatory role for actin on the Na^+ channel activity in A6 cells. Depolymerization of actin filaments, or the addition of short actin filaments, increased Na^+ channel activity in cell-attached or excised patches, while monomeric actin or long filaments had no effect (Cantiello *et al.*, 1991). It is possible that, in the AVP induced increase in the number of open Na^+ channels, actin may be involved in the recruitment of Na^+ channels in a manner analogous to that in which the filaments bring about the fusion of water channels with the cell membrane in toad bladder (Holmgren *et al.*, 1992; Schafer and Hawk, 1992). In A6 cell patches, disruption of the endogenous actin filaments by cytochalasin D prevents the activation of Na^+ channels by protein kinase A (Prat *et al.*, 1993b). Results from these experiments indicated that actin filament organization is involved in the PKA activation of epithelial Na^+ channels.

Chapter 3

Aims

This particular project originated as result of our principal research into the regulation of Na^+ reabsorption across apical membranes of tight, Na^+-transporting epithelia. We have examined the non-hormonal regulatory mechanisms, and the hormonal regulatory mechanisms of the Na^+ channel densities on isolated frog skin epithelium.

Earlier electrophysiological studies from our laboratory have shown that AVP stimulated Na^+ reabsorption across renal model tissue ventral frog skin epithelium by increasing the permeability of the apical membrane. More recent molecular results from our and other laboratories demonstrated that the increased permeability is caused by large increases (>200%) in the number of open Na^+ channels. The open probability of the channels remains unchanged.

We decided to extend our studies to examine the mechanisms whereby luminal Na^+ concentration directly controls the properties of Na^+ channels. It is well-known that in the kidney the Na^+ permeability of the apical membrane of distal cells in the nephron is changed in response to luminal Na^+. The mechanism of this autoregulatory process is unknown. The issue is further complicated because results from patch clamp and noise analysis of the channels are often at variance. We found that lowering the Na^+ concentration increased the number of Na^+ open channels to compensate for the decrease in single channel current. This occurred by an increase in open probability of the channels. Our results are supported by recent patch clamp on renal A6 cells, but are different from earlier patch clamp data.

An increase in the number of open channels can occur in one or both of the following ways: (1) by an increase in open probability and/or (2) by increase in the total number of channels (open + closed). From our results it seems that the mechanisms for increase in the number of open Na^+ channels in hormonal or non-hormonal regulation are different. An increase in the total number of channels may occur by (1) activation of "electrical silent" channels already residing in the membrane or (2) by recruiting new channels, probably from the subapical cytoplasm. If the latter mechanism is the correct one then, by analogy to other epithelia, the cytoskeleton could be involved in the insertion of new channels into the membrane. We intend to resolve:

(1) Whether changes in open channel densities occur by increase in open probability and/or total number of channels.

(2) Whether the cytoskeleton is involved in the regulation of changes in channel densities.

This critical information will increase our insight into the mechanism whereby Na^+ reabsorption occurs in the distal nephron. It could possibly have further pharmacological and/or clinical relevance.

In this project we tried to resolve whether AVP and luminal Na^+ concentrations modulate apical Na^+ channels by separate mechanisms. We are especially keen to determine whether the luminal factors effect Na^+ channels by changes predominantly in open probability or in total channel density. Next we intended to resolve which of the mechanisms are used to bring about changes in open channel densities. Activation of existing membrane channels or recruitment from cytoplasmic pools. Preliminary experiments in our laboratory have indicated that the cytoskeleton might be involved in the recruitment process. We studied the mechanism by: (1) altering the microtubules of cells with colchicine to test the selective targeting of vesicles theory. (2) by

disrupting actin filaments with cytochalasin B to study the possible effects on vesicle delivery at the apical membrane. Similar studies have been done to study the effects of the recruitment of water channels under influence of ADH. Such studies have not been done on Na^+ channel insertion. In this way we may find evidence to support our theory that open channels are recruited from cytoplasmic stores by cAMP-independent mechanism, while the number of open channels is increased by activation of existing channels by cAMP-dependent mechanism.

Chapter 4

Materials and Methods

4.1 Electrophysiology

4.1.1 Tissue preparation

Studies were done on isolated abdominal skin of the frog *Rana fuscigula*. This species was chosen for its ion transporting features which are characteristically similar to those of other tight epithelia. Frogs (~10 cm) were stored in storage tanks at room temperature (20 to 25 °C) in distilled water with access above water to a dry surface, and were fed with meal worms twice a week. Any frogs which appeared to be infected with " red leg " were not considered for the study, and usually died within a couple of days.

Frogs were sacrificed by decapitation and then the spinal cord was pithed with a needle. The abdominal skin was dissected ventrally, then gently scraped with a scalpel blade and rinsed in Ringer solution on a sylgard plate. About 80% of the corium was removed during scraping as to diminish the unstirred layer and allowed rapid access of the drugs from the serosal solution to the epidermal cells. The isolated epithelia used in the experiments were prepared from abdominal skins by the method of Fisher *et al.* (1980). Concisely, this entailed applying cyanoacrylate tissue glue (Eurecryl™, Silicone Technical Products, South Africa) to the rim of a polycarbonate (perspex) ring and placing it onto the skin sample so that the mucosal surface adhered to the ring. The serosal side was then exposed for 2 hours to a solution containing 50 I.U. collagenase/ml Ringer solution at room temperature.

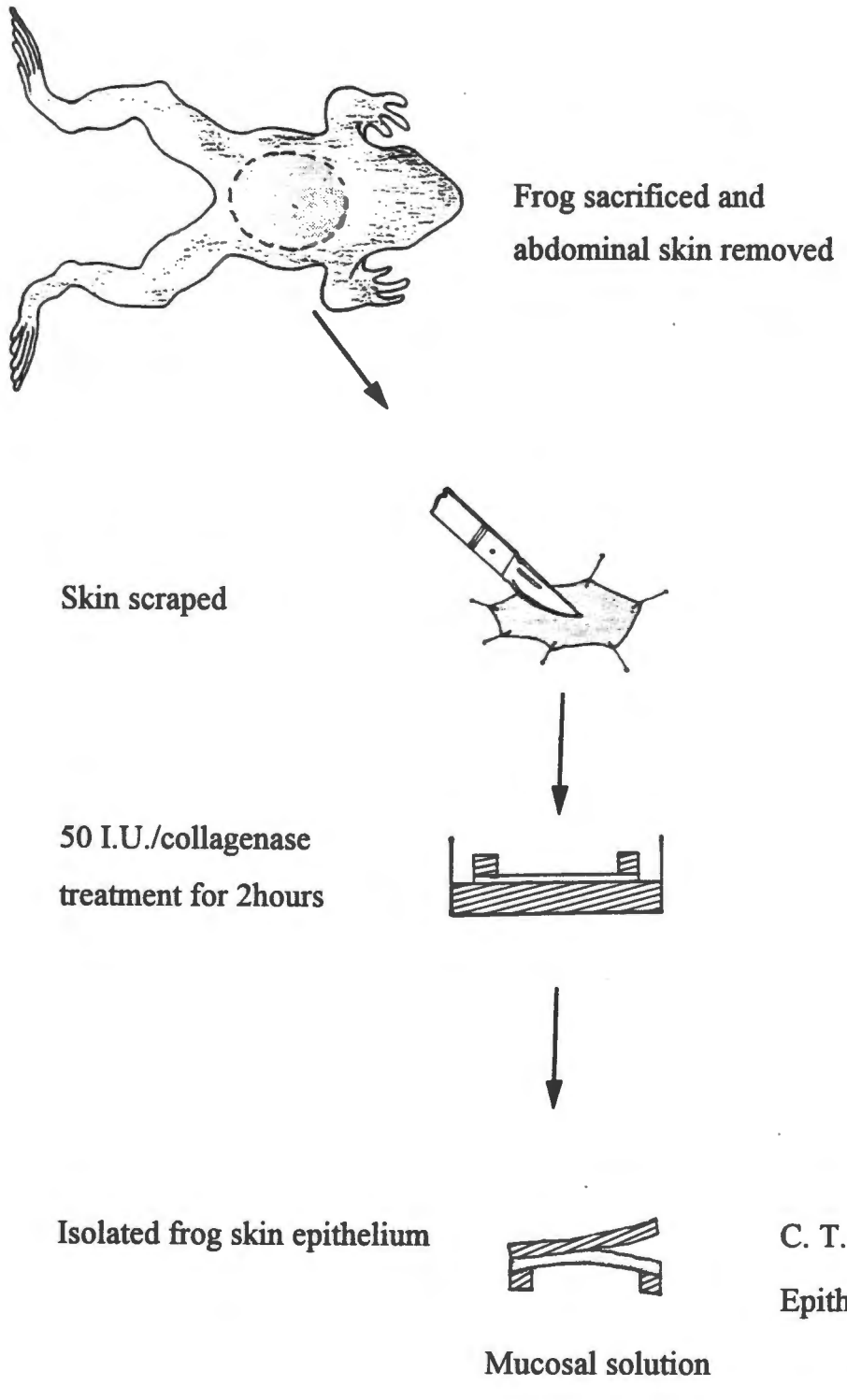

Fig. 4.1 Tissue preparation (Details in 4.1.1)

After the enzyme treatment, the underlying connective tissue (C. T.) was gently peeled away with forceps to leave behind the epithelial layer adhering to the edges of the polycarbonate ring (Fig. 4.1).

4.1.2 Tissue mounting

The isolated frog epithelium was glued between two Lucite gaskets with cyanocrylate tissue glue, then the two gaskets were held onto an Ussing-type chamber with silicone grease (Dow Corning high vacuum grease) which minimized edge damage of the tissue (Fig. 4.2) (Helman and Miller, 1971).

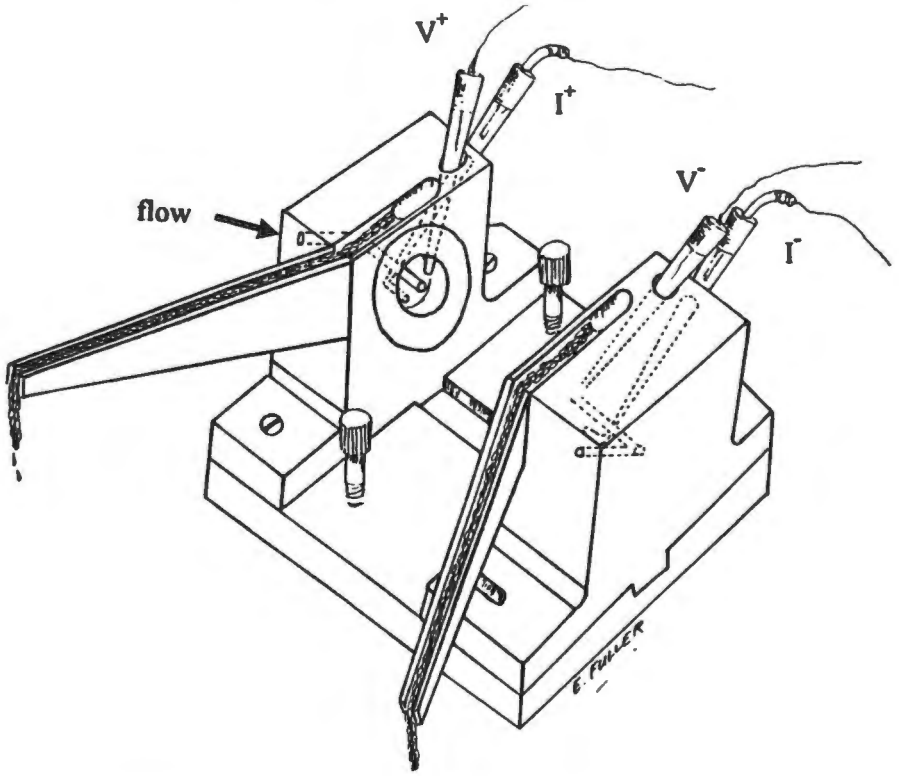

Fig. 4.2 Ussing-type chamber to permit continuous flow of solutions during fluctuation analysis. The chamber volume is about 0.6 ml. Spillways containing wicks made from paper tissue allow for the solution to leave the chamber. Fluid is not usually recirculated. The symmetrical chambers contain the appropriate inlets which are low resistance bridges for current (I) passing and voltage (V) recording via Ag/AgCl electrodes to the voltage clamp (Helman and Miller, 1971).

The tissues were bathed symmetrically in a Ringer solution. The volume of the chamber is about 0.6 ml and the area of tissue exposed to bathing solutions is 0.75 cm^2. The chambers were continuously perfused with Ringer solution by gravity from reservoirs at rates of ~ 9 ml/min, allowing a constant flow of solutions between and during periods of data acquisition of the power density spectra (PDS). This not only facilitated exchanges of solution, but avoided the usual flushing transits that occur after the flow of the bathing solutions is stopped. Background spectra have indicated that there is less $1/f$ noise during continuous flow than during stopped flow experiments (Abramcheck *et al.*, 1985).

4.1.3 Solutions and chemicals

Collagenase type II (Worthington Biochemicals, New Jersey) was used at a final concentration of 50 I.U./ml Ringer to isolate the frog epithelium. All tissues were bathed in Cl/HCO_3 Ringer solution which consisted of 110 mM NaCl, 2.4 mM $KHCO_3$ and 2.0 mM $CaCl_2$ and equilibrated with air at a pH of 8.1. The osmolarity of the Ringer solution was approximately 220 mosm/kg. For the low Na^+ experiments, Ringer solutions were prepared by isosmolar replacement of NaCl with tetramethylammonium chloride. Experimental changes in Na^+ concentrations were made to the mucosal solution alone, maintaining the Na^+ concentration in the serosal solution at 110 mM. The Ringer solutions were checked for constancy of ion content by flow cytometry, and osmolarity by an osmometer. For noise analysis, 6-chloro-3,5-diamino-pyrazine-2-carboxamide (CDPC) was purchased from Aldrich Chemical Company (Milwaukee) and made up to the appropriate concentrations (10, 20, 30, 40, and 50 μM) in the mucosal Ringer solution.

Amiloride, used at concentration of 10^{-4} M, was donated by Merck, Sharp and Dohme Research Laboratories.

For the depolymerizing drug studies, both surfaces of the tissues were perfused with Ringer solution containing either 100 μM colchicine (Sigma Chemical Co. St. Louis) to disrupt microtubules or 10 μg/ml cytochalasin B (CB) to disrupt microfilaments. 39.94 mg Colchicine was dissolved in 1000 ml Ringer solution at a final concentration of 100 μM and made fresh every time. A stock solution of CB (Sigma Chemical Co. St. Louis) was prepared by dissolving (2 mg/ml) in dimethyl sulfoxide (DMSO) and stored at -4 °C in the dark. The final concentrations of CB and DMSO in Ringer solution were 10 μg/ml (~21 μM) and 0.5%, respectively. The tissues were first treated in either colchicine for 3 hours, or for 2 hours in CB at room temperature and during this time the I_{SC} was continuously monitored and the experiments were only started when I_{SC} had reached a steady-state value. Colchicine and CB were continuously present during the experimental manipulations. Control perfusion with 0.5% DMSO alone showed no significant effect on the Na^+ transport rate.

For the hormonal-regulation study, arginine-vasopressin (AVP) (Sigma Chemical Co. St. Louis) was dissolved in Ringer solution at a final concentration of 30 mU/ml in the serosal bathing solution.

4.1.4 Application of the current fluctuation analysis technique

The technique of noise analysis has been successfully used for the study of ion channel epithelia, especially for the study of channel kinetics, single channel current and the regulation of channel densities. This method needs a shielded cage, a low-noise voltage clamp and a commercially available personal computer system. Fluctuation analysis requires the use of specific Na^+ channel blockers to induce fluctuations in current. From the fluctuations certain information about the Na^+ channel properties may be obtained (Van Driessche and Lindemann, 1979).

4.1.4.1 Electrodes and electrical connections

The current and voltage electrodes were made with silver (Ag) wires, which were scraped to remove oxides and coated with chloride by an electrocoating process before each experiment. 5M NaCl/agar (2%) (May & Baker Ltd., UK.) bridges were used to prepare four Ag/AgCl electrodes. Two electrodes served as current electrodes; two others were voltage electrodes. The inter-electrode potential differences were measured by a multimeter, and were kept as low as possible (< 1 mV), in order to reduce the contribution of the current noise source of the input stage of the voltage amplifier to the total noise signal. This was again checked and recorded at the end of each experiment. Careful design of low resistance electrodes is a essential for the electronic circuitry. KCl/agar (3%) is more commonly used because the two ion species have very similar motilities whereas the motilities of Na^+ and Cl^- are not as close. In our laboratory NaCl/agar bridges were used instead of KCl/agar bridges, because leaks of KCl might influence the characteristics of the preparation more seriously than would NaCl leaks (Van Driessche and Erlij, 1983).

The Ussing-type chamber with tissue and electrodes was set up in a shielded (Faraday) cage and all electrical connections were earthed and voltage clamp apparatus was powered from DC batteries (±15 V) rather than an AC electrical source, to reduce the background noise from the equipment as much as possible.

Experiments were performed at room temperature and the macroscopic current was recorded by a chart recorder (Linear 1200, Anatech Instruments Ltd., South Africa).

4.1.4.2 Low -noise equipment

The tissues were continuously short-circuited with a low-noise voltage clamp (Fig. 4.3) (Van Driessche and Lindemann, 1978; Van Driessche and Gullentops, 1982).

Under short-circuited conditions the I_{SC} represents mainly the ion passage across the transcellular pathway (Fig. 2.1). The current input into the voltage clamp is via a differential voltage amplifier (DA) that amplifies the signal 100 times. This is connected to a feedback amplifier (FBA) which clamps the tissue to a particular command voltage for e.g. 0 mV. The current output is fed into a noise analysis system containing prefilters, aliasing filters and gain controls. The current output of the tissue is measured by a current to voltage converter (CA).

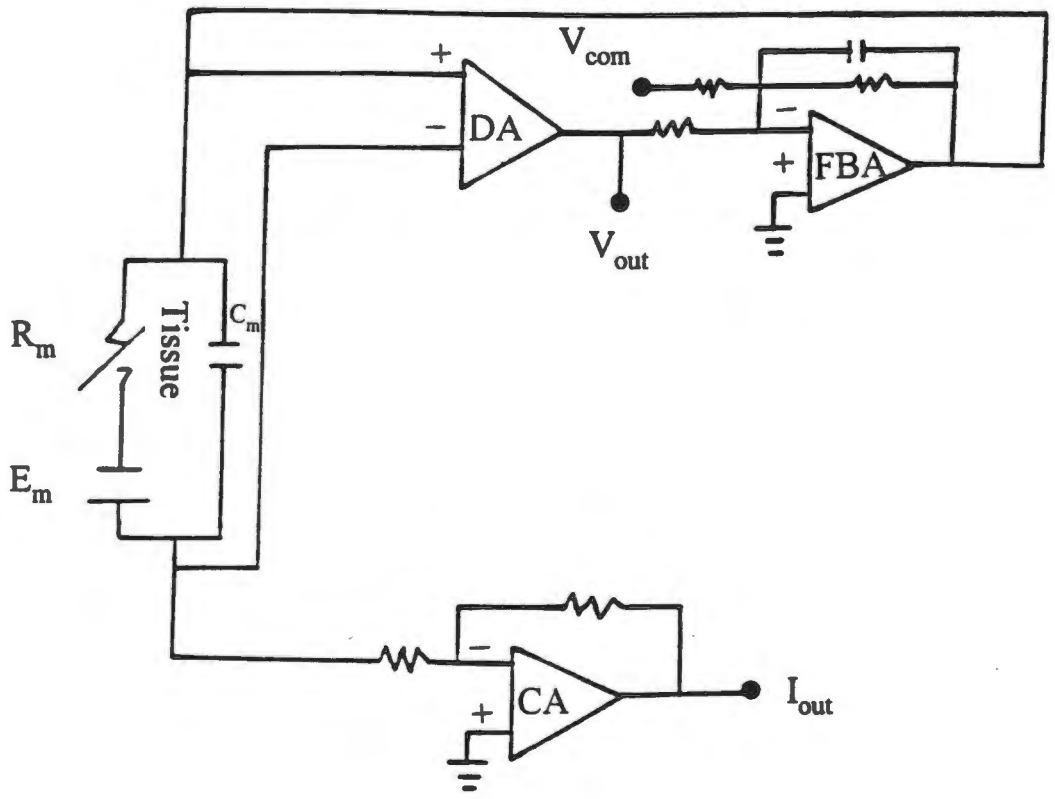

Fig 4.3 Voltage clamp circuit with an input and differential voltage amplifier (DA), and feedback amplifier (FBA) in a circuit. The transepithelial voltage is clamped by applying a DC voltage to V_{com} (command voltage) of the FBA. The current output (I_{out}) of the tissue is measured by a current to voltage converter (CA) (Modified from Van Driessche and Gullentops, 1982).

4.1.4.3 Data capture and processing

For the data capture of fluctuation analysis, the electrodes provided the continuous recording of the short-circuit current I_{SC} across the membrane. In order to analyse the current fluctuations, the AC and DC components of the I_{SC} were separated by a high-pass rectifying current filter and the AC current was amplified 1000 times. After anti-aliasing filtering through a low-pass filter, which filtered out the high amplitude AC component, the signal was digitised with an analog-to-digital (A/D) converter (RTI 800, Analog Devices Inc., Norwood, Mass., USA.) (this procedure is described by Desmedt *et al.*, 1993). We used a fundamental frequency of 0.5 Hz. to derive power density spectra (PDS) from time domain to frequency domain by means of fast Fourier transformed (algorithm described by Cooley *et al.* 1967) records of 4096 points collected over a 2 s period at each concentration of blocker. Averaged PDS of 2048 frequencies were obtained from 50 or 60 sweeps of data. The digitised signals were monitored on an oscilloscope and recorded on an IBM® compatible 486 computer using a data acquisition program and later stored on disc. Spectra containing relaxation noise were fitted by non-linear, least squares regression analysis (described by Brown and Dennis, 1972) with the sum of a Lorentzian component and an A/f^{α} term to determine the low frequency plateau value (S_o) and radian corner frequency, $2\pi f_c$ according to the following formula:

$$S(f) = \frac{S_o}{1 + (f/f_c)^2} + \frac{A}{f^{\alpha}}$$

where A is the amplitude of the low-frequency noise component at $f = 1$ Hz. and α its slope. The data acquisition (software) programme " Noise " obtained from Professor W. Van Driessche and described previously by De Wolf and Van Driessche (1986), was used in our laboratory for continuous sampling of data. This software was programmed in accordance with standard analysis procedures by K. Wessels, and the

hardware was developed by G. Raskin, K. U. Leuven. For analysing data, the program "Fitpow" was used.

4.1.4.4 Blocker-induced fluctuation analysis

Blocker-induced fluctuation analysis of apical membrane Na^+ channels was performed with the weak electroneutral blocker CDPC. Two different protocols were used: staircase protocol and time course protocol. The staircase protocol, as described by Helman and Baxendale (1990), permitted determination of the blocker's concentration dependencies of single channel currents and of channel densities. The time course protocol allowed estimation of the rates of change of channel densities and single channel current under experimental conditions (Els and Helman, 1991). The data were analysed according to a three-state model recently developed by Helman and Baxendale (1990), describing channels distributed between open, closed and blocked states. Microscopic fluctuations in I_{SC} were induced by the serial introduction of 10 to 50 μM CDPC into the mucosal solution. Following noise analysis, the blocker was completely washed out from the mucosal solution and the I_{SC} allowed to stabilize. Membrane conductance can be measured by supplying 3 mV unipolar pulses, which were applied via a voltage clamp every 14 s, and then measuring the change in I_{SC} (ΔI) according to the Ohm's Law equation:

$$\Delta V = \Delta I \times R$$

$$R = \frac{\Delta V}{\Delta I}$$

$$G_m = \frac{\Delta I}{\Delta V}$$

where V is voltage, ΔI is the change in current due to ΔV = 3 mV, and G_m is membrane conductance. The sodium macroscopic current (I_{Na}) was determined by subtracting the residual current after about 15 min following the addition of a high

affinity sodium channel blocker, amiloride, at a final concentration of 10^{-4} M, to the mucosal solution from the I_{SC} at the end of each experiment. ($I_{Na} = I_{SC} - I_{amil.}$)

Staircase protocols: We assumed a simple three-state model where channels are distributed between closed, open, and blocked states and the blocker molecules are in constant association and dissociation with the open channels represented by rate coefficiency k_{ob} and k_{bo}, respectively. The closed to open, and open to closed, fluctuation is given by rate coefficients β and α respectively.

$$N_c \underset{\alpha}{\overset{\beta}{\rightleftarrows}} N_O \underset{kbo}{\overset{kob[B]}{\rightleftarrows}} N_b$$

The on- (k_{ob}) and off- (k_{bo}) rate coefficients of blocker interaction with the open state of the channel were determined from the slope and intercept of the rate-concentration plots ([B]-$2\pi f_c$ relationship) according to equation:

$$2\pi f_c = k_{ob}[B] + k_b \qquad \text{(Eq. 1)}$$

The equilibrium blocker coefficient of open channels (K_B) was calculated from:

$$K_B = k_{bo} / k_{ob} \qquad \text{(Eq. 2)}$$

The macroscopic I_{Na}, together with S_O, $2\pi f_c$ and the on-rate coefficient were used to calculate the mean single channel Na^+ current (i_{Na}) at each [B] according to Eq. 3.

$$i_{Na,B} = [\, S_O \times (2\pi f_c)^2 \,] / (4 \times I_{Na} \times k_{ob} \times [B]) \qquad \text{(Eq. 3)}$$

Note that the subscript ('B) included with the usual notations will indicate that a measurement was made in the presence of blocker. Estimation of values for i_{Na} in the absence of blocker were obtained by extrapolation to zero [B] (Fig. 5.4).

Open channel density (N_O), in the absence of blocker, was calculated from the quotient of I_{Na}/ i_{Na}. With channels fluctuating between open and blocked states (N_b), the

density of channels in open and blocked states (N_{ob}) at each [B] of the channels was calculated according to mass law action from Eq. 4.

$$N_{ob} = N_{O,B} (1 + [B] / K_B)$$

$$= N_{O,B} + N_b \qquad \text{(Eq. 4)}$$

Analysing data according to a three-state model allowed us to estimate the open probability of spontaneuous fluctuations. Open channel probability in the absence of blocker (β'), defined by $\beta / (\beta+\alpha)$, was determined by first calculating apparent open probabilities at each blocker concentration (β'_B) Eq. 5 (Helman and Baxendale, 1990; Helmann and Kizer, 1990; Els and Helman, 1991) and then extrapolating values to zero blocker concentration by linear regression in the β'_B - [B] relationship (Fig. 5.4).

$$\beta'_B = [1- (N_{O,B} / N_O)] / (N_{O,B} / N_O) ([B] / K_B)$$

$$= (N_O / N_{O,B} -1) / ([B] / K_B) \qquad \text{(Eq. 5)}$$

The total channel density (N_T), the sum of electrically active open and closed channels in the absence of blocker, was calculated from:

$$N_T = (N_O + N_C) = N_O / \beta' \qquad \text{(Eq. 6)}$$

Staircase protocols are used during control and experimental conditions when the macroscopic transport rates are in apparent stable conditions.

4.1.4.5 Time course protocol

In order to determine time-dependent changes in single channel current, and in channel densities caused by a reduction in the mucosal sodium concentration, experiments were done according to a protocol described elsewhere (Els and Helman, 1991). Briefly, an initial noise analysis was performed as described in the 4.1.4.4, to get

steady-state values of k_{ob}. Thereafter, 20 μM CDPC were continuously present in the mucosal solution during the time course control period of about 20 minutes, followed by the experimental period. During this time PDS were measured every 4 minutes to obtain rates of change of $S_{O,B}$ and $f_{c,B}$. At the same time, we also measured $I_{Na,B}$. It was established with general protocol experiments that the k_{ob} for CDPC was not changed by reducing the mucosal sodium concentration. These values were then used to calculated changes in i_{Na} and $N_{O,B}$ in the presence of blocker during periods in 110 and 20 mM Na^+. These results are shown in Fig. 5.5.

4.1.4.6 Statistical analysis

Data obtained was statistically analysed in the Quattro® Pro (Borland International, Inc., USA.) spreadsheet. Equations for current fluctuation analysis were programmed into the spreadsheet with automatic calculation on entry of data. All graphs were prepared with Sigma Plot® (Jandel Scientific, USA.) and Harvard™ Graphics (Software Publishing Corporation, USA.). Statistical data are presented as means ± SEM. The Student's *t* test, on paired data, was used to determine the significance ($P<0.05$) of differences between means by using the programme Epistat (copyright from Tracy L. Gustafson, 1984).

The use of experimental animals (tissues) was in accordance with the guidelines published by the South African Medical Research Council. Permission was granted by the Animal Research Review Committee of the Faculty of Medicine, University of Cape Town, South Africa.

4.2 Cytochemistry

This study aimed to determine the organisation of certain cytoskeletal elements in frog skin epithelial cells.

4.2.1 Tissue preparation for light microscopy

The preparation of isolated frog epithelia has been shown in the section 4.1.1. For studies of drug depolymerization of the cytoskeleton, tissue samples were suspended in air-bubbled Ringer solution containing either 100 µM colchicine for 3 h or 10 µg/ml cytochalasin B for 2 h at room temperature before fixation.

4.2.1.1 Pretreatment of tissue for immunofluorescence microscopy

For microtubules : Prepared resin sections.

Control (colchicine-untreated) and colchicine treated tissues were fixed at room temperature with 3% paraformaldehyde in 0.1 M phosphate buffer saline (PBS) pH 7.6 for 30 min, then removed, cut into smaller pieces and fixed for a further 30 min with 3% paraformaldehyde (in 0.1 M PBS) at 4 °C. After washing 3 times in 0.1 M PBS to remove the fixative, the tissues were dehydrated in ascending grades of ethanol from 50% (v/v) to absolute (100%) two changes of 10 min each, followed by two changes of propylene oxide (1,2-epoxypropane) of 5 min each. Infiltration of the tissue with resin was achieved using a 1:1 mixture of propylene oxide and resin at room temperature for 1 h. Tissues were further infiltrated using pure resin at 40 °C overnight. The following day tissues were transferred to fresh resin containing the accelerator DMP-30 (2,4,6-tri-dimethylaminomethyl-phenol) (0.71g DMP-30/15g resin) and left for 1 h at room temperature. Final infiltration took place at 40 °C for a further hour. Samples were embedded in fresh resin using suitably labelled prefilled moulds and polymerised at 60 °C for 48 h. Epoxy resin (Araldite CY 212, TAAB, UK.) was used for this procedure. This embedding process was described previously by Luft, 1973.

Semithin (1 µm) epoxy resin sections were cut using a Reichert-Jung ultramicrotome and glass knives made on a LKB Type 7801B knifemaker. Sections were transferred

to drops of water on glass slides, and dried on a warmplate prior to staining with toludine blue.

For microfilaments: Prepared cryosections.

For visualisation of actin, immediately after isolation small pieces of epithelium were immersed and fixed in 3% paraformaldehyde buffered with 0.1 M PBS (pH 7.6) for 1 h, then rinsed 3 times for 10 min at room temperature in phosphate buffer (pH 7.6) with 5% sucrose. Tissues were cryoprotected using PBS containing 10%, 15%, and 20% sucrose for 4 h at 4 °C each time. The addition of sucrose made blocks less brittle, cutting easier and minimised damage due to the formation of ice crystals (Tokuyasu, 1973). After cryoprotection, tissues were infiltrated in a mixture of 20% sucrose in 0.1M PBS (pH 7.6) and Tissue-Tek OCT embedding compound (Miles; Kankakee, IL) in a ratio of 2:1 for 30 min at room temperature. Tissues were transferred to an aluminum embedding mould filled with fresh sucrose/phosphate buffer/OCT in the same ratio used for infiltration. Finally, the blocks were frozen in liquid nitrogen and stored at -90 °C. Cryosections (2-4 µm thick) were cut at -15 to -40 °C on a SLEE (London) cryostat using a steel knife, mounted on gelatin-coated glass slides and dried at room temperature. The slides were stored at -90 °C until required. Before processing for immunocytochemistry, the slides were taken from the freezer, allowed to warm to room temperature, and then air-dried. This improved method for cryosections was introduced by Barthel and Raymond, (1990).

4.2.1.2 Immunostaining for microtubules and microfilaments

For microtubules: Immunocytochemistry was done with 1 µm semithin sections of resin embedded tissue. All steps were performed at room temperature. Phosphate buffer saline (PBS) at pH 7.6 was used for the preparation of various reagents as indicated. Slides with 1 µm resin sections were deplasticized for 10 min at room

temperature in a solution of saturated NaOH in absolute ethanol (sodium ethoxide), diluted 1:1 with fresh absolute ethanol. After 10 min incubation, slides were quickly washed three times in absolute ethanol for 2 min each to avoid drying. Then, slides were hydrated through a graded alcohol series (95%, 70%, 50%, 2 min each, and distilled water 2 min twice). The sections were immediately rinsed with 0.1 M PBS twice, for 5 min each. The deplasticization was first introduced by Mar and Wight, (1988).

This staining procedure was based on a method of Kurihara *et al.* (1990). The indirect immunostaining protocol for microtubules was as follows:

(a) Deplasticized sections were placed in 0.5% Triton X-100 for 10 min.

(b) Then briefly washed in 0.1 M PBS, twice in 10 min.

(c) Non-specific staining was blocked by 1:20 normal sheep serum at room temperature for 10 min.

(d) Excess serum was drawn off with a paper tissue and the slide was wiped, except the area of the section which should remain moist. The slides were placed horizontally on a rack in a damp chamber or large Petri dish containing some wet cotton wool or filter paper.

(e) Each section was covered with a drop (30 µl) of primary antibody (rat monoclonal antibody against tubulin; Serotec, UK.), at a dilution of 1:100 in 0.1 M PBS containing 0.1% saponin and 0.05% sodium azide, for 1 h at room temperature and left overnight at 4 °C.

(f) The following morning the sections were washed 3 times in 0.1 M PBS, each rinse lasting 5 min, then, except for the area of the section, the slides were wiped dry.

(g) One drop of the secondary antibody, fluorescein isothiocyanate (FITC)-labelled sheep anti-rat IgG (Amersham, Amersham Laboratories, England), was applied at a dilution of 1:40 in 0.1 M PBS and left on the slide for 1 h at room temperature.

(h) Slides were rinsed 3 times in 0.1 M PBS, with each rinse lasting 5 min.

(i) Slides were mounted in 0.1 M PBS:glycerine, 1:1. Mounting medium was added (Vectashield™, Vector Laboratories, Inc. USA) to prevent fading (Johnson *et al.*, 1982).

(j) Finally, the slides were viewed using a Leitz epifluorescent microscope and photographed with a Leitz photomicrographic camera using Fujichrome 400 film.

In negative control experiments, incubation with the primary antibody was omitted. In positive control experiments, rat embryonic pancreas was used.

***For microfilaments*:** Actin was stained by direct immunofluorescence similar to the method used by Hugon *et al.* (1989) on toad bladder epithelial cells. Cryosections were removed from the freezer and dried for 30 min at room temperature before immunostaining according to the following protocol:

(a) The thick sections were postfixed for 15 min in pure acetone at -20 °C, then rinsed in 0.1 M PBS for 5 min each time.

(b) A solution of rhodamine-phalloidin (Molecular Probes Inc., USA) in 0.5% TritonX-100/PBS at a twenty-fold dilution (0.16 µM) was added and left on the section at room temperature for 1 h.

(c) The slides were rinsed immediately in 0.1 M PBS and mounted with PBS/glycerine-mounting medium (Vectashield™, Vector laboratories Inc., USA).

(d) Finally, the slides were observed and photographed on a Zeiss photomicroscope with epifluorescence attachment.

In negative control experiments, the sections were treated according to the mehtod of Sugimoto *et al.* (1990) for 1 h at room temperature with a mixture of 0.16 μM rhodamine-phalloidin and 8 μM unlabelled phalloidin (Boehringer Mannheim, Germany). In positive control experiments, we used the epithelial cells from rat thyroid.

4.2.2 Tissue preparation for transmission electron microscopy (TEM)

To localise actin and to show the effects of cytochalasin B (CB) and arginine-vasopressin (AVP) by electron microscopy, we adapted a postembedding immunigold method used by Gao *et al.* (1992) in studies of toad bladder and rat collecting duct. Isolated frog epithelia were obtained in the manners described in section 4.1.1. The tissue was cut into 4 pieces: One piece was incubated with either CB, AVP or a mixture of CB/AVP, and the fourth piece was used for a control.

4.2.2.1 Summary processing protocols for standard TEM

A basic protocol for the preparation of tissue for transmission electron microscopy (TEM) consisted of tissue processing (primary and secondary fixation, followed by dehydration and infiltration of the tissue with resin) and embedding the specimen in resin. This permitted the cutting of thin sections suitable for viewing with the electron microscope. Various primary and secondary fixations were suggested (Viale *et al.*, 1985; Mar and Wight, 1988; Gao *et al.*, 1992). Finally, the technique was carried out by using suitable fixation protocols and embedding in epoxy resin.

A routine procedure for the TEM specimen was as follows:

(a) Fresh isolated epithelia were briefly rinsed with 0.1 M PBS and immediately fixed for 30 min at room temperature with a mixture of 1.5% paraformaldehyde and 1% glutaraldehyde in PBS at pH 7.6, followed by further fixation at 4 °C for 90 min.

(b) Washed 3 times in 0.1 M PBS for 10 min each, then cut into further small pieces.

(c) Standardized methods for dehydration of tissue:

50% ethanol for 10 min.
70% ethanol for 10 min.
90% ethanol for 10 min.
100% ethanol 2 times for 10 min each.
Propylene oxide (P.O.) 2 times for 5 min each.

(d) Infiltration of the tissue with resin was done as follows:

The detailed formulation of Epon/Araldite is shown in the Appendix.

1:1 mixture of P.O. and resin for 1 h at room temperature.
Pure resin for 18 h at 40 °C.
A mixture of resin and accelerator for 1 h at room temperature.
A mixture of resin and accelerator for 1 h at 40 °C.

(e) Tissues were embedded in fresh epoxy resin (Epon/Araldite) and the blocks were polymerized for 48 h at 60 °C.

4.2.2.2. Sectioning of tissues for TEM

Toludine blue staining of 1 μm thick sections was first used to select the most suitable blocks for each experiment.

Blocks were trimmed by hand using a steel blade, or with a mechanical trimmer, to expose the cut surface. Silver grey to pale gold ultrathin sections were cut on a Reichert-Jung Ultracut using glass knives made on a LKB knifemaker. These sections

were stretched by chloroform fumes before being collected on uncoated 200 mesh nickel grids for immunoelectron microscopy. Generally speaking, smaller, additional thick sections, cut after thin sectioning, often yielded better control of the thick sections, and allowed better light microscopical correlation with the area selected on the thin sections.

4.2.2.3 Immunogold staining for TEM

To distinguish differences between actin filaments (F-actin), or to determine accurately the effects of depolymerisation and AVP on the filaments required higher resolution. The indirect immunogold staining procedure used was an adapted method of Gao *et al.* (1992).

The grid-mounted tissue sections were dried overnight at room temperature and then immunostained for the localization of actin filaments. For electron microscopic study, grids were always kept covered in moist chambers (Petri dishes with moist filter paper on the bottom) between incubations and washes. Incubations and washes were performed at room temperature by floating grids, section facing down, on droplets of the immunolabelling and washing solutions placed on clean pieces of Parafilm. Care was taken not to wet the reverse side of the grids or allow the section to dry. Grids were transferred between drops with anti-capillary forceps to minimize carry-over of solutions. Droplets of buffer washes were administered by syringes fitted with 0.2 μm Millipore filters (Millipore, USA).

The primary antibody used in this study was a purified mouse monoclonal immunoglobulin G (IgG) antibody to chicken gizzard actin (Amersham Laboratories, UK). The secondary antibody was goat anti-mouse IgG coating the surface of either 15 or 10 nm gold particles (Electron Microscopy Sciences, USA).

The immunogold staining procedure on resin sections was as follows:

(a) Non-osmicated sections on 200 mesh nickle grids were etched, by being placed on a droplet of 5% hydrogen peroxide (H_2O_2) for 5 min, to improve antigenic immunoreactivity.

(b) Grids were placed on drops of distilled water for 3 min then jet washed with 10 ml distilled water and dried on fibre free paper.

(c) Grids were submerged for 15 min in the 0.01 M PBS containing 1% bovine serum albumin (BSA) (Fraction V, BDH Chemicals Ltd.,Poole, UK) and 5% normal goat serum to reduce nonspecific background staining.

(d) Drained on fibre free paper.

(e) Grids were then transferred for 2 h to 30 µl drops of the primary monoclonal antibody diluted to a ratio of 1:250 in 0.01 M PBS.

(f) After incubation of the primary antibody, grids were rinsed 4 times with 0.05% Tween 20 in 0.01 M PBS and 4 times with 1% BSA in 0.01 M PBS, for 5 min each time.

(g) Grids were subsequently incubated for 1 h with secondary antibody goat anti-mouse IgG on 10 and 15-nm gold diluted to a final concentration of 1:50 in 0.01 M PBS.

(h) Grids were then rinsed 4 times in PBS, and 4 times in distilled water for 5 min each.

(i) Counterstained with 2% uranyl acetate for 10 min.

(j) Jet washed with distilled water.

(k) Counterstained with lead citrate for 5 min.

(l) Jet washed with distilled water.

(m) The grids were examined and photographed in a Hitachi (Model H-600, Tokyo, Japan) electron microscope operating at 75 kV accelerating voltage.

The specificity of the gold labelling was tested in control specimens by omitting the primary antibody from the protocol and incubating only with the antibody diluent. As a positive control, we stained and examined filament containing intestinal epithelial cells of the frog.

Chapter 5

Results

5.1 Electrophysiology

5.1.1 Steady-state control data from current fluctuation (noise) analysis

It was important to perform initial experiments to acquire the elecrophysiological properties of *Rana fuscigula*. Tissues were studied with CDPC-induced noise analysis during control and experimental conditions according to protocols shown in Fig. 5.1. After exposure to the sequential CDPC concentrations (10 to 50 μM), the blocker was washed out from the apical bathing solution. CDPC caused relatively small, graded inhibitions of I_{Na} not exceeding about 25% (Fig. 5.1) and hence, analyses were done under conditions close to spontaneous rates of apical Na^+ entry (Helman and Baxendale, 1990). Introduction of CDPC induced a single Lorentzian in the PDS, whose f_c varied linearly as a function of [B], allowing estimation of the on- and off-rate coefficients for blocker interaction with the Na^+ channel (Fig. 5.4C). Values for f_c ranged between about 25 and 90 Hz. The plateau value (S_o) of the Lorentzian displayed the expected biphasic relationship with [CDPC] (Fig. 5.4B).

Variability of channel kinetics among species is an important consideration when speculating on transport mechanisms. With this in mind we began by presenting the steady-state control data, the first reported for this species. The means of steady-state values collected during control periods from different groups of experiments are summarized in Table 1. The I_{Na} averaged 10.71 μA/cm², significantly lower than mean values for frog skin from many other species under similar conditions (see

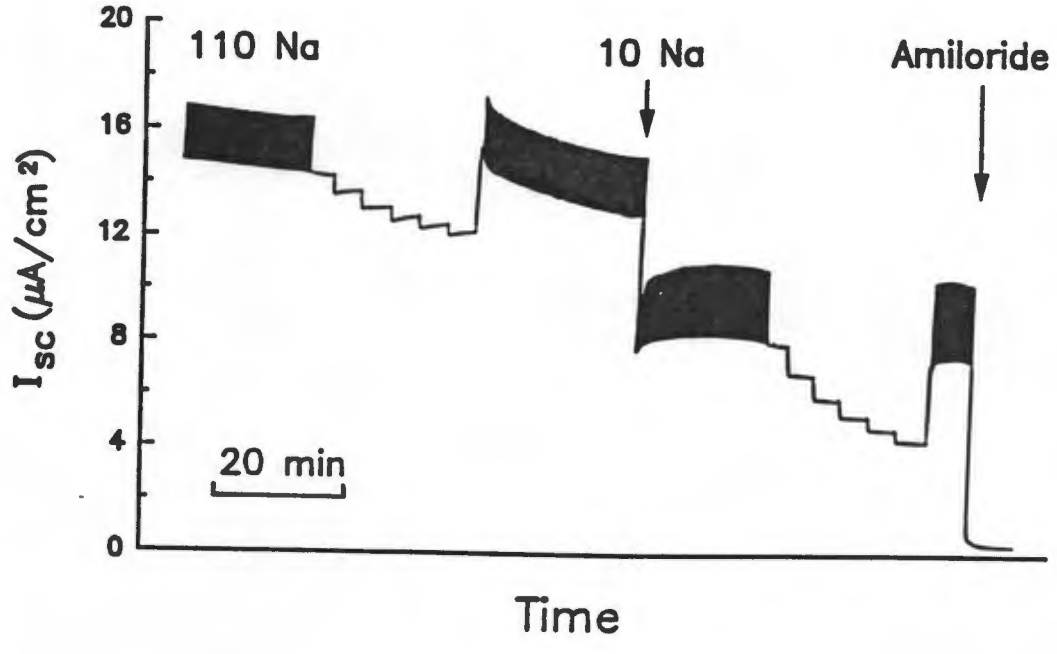

Fig. 5.1 Strip chart recording of an experiment to determine changes in Na^+ channel densities. Tissue perfused with Ringer solutions containing consecutively 110 mM and 10 mM Na^+ in the mucosal solution, were exposed to a staircase increase of CDPC concentrations (10 to 50 μM). The PDS were measured during periods when the pulse generator was turned off. After noise analysis had been completed, the CDPC was washed out and the I_{SC} was allowed to stabilize. At the end of each experiment, amiloride (100 μM) was added to the mucosal solution to determine the amiloride-sensitive I_{SC}, that averaged near 1 μA/cm². Note the increase in the transepithelial conductance from 750 to 920 μS during the relaxation in the I_{SC} after exposure to 10 mM Na^+ in the mucosal solution.

Helman and Kizer, 1990). Often skins with low steady-state control currents were unsuitable for our experiments, since experimental conditions and time-dependent transients reduced the I_{SC} to such low values (1 or 2 μA/cm²) that current fluctuation analysis became unreliable. Accordingly, there were very few skins with steady-state currents large enough to investigate the effects of very low mucosal Na^+ (5 or 10 mM) on the channel kinetics. In most experiments we investigated effects of lowering to 20 mM Na^+.

Table 1: Summary of steady-state values of epithelial Na^+ channels in 110 mM NaCl Ringer

I_{Na} (μA/cm²)	i_{Na} pA	N_O (10^6/cm²)	β'	N_T (10^6/cm²)	k_{ob} (rad/s·μM)	k_{bo} (rad/s)	K_B (μM)
10.71	0.59	21.6	0.38	65.6	4.73	171.7	37.1
±0.98	±0.03	±2.2	±0.02	±8.7	±0.16	±6.8	±1.3
(3.9-27.3)	(0.37-0.90)	(6.1-54.5)	(0.24-0.58)	(7.0-200.8)	(3.6-6.2)	(125.8-234.6)	(24.4-45.8)

Values expressed as means ± S.E.M. (Range) (n = 31)

Epithelial Na^+ channels are generally low conductance channels, with single-channel conductances ranging from 3 to 20 pS (Reviewed by Garty and Benos, 1988; Els and Helman, 1989). In agreement, i_{Na} averaged 0.59 pA, a value comparable to previous results with the patch clamp and noise analysis (see Helman and Baxendale, 1990; Helman and Kizer, 1990). We calculated that, assuming a mean apical membrane voltage of 85 mV and intracellular Na^+ concentration of 14.5 mM (Els and Helman, 1991), single-channel conductance would be about 4.3 pS. Since the value of the mean i_{Na} was not significantly different from other studies on frog skin, the low range for I_{Na} could be explained in terms of the relatively small number of open Na^+

channels, which averaged 21.6 million/cm² in the presence of 110 mM NaCl. Channel open probability averaged 0.38, a value similar to that measured with the patch clamp (Palmer and Frindt, 1988) and with noise analysis (Helman and Baxendale, 1990) and had shown no correlation with I_{Na}. Total channel densities that ranged between 7 and 200 million/cm² paralleled differences in N_O. We also collected 69 records from the control data to analyse the correlation amongst Na^+ channel properties. We found no significant relationships correlated between the I_{Na} and i_{Na} or β' (Table 2). Table 2 shows N_O increased with I_{Na} indicating that the extent of Na^+ transport across tight epithelia was in effect mainly due to the N_O. From the control data (Fig. 5.2), a Linear regression correlation was found between the I_{Na} and N_O.

Table 2: Frog skin control data

N	I_{Na} (μA/cm²)	i_{Na} (pA)	N_o (10^6/cm²)	β'
5	2.79 ± 0.21	0.43 ± 0.02	6.86 ± 0.82	0.58 ± 0.06
12	4.90 ± 0.40	0.66 ± 0.04	8.04 ± 1.20	0.43 ± 0.04
14	8.08 ± 0.74	0.58 ± 0.03	14.48 ± 1.60	0.40 ± 0.04
13	10.99 ± 0.98	0.58 ± 0.03	19.70 ± 2.20	0.36 ± 0.02
11	13.51 ± 1.25	0.52 ± 0.03	27.06 ± 2.62	0.37 ± 0.02
14	17.17 ± 2.22	0.55 ± 0.04	32.69 ± 3.11	0.30 ± 0.02
5	25.84 ± 3.41	0.50 ± 0.03	52.01 ± 5.55	0.43 ± 0.04

Values are means ± S.E.M. ("N" refers to the sample number of the group).

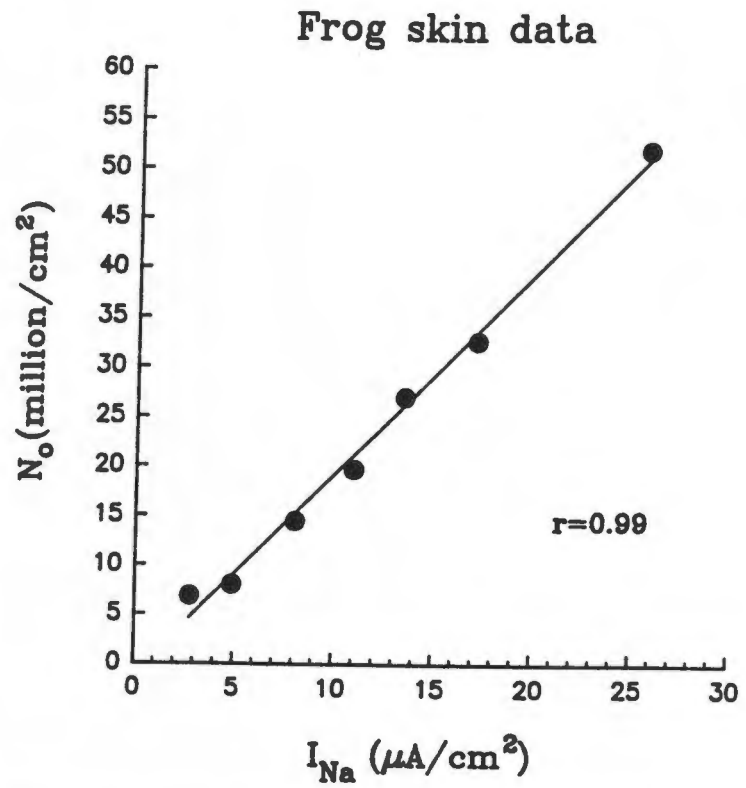

Fig. 5.2 N_O increases with I_{Na}, Linear regression was performed on this data (69 records), and the best correlation was found between the I_{Na} and N_O (r = 0.99, r is the regression coefficient).

The blocker rate coefficients varied widely. k_{ob} averaged 4.73 rad/s·μM, significantly lower than the 7 rad/s·μM determined with CDPC for *Rana pipiens* (Els and Helman, 1991), but higher than in skins from *Rana esculenta* and *Rana temporaria* (Helman and Kizer, 1990). k_{bo} averaged 171.7 rad/s, again slightly lower than in *Rana pipiens* where the off-rate coefficients averaged about 200 rad/s. The reasons for the variability of rate coefficients among tissues of the same and also of different species are unknown. It may indicate that the blocker binding site can be regulated, but membrane potentials, structural and other factors may also be responsible (Helman and Kizer, 1990).

5.1.2 Effects of reducing the mucosal Na^+ concentration

5.1.2.1 Macroscopic current kinetics

After reaching stable transport rates of apical Na^+ entry (I_{Na}) in short-circuited isolated skins, control tissues were exposed to sudden changes in mucosal Na^+ concentrations according to the experimental protocol shown in Fig. 5.3. A reduction of the Na^+ concentration in the mucosal solution produced a transient decrease in the rate of Na^+ entry into the cells. Within seconds of reducing the mucosal Na^+ concentration to 20 mM or lower, the I_{SC} decreased to a minimum value followed by a relatively slow return to a new but lower steady-state level. The slow component for the relaxation in I_{SC} could be fitted by a single exponential, typically with time constants of about 9 min for tissues exposed to 20 mM Na^+. After 20 min recovery, levels of I_{SC} averaged about 24% or 35% below original levels in 20 and 10 mM Na^+, respectively (Table 3). Concurrently, after changing the mucosal Na^+ to 20 mM, the transepithelial conductance increased by 39% from a mean 436 ± 51 to 581 ± 40 μS.

5.1.2.2 Reduction in mucosal Na concentration increased channel densities

Figure 5.4 shows the changes of S_o and $2\pi f_c$ of the CDPC-induced Lorentzians caused by a decrease in luminal Na^+ to 10 mM. A large decrease in the mean value of S_o was caused by the drop in mucosal Na^+ (Fig. 5.4B) while it had little effect on the on- and off-rate coefficients (Fig. 5.4C). Thus k_{ob} did not change significantly while k_{bo} decreased by only 7%, which was the main reason why the K_B reduced from about 41 to 36 μM (Table 3).

We investigated the effects of decreasing the mucosal Na^+ concentration on two groups of skins. On a group of eight epithelia, selected on the basis of their inherent higher transport rates, the effects of a reduction to 10 mM were examined. The

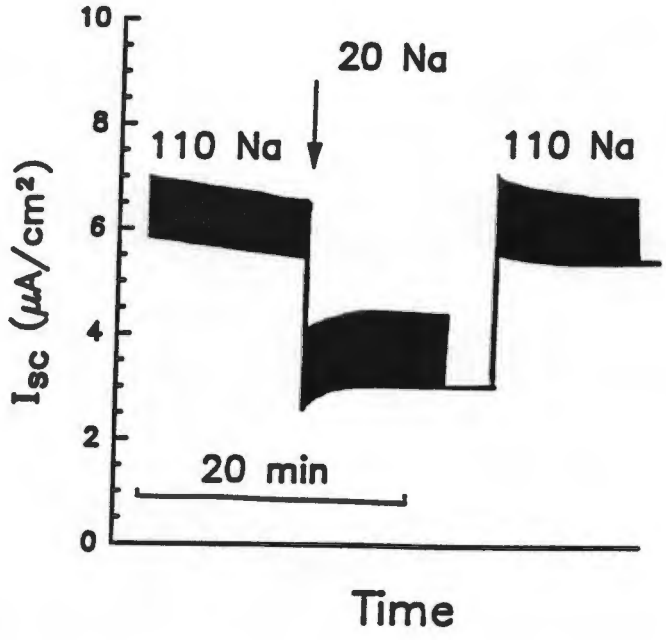

Fig. 5.3 An example of an experiment to show autoregulation of the I_{sc} in isolated frog skin epithelium. The solid line is the recording of the I_{sc}. The upward deflections are responses to a 3 mV pulse applied every 15 seconds, and the difference of the deflections of the I_{sc} was used to calculate the transepithelial conductance. Initially the tissue was exposed to 110 mM Na^+ Ringer solution on both sides. Replacing the mucosal with isosmolar Ringer containing 20 mM Na^+ caused a rapid inhibition of the I_{sc} followed by a slow recovery towards a new steady-state. The relaxation in the I_{sc} was brought about by an increase in the transepithelial Na^+ conductance from 375 to 460 μS. A return to 110 mM Na^+ Ringer solution reversed all macroscopic changes and the conductance slowly decreased to a value of 410 μS after 10 min.

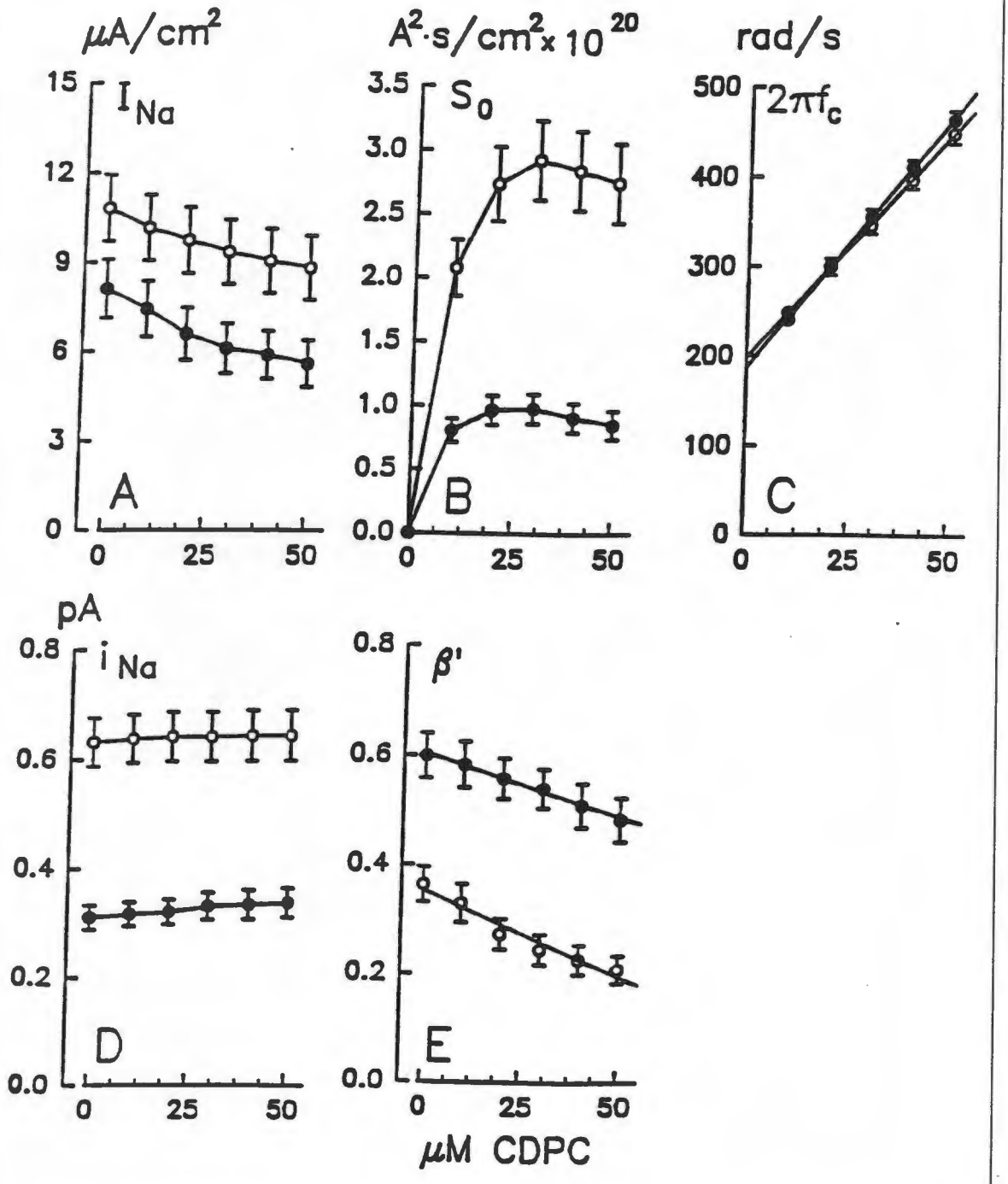

Fig. 5.4 CDPC-dependent changes of I_{Na}, S_O, $2\pi f_c$, i_{Na} and β' in tissues perfused with 110 mM Na^+ (o) and 10 mM Na^+ (•) in the mucosal solutions. Mean changes of these parameters are summarized in Table 3.

compensatory changes in this group were the largest and best illustrated effects of decreasing mucosal Na^+ concentration. Unfortunately, the intrinsic transport rates and channel densities of the majority of frog skins were much lower than in this sample. Since our depolymerising studies and time-related transients further reduced the I_{SC} to even lower levels, it was not feasible to study with noise analysis effects in 10 mM Na^+, consequently, we were bound in all other experiments to examine the effects of reducing mucosal Na^+ to 20 mM. For comparison, we summarized in Table 3 the effects on Na^+ channels of reducing mucosal Na^+ to 10 and to 20 mM. One can observe that, while the magnitude of changes in channel densities (N_T) was smaller than in the 20 mM Na^+ experimental group, the pattern of changes was still similar.

Decreasing the mucosal Na^+ concentration lowers the electrochemical driving force for Na^+ across the apical membrane, resulting in a lower transport rate. After 20 min in 10 mM Na^+, and in compensation for the decrease in i_{Na}, the mean number of open channels had increased markedly by 158% from nearly 27 to 64 million/cm² (Table 3), being the main mechanism responsible for the relaxation of the I_{Na} towards the original level (refer to Fig. 5.5). Increases of open channel density may arise by recruitment of channels from closed to open state (a change of open channel probability, β'), and/or by an increase in the total channel density (Els and Helman, 1991). Foremost, we determined that the reduction in mucosal Na^+ to either 10 or 20 mM consistently increased channel open probability. In 10 mM Na^+, β' increased by 63% from a mean of 0.35 to 0.55 (Table 3). This mechanism alone could not account for the large increase in N_O. We also calculated that concurrently with the increase in N_O, N_T had increased significantly by an average of 81% from 74 to 120 million/cm² (Table 3).

Table 3: Effects of decreased mucosal Na^+ on epithelial Na^+ channels

		Control	Experiment	E/C
I_{Na} (μA/cm²)				
	10 mM	14.22 ± 1.60	9.47 ± 1.03	0.65 ± 0.02
	20 mM	10.69 ± 1.04	8.14 ± 0.93	0.76 ± 0.04
i_{Na} (pA)				
	10 mM	0.57 ± 0.04	0.16 ± 0.01	0.28 ± 0.02
	20 mM	0.65 ± 0.04	0.30 ± 0.02	0.47 ± 0.01
N_o (10^6 /cm²)				
	10 mM	26.6 ± 4.6	64.3 ± 11.0	2.58 ± 0.37
	20 mM	17.8 ± 2.3	29.4 ± 4.3	1.65 ± 0.10
β'				
	10 mM	0.35 ± 0.04	0.55 ± 0.04	1.63 ± 0.16
	20 mM	0.40 ± 0.03	0.61 ± 0.03	1.55 ± 0.08
N_T (10^6/cm²)				
	10 mM	74.8 ± 13.8	120.7 ± 20.6	1.81 ± 0.30
	20 mM	49.2 ± 12.5	57.5 ± 14.7	1.24 ± 0.10
k_{ob} (rad/s·μM)				
	10 mM	5.26 ± 0.30	5.96 ± 0.57	1.12 ± 0.07 *
	20 mM	5.13 ± 0.13	5.52 ± 0.11	1.08 ± 0.02 *
k_{bo} (rad/s)				
	10 mM	215.4 ± 14.8	204.6 ± 12.7	0.93 ± 0.01
	20 mM	193.9 ± 8.4	186.4 ± 8.4	0.96 ± 0.02
K_B (μM)				
	10 mM	41.2 ± 2.9	35.8 ± 3.6	0.84 ± 0.06
	20 mM	38.6 ± 1.9	34.4 ± 1.7	0.90 ± 0.02

The three columns represent values from paired experiments where the mucosal Ringer solution was reduced from 110 mM Na^+ to 10 mM Na^+ (n = 8), and to 20 mM Na^+ (n = 14), respectively. All values are means ± S.E.M. Non-significant changes ($p < 0.05$) assessed on a paired basis are indicated by *.

Therefore, both mechanisms are used by these cells to stabilize the Na^+ transport rate. The changes were readily reversible on return to 110 mM Na^+ (Data not shown).

5.1.2.3 Reduction in mucosal sodium concentration causes rapid changes in N_O

We also performed an experiment to study the time course of changes in N_O induced by reducing the mucosal Na^+ to 20 mM. The control data for this group of six skins was as follows: I_{Na} averaged 16.17 ± 3.2 μA/cm²; mean i_{Na} was 0.56 ± 0.03 pA; N_O averaged 29.0 ± 6.2 million/cm²; k_{ob} was 4.80 ± 0.51 rad/s·μM; k_{bo} was 152.1 ± 1.3; K_B was 33.6 ± 3.6 μM; mean β' was 0.28 ± 0.02 and the mean N_T was 109.2 ± 16.3 million/cm².

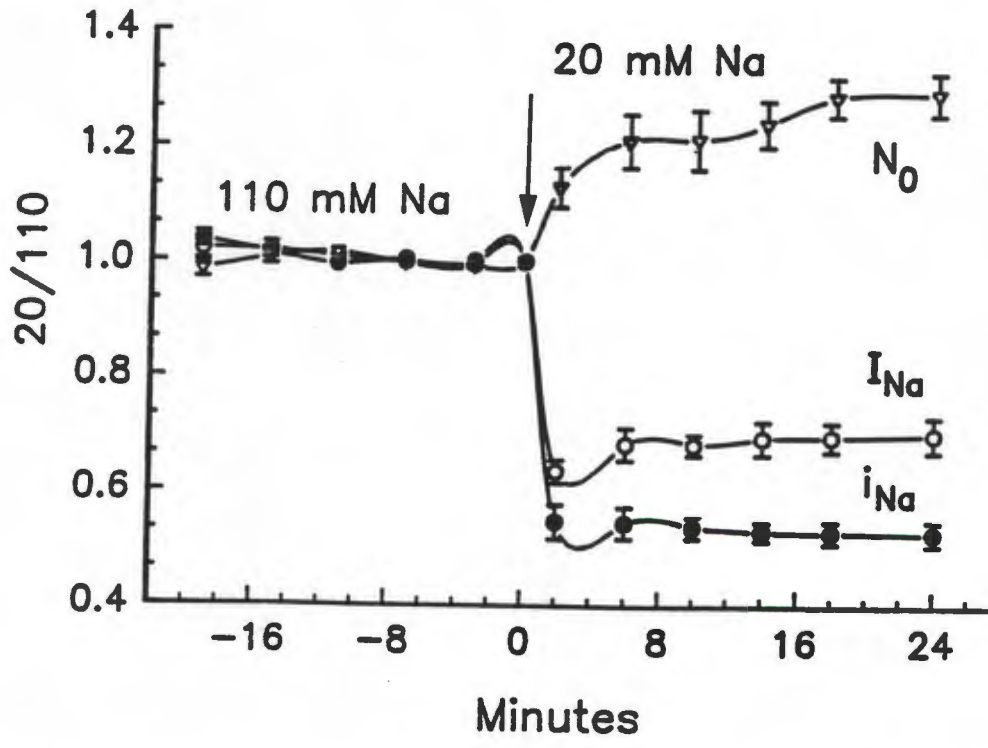

Fig. 5.5 Response of I_{Na}, N_O, and i_{Na} to a reduction in mucosal Na^+ concentration from 110 mM to 20 mM as determined with the time-course protocol. Data are expressed as values in 20 mM Na^+/ values in 110 mM Na^+ (20/110). The control values for this group of tissues (n = 6) appear in the text. Each noise analysis took about 2.5 minutes to complete.

The results illustrated in Fig. 5.5 were consistent with our initial observation (Table 3). A reduction in mucosal Na^+ concentration decreased i_{Na} by about 57% within 2 minutes and continued to decline at a lesser rate for the next 20 min. Despite the reduction in i_{Na}, the I_{Na} returned to within 30% of the original value because of a concurrent increase in N_O. Of interest was the rate at which new open channels were recruited. We determined that an increase in N_O took place within the first 2 minutes. This ruled out any possibility that new open channels were recruited by synthesis. After the initial increase, N_O continued to increase steadily for the next 20 min, approaching a new steady state, and being primarily responsible for the relaxation of I_{Na} towards the original control level.

5.1.3 Effects of depolymerizing the cytoskeleton on autoregulatory mechanism of Na^+ channel densities

The rapid recruitment of new active channels in response to changes in the luminal Na^+ concentration may be from quiescent apical channels or from a pool residing in some cytoplasmic site. To test the latter hypothesis we also investigated whether the cytoskeleton was involved in the autoregulation of channel densities in response to a change in mucosal Na^+ to 20 mM. It has become established that the cytoskeleton plays a central role in the regulation of epithelial cell membrane function by continually inserting and removing selected components. Best known is the role of the cytoskeleton in regulating the water channels by vasopressin (Pearl and Taylor, 1985).

5.1.3.1 Disrupting microtubules by colchicine did not alter the effects of reduced mucosal sodium concentration

The data of disrupting microtubules on frog skin epithelia by colchicine are summarized in Table 4. It shows the effects of 100 μM colchicine on epithelial Na^+

channels. The mean macroscopic I_{Na} was significantly decreased by 44% in the presence of colchicine. Since the control i_{Na} averaged 0.53 pA and was not changed significantly by colchicine to 0.49 pA, the data in Table 4 makes it clear that decrease of I_{Na} by colchicine was due to a reduction of N_O from means of 21.3 to 14.6 million/cm^2. Significantly, the changes in N_O caused by colchicine were decreased principally through changes of N_T (open + closed channels). The mean open probability (β') of control group averaged 0.37 and this was increased to 0.47 after treating tissues with colchicine for 3 hours. A summary of CDPC blocker rate coefficients is given in Table 4. Colchicine treatment of these tissues caused on average a 13% decrease of k_{ob} and a 6% increase of k_{bo}, and hence a 24% increase of the control K_B that averaged 42.9 μM.

Table 4: Effects of 100 μM colchicine on epithelial Na^+ channels

	110 mM (C)	Colchicine (E)	E/C
I_{Na} (μA/cm²)	9.93 ± 1.78	6.16 ± 1.18	0.56 ± 0.05
i_{Na} (pA)	0.53 ± 0.06	0.49 ± 0.05	0.95 ± 0.06*
N_o (10^6 /cm²)	21.3 ± 5.8	14.6 ± 3.7	0.59 ± 0.06
β'	0.37 ± 0.02	0.47 ± 0.04	1.32 ± 0.10
N_T (10^6/cm²)	59.6 ± 17.5	35.2 ± 10.2	0.47 ± 0.04
k_{ob} (rad/s·μM)	4.10 ± 0.29	3.63 ± 0.33	0.87 ± 0.05
k_{bo} (rad/s)	144.9 ± 8.7	144.7 ± 8.9	1.06 ± 0.05*
K_B (μM)	36.5 ± 3.6	42.9 ± 4.1	1.24 ± 0.08*

Values are means ± S.E.M. (n = 6). Non-significant changes ($p < 0.05$) assessed on a paired basis are indicated by *.

Autoregulatory changes in channel densities, induced by a reduction in mucosal Na^+ concentration to 20 mM, were not affected by depolymerization of the microtubules with 100 µM colchicine for 3 hours (Table 5). The manoeuvre decreased the i_{Na} to 0.26 pA, a decrease by nearly identical proportions as previously shown (Table 3). Despite the reduction in entry rate, the I_{Na} recovered to within 30% of earlier steady-state levels after 20 min, mainly due to a 50% increase in the number of open channels from 19.3 to 27.4 million/cm^2. The change in open channel density (N_O) was primarily brought about by a 40% increase in the channel open probability (β'), since N_T did not change significantly from control values.

Table 5: Effects of decreased mucosal Na^+ on epithelial Na^+ channels after treatment with 100 µM colchicine

	110 mM (C)	20 mM (E)	E/C
I_{Na} (µA/cm^2)	9.89 ± 1.42	6.89 ± 1.09	0.71 ± 0.02
i_{Na} (pA)	0.55 ± 0.04	0.26 ± 0.02	0.48 ± 0.03
N_o (10^6 /cm^2)	19.3 ± 3.0	27.4 ± 4.5	1.50 ± 0.15
β'	0.46 ± 0.04	0.61 ± 0.03	1.40 ± 0.15
N_T (10^6/cm^2)	49.5 ± 15.1	50.1 ± 9.0	1.26 ± 0.20*
k_{ob} (rad/s·µM)	3.98 ± 0.17	4.39 ± 0.14	1.12 ± 0.03
k_{bo} (rad/s)	122.6 ± 6.1	121.1 ± 6.4	0.99 ± 0.03*
K_B (µM)	31.6 ± 2.4	27.7 ± 1.7	0.89 ± 0.05*

Values are means ± S.E.M. (n = 8). Non-significant changes ($p < 0.05$) assessed on a paired basis are indicated by *.

5.1.3.2 Disrupting microfilaments by cytochalasin B blocks the increase in open channel density

We first performed experiments to study the direct effects of cytochalasin B (CB) treatment for 2 hours on frog skin epithelia. Data are presented in Table 6 on steady-state control values (110 mM Na) and experimental values (CB) of Na^+ channels. It appears that CB had little direct effect on the channels after 2 hours. By which time the I_{Na} had declined to 74% of mean control values (also see Fig. 5.6).

Table 6: Effects of cytochalasin B on apical membrane Na^+ channels

	110 mM (C)	Cytochalasin B (E)	E/C
I_{Na} ($\mu A/cm^2$)	13.47 ± 1.41	9.85 ± 0.84	0.74 ± 0.02
i_{Na} (pA)	0.62 ± 0.08	0.67 ± 0.06	1.13 ± 0.11*
N_o (10^6 /cm^2)	23.9 ± 4.2	15.8 ± 2.6	0.69 ± 0.07
β'	0.39 ± 0.04	0.47 ± 0.05	1.26 ± 0.15*
N_T (10^6/cm^2)	63.9 ± 10.9	35.5 ± 6.8	0.59 ± 0.10
k_{ob} (rad/s·μM)	5.11 ± 0.32	4.64 ± 0.49	0.90 ± 0.07*
k_{bo} (rad/s)	229.2 ± 28.7	247.0 ± 27.0	1.10 ± 0.06*
K_B (μM)	43.9 ± 3.8	54.9 ± 6.9	1.26 ± 0.12*

Values are means ± S.E.M. (n=6). Non-significant changes ($p < 0.05$) assessed on a paired basis are indicated by *.

This was due mainly to a 31% decrease in N_O since single channel current (i_{Na}) did not change during this time. Whether this was a direct effect, or merely represents a

time-related transient, is not known. During this experiment, the open probability of the channels was increased by 26% and the rate coefficients did not change significantly.

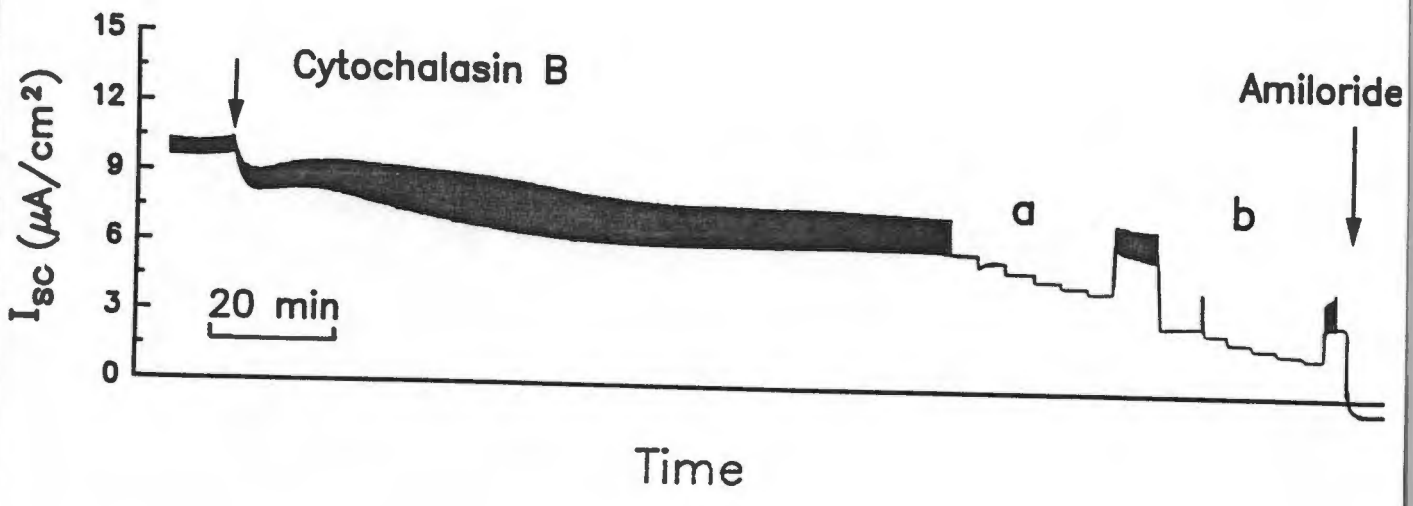

Fig. 5.6 A strip chart recording of an experiment to determine autoregulation changes in channel densities after the tissue had been treated in cytochalasin B (10 μg/ml) for 2 hours. The upward current deflections in response to 3 mV pulses are indicative of the transepithelial conductance of the tissue. Noise analysis was performed with tissues exposed to 110 mM Na^+ Ringer during period (a), and when tissues were exposed to 20 mM Na^+ Ringer solution during period (b). Note the absence of any relaxation in the I_{sc} immediately prior to period (b). During control steady-state conditions the mean transepithelial conductance was 260 μS. This increased to 430 μS immediately prior to period a.

We also performed another group of experiments to study the autoregulation changes in channel densities after epithelial tissues had been treated by 10 μg/ml CB for 2 hours. Figure 5.6 shows that within 5 min of placing isolated frog epithelia in CB, the I_{SC} decreased by about 2 to 5 μA/cm², and, thereafter, continued to decline at a slower rate to a new steady-state level after about 90 min. Concurrently, the transepithelial conductance increased by between 50% and 100%. The microfilament-disrupting drug treatment caused very little change in the properties of the channels (Table 6). This becomes apparent when comparing the values in 110 mM Na^+ from two groups with nearly identical macroscopic transport rates (Table 3 and 7).

Table 7: Effects of decreased mucosal Na^+ on epithelial Na^+ channels after treatment with 10 μg/ml cytochalasin B

	110 mM (C)	20 mM (E)	E/C
I_{Na} (μA/cm²)	10.10 ± 1.07	6.32 ± 1.07	0.63 ± 0.05
i_{Na} (pA)	0.42 ± 0.03	0.27 ± 0.02	0.65 ± 0.04
N_o (10^6 /cm²)	24.3 ± 2.4	23.5 ± 2.4	0.99 ± 0.12*
β'	0.43 ± 0.04	0.67 ± 0.03	1.69 ± 0.17
N_T (10^6/cm²)	59.5 ± 8.3	46.6 ± 10.1	0.89 ± 0.28*
k_{ob} (rad/s·μM)	4.01 ± 0.25	4.24 ± 0.25	1.06 ± 0.04*
k_{bo} (rad/s)	120.8 ± 5.3	129.0 ± 4.8	1.08 ± 0.04*
K_B (μM)	30.7 ± 1.6	31.1 ± 1.7	1.03 ± 0.06*

Values are means ± S.E.M. (n = 9). Non-significant changes ($p < 0.05$) assessed on a paired basis are indicated by *.

The main difference was that i_{Na} averaged 0.42 pA in cytochalasin-treated tissues, about 30% lower than mean values in 110 mM Na^+. Consequently, the mean N_O was correspondingly slightly higher than in the untreated group.

The ability of the tissues to increase their membrane Na^+ permeability in response to a reduction in the rate of Na^+ entry was diminished by depolymerization of the microfilaments (Fig. 5.7).

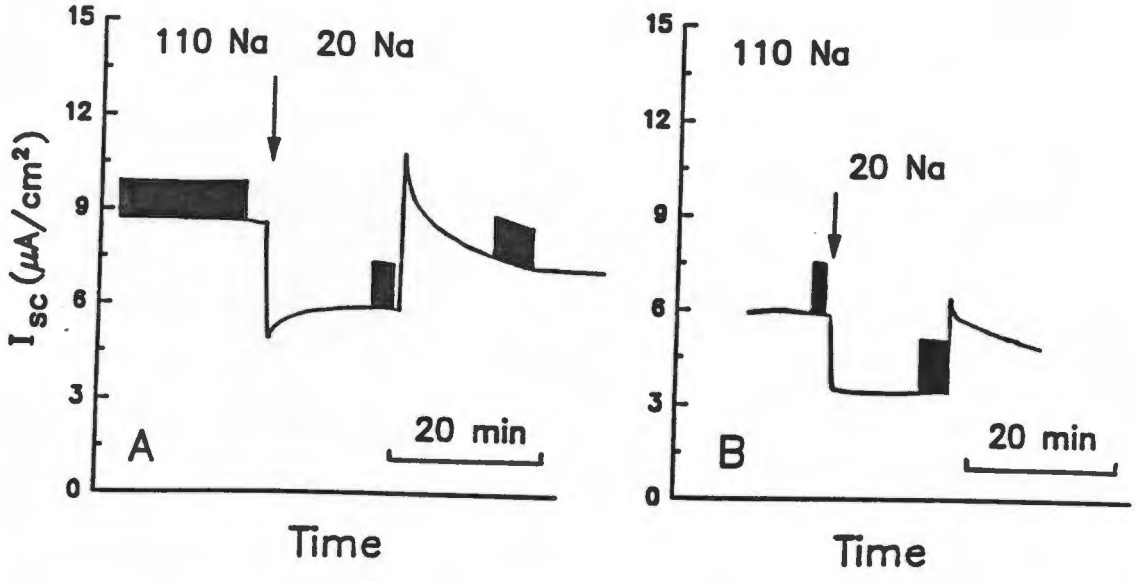

Fig. 5.7 Disruption of microfilaments with cytochalasin B (CB) prevents autoregulatory relaxation of the Na^+ transport rate. Panel A shows the normal response of the I_{SC} when we decrease the mucosal Na^+ from 110 to 20 mM. After about 20 min, the tissue was returned to 110 mM Na^+ Ringer and changes in I_{SC} and the transepithelial conductance were reversed. Notice the big overshoot of the I_{SC} followed by a return towards original levels. Panel B is from the same tissue but after treatment with CB to prevent polymerization of the microfilaments. Also note that there is little sign of any relaxation of the I_{SC} in response to a decrease in mucosal Na^+ to 20 mM, and the overshoot is much reduced on return to 110 mM Na^+ Ringer solution.

After the cytochalasin B treatment and in response to a reduction in mucosal Na^+ to 20 mM, the I_{Na} recovered to within 37% of previous levels compared to a recovery of within 24% for the tissue not treated with CB (Table 3 and 7). Results with current fluctuation analysis showed that, unlike before, this was as a result of an inability by the tissues to autoregulate channel densities. Significantly, a decrease in mucosal Na^+ to 20 mM did not produce the expected increase in N_O which remained essentially unchanged at control values near 24 million/cm². The mean open probability (β') still increased as before, from 0.43 to 0.67 despite treatment with CB. Accordingly, N_T did not increase, but actually reduced slightly, but not significantly, from about 60 to 47 million/cm². We confirmed these results in two skins with significantly higher transport rates and channel densities (data not shown). Subjecting these cytochalasin-treated tissues to an even greater reduction in mucosal Na^+ (110 to 10 mM Na^+) failed to produce any increase in the number of open channels (N_O), or the total number of Na^+ channels (N_T).

5.1.4 Disrupting Actin Filaments did not Interfere with the Regulation of Na^+ Channels by AVP

The hormonal control of Na^+ channels by vasopressin has been intensively studied by noise analysis and patch clamp. Using noise analysis, Li *et al.* (1982) have shown that oxytocin (which also elicits an antidiuretic response) increases Na^+ permeability by increasing the Na^+ channel density from 1.03 to 4.4 Na^+ channels per 10 fF, with little change in single-channel conductance and in channel open probability of the toad uninary bladder cells. In a previous study, Els and Helman (1991) demonstrated that vasopressin increases apical membrane Na^+ conductance by raising the number of open Na^+ channels from 67.8 to 96.3 million/cm² in the apical membranes of the frog skin epithelial cells. Similarly, Marunaka and Eaton (1991) demonstrated that AVP causes an increase in the number of active Na^+ channels in the patches (each patch

increased from 2 to 6 channels) of the apical membrane, with no change in the P_o (about 0.4). In the collecting duct and toad urinary bladder, actin microfilaments are implicated in the mechanism whereby vasopressin induces an increase in transepithelial water transport. We know the response of AVP on the epithelial tissues is very complicated, because AVP caused large increases in N_O and N_T. This was the reason why we performed the underlying experiments to examine whether disruption of the actin cytoskeleton would have any effect on the hormonally-induced changes in channel densities caused by AVP.

5.1.4.1 Steady-state experiments

Current fluctuation analysis of apical membrane Na^+ channels was carried out on the isolated frog epithelial tissues during control and experimental periods following experimental protocols shown in the strip chart recording (Fig. 5.8A and B). During both control periods, a sequence of increasing CDPC concentrations was used to inhibit the macroscopic currents of apical Na^+ entry. After a complete washout of CDPC from the apical solution, and the relaxation of the I_{Na} towards a new steady-state, epithelia were then treated with vasopressin for about 30 minutes (Fig. 5.8). Thereafter, the tissues were again subjected to CDPC-induced noise analysis with the protocols identical to those of the control period. Following the washout of CDPC from the mucosal solution, the tissues were given 100 μM amiloride from the mucosal solution for determination of the amiloride-sensitive Na^+ current defined as I_{Na}.

5.1.4.2 Macroscopic changes of I_{Na}

The changes of I_{Na} in response to 30 mU/ml AVP are summarized in Table 8. The values of I_{Na} reported in Table 8 were measured immediately before stimulation of

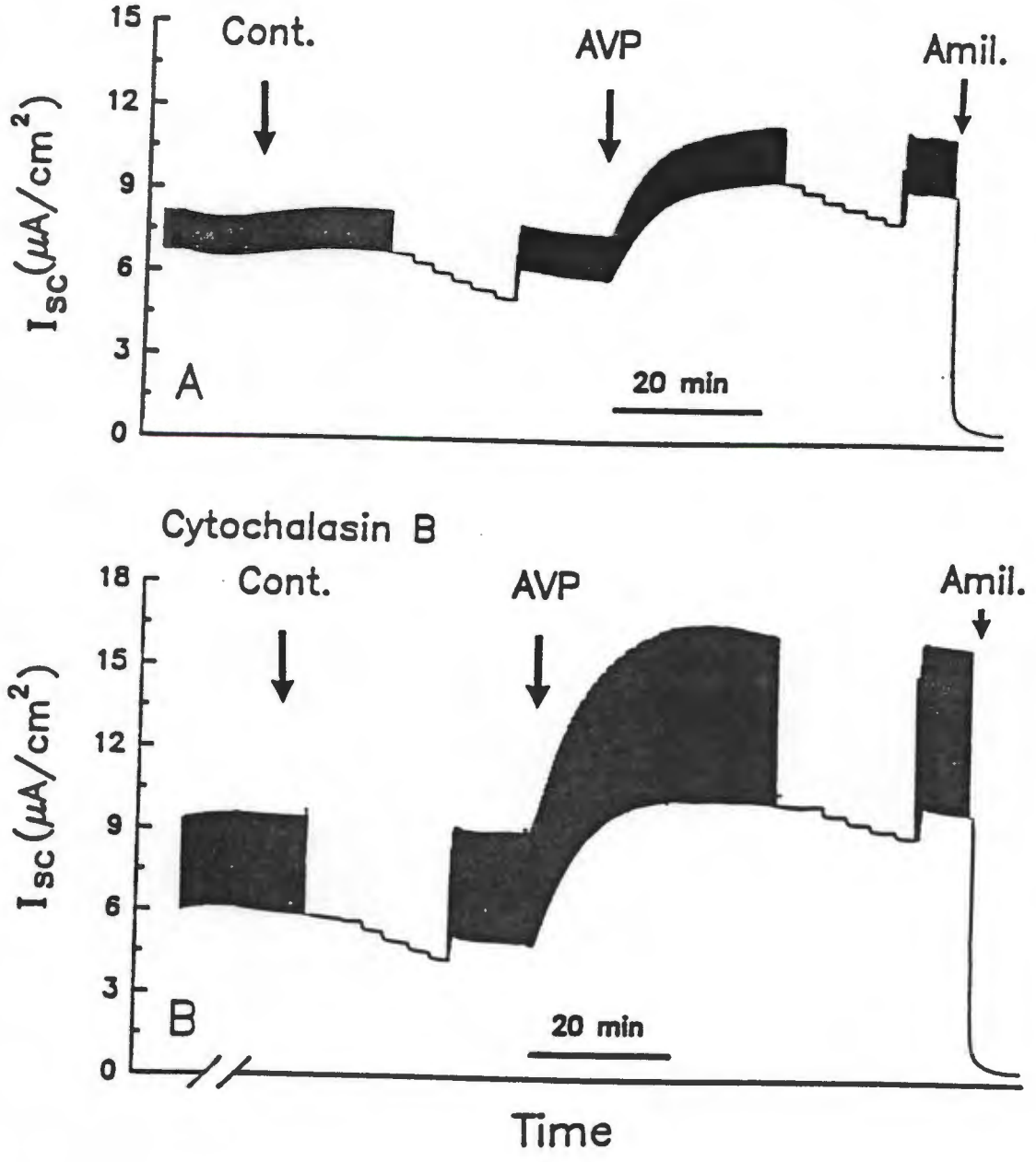

Fig. 5.8 Strip chart recordings of a paired experiment to determine the regulation of Na^+ channels by AVP. Noise analysis was performed during the control and experimental periods. The recording in panel A demonstrates the usual response of AVP. Notice after 20 min AVP stimulation, the transepithelial conductance had increased from 566 μS to 733 μS. The recording in panel B is from the same tissue but after treatment with cytochalasin B, for about 2 hours, to depolymerize the microfilaments. Notice that there is a big increase in the transepithelial conductance after the CB treated experiment; also there is about a triple increase in the transepithelial conductance from 816 μS to 2.18 mS while the tissue was stimulated with AVP.

AVP, and at a steady-state of the response, just prior to the addition of CDPC to the mucosal solution. In the CB-untreated tissues, after the addition of AVP for about 25 to 30 min the control I_{Na} was stimulated from averaged 9.38 ± 1.26 to 14.44 ± 2.26 μA/cm². The effects of AVP on I_{Na} were reversible (Fig. 5.8A), and after allowing the tissues to recover to unstimulated steady-state, the tissues were treated with 100 μM Amiloride which ensured the complete blockage of Na^+ channels, and, therefore, complete inhibition of the Na^+ current component (Helman and Baxendale, 1990). In the CB-treated tissues the addition of AVP also caused a stimulation of the transport rate within 2 minutes, and the I_{Na} was increased from averaged 6.39 ± 0.96 to 9.11 ± 1.46 μA/cm². In the paired experiments, the addition of AVP caused no significant difference in the E/C values of Na^+ transport rate between CB-treated and untreated groups (Table 8).

5.1.4.3 Results from noise analysis

Summarized in Fig. 5.9 are the changes of S_o and $2\pi f_c$ of the blocker-induced Lorentzian and the blocker-dependent changes of macroscopic I_{Na} measured in control, and experimental periods of 11 paired epithelia treated with 30 mU/ml AVP. For convenience, the mean changes of I_{Na}, S_o, $2\pi f_c$, and i_{Na} were shown in Fig. 4.8, although analysis was done for each individual tissue providing the statistical information given in Fig. 5.9 and Table 8. By comparison with the data presented in Table 1 and 3, it is clear that the properties of the tissues used in the current experiments were similar to those used in the previous experiments. As before, CDPC caused a relatively small but graded inhibition of I_{Na} at concentrations of 10 to 50 μM CDPC (Fig. 5.9A and E), S_o showed the expected biphasic dependency on CDPC concentrations with $2\pi f_c$ rising linearly with increase in the CDPC concentrations (Fig. 5.9B and C). In determining how I_{Na} is increased by AVP, the Lorentzian values S_o and f_c are important, because they relate to the channel kinetics (k_{ob} and k_{bo}).

Table 8: Summary of effects of AVP on apical membrane Na^+ channels in untreated and CB-treated epithelial cells

	Control (C)	AVP (E)	E/C
I_{Na} (μA/cm²)			
untreated	9.38 ± 1.26	14.44 ± 2.26	1.562 ± 0.128
CB-treated	6.39 ± 0.96	9.11 ± 1.46	1.464 ± 0.137
i_{Na} (pA)			
untreated	0.65 ± 0.04	0.45 ± 0.05	0.681 ± 0.047
CB-treated	0.58 ± 0.04	0.44 ± 0.03	0.795 ± 0.065
N_o (10^6 /cm²)			
untreated	16.1 ± 3.6	39.3 ± 9.2	2.435 ± 0.281
CB-treated	12.3 ± 2.7	21.3 ± 3.5	2.033 ± 0.296
β'			
untreated	0.45 ± 0.05	0.40 ± 0.04	0.928 ± 0.096 *
CB-treated	0.47 ± 0.06	0.40 ± 0.05	0.925 ± 0.124 *
N_T (10^6/cm²)			
untreated	39.7 ± 9.1	115.3 ± 29.8	2.925 ± 0.561
CB-treated	27.3 ± 4.1	58.2 ± 10.1	2.852 ± 0.716
k_{ob} (rad/s·μM)			
untreated	4.39 ± 0.11	4.37 ± 0.11	0.999 ± 0.015 *
CB-treated	4.40 ± 0.21	4.39 ± 0.20	1.008 ± 0.046 *
k_{bo} (rad/s)			
untreated	216.0 ± 8.8	232.0 ± 11.8	1.074 ± 0.032
CB-treated	237.5 ± 11.7	268.8 ± 18.8	1.126 ± 0.042
K_B (μM)			
untreated	49.9 ± 2.9	53.5 ± 3.3	1.078 ± 0.043 *
CB-treated	55.3 ± 3.9	61.5 ± 3.5	1.141 ± 0.068 *

Values are means ± S.E.M. (n = 11). Non-significant changes ($p < 0.05$) assessed on a paired basis are indicated by *.

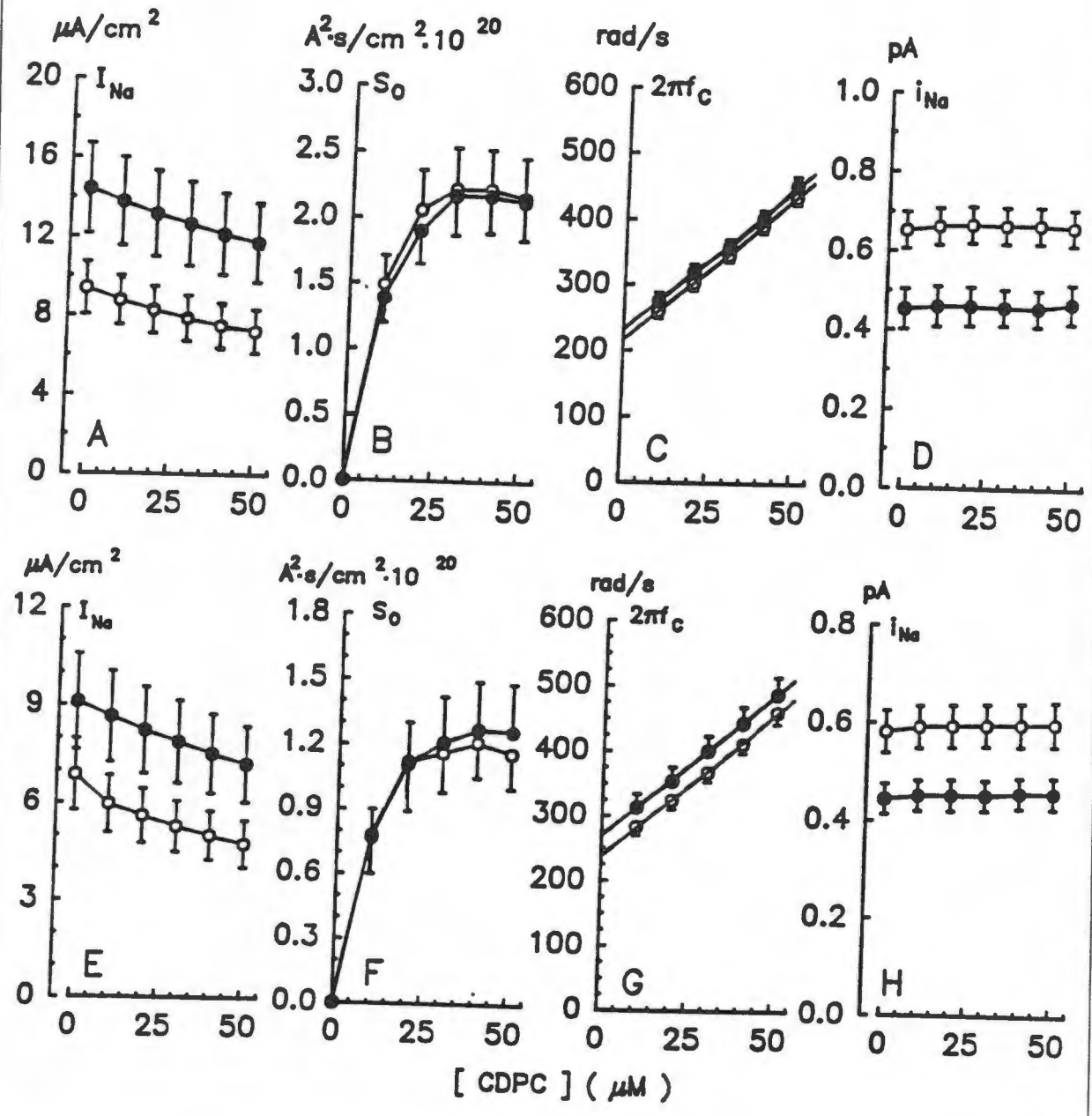

Fig 5.9 Blocker-dependent changes of I_{Na}, S_O, $2\pi f_c$, and i_{Na} in control (110 mM Na^+) (o), and experimental (30 mU/ml AVP) (•) periods. A-D show the CB-untreated tissues in response to AVP. E-H show the CB-treated tissues in response to AVP. Values are means ± S.E.M.

The Lorentzian in the presence of AVP has a slightly lower power than in the control. This indicates a smaller S_O value at different blocker concentrations, and at the various blocker concentrations also shows a linear increase with no change in the slope (Fig. 5.9B, C, F, G). It was clear in all the experiments on both groups (CB-untreated and CB-treated) that AVP caused a small but significant increase in the off-rate coefficient k_{bo}, with no significant change of the on-rate coefficient k_{ob}. The increases of k_{bo} averaged about 7% (untreated) and 12% (CB-treated). Accordingly, K_B increased from 49.9 ± 2.9 to 53.5 ± 3.3 μM in untreated experiments, and from 55.3 ± 3.9 to 61.5 ± 3.5 in CB-treated experiments.

The i_{Na} remained essentially constant with increasing CDPC concentrations, further there was a slight increase with blocker concentration. Extrapolation of i_{Na} to zero blocker concentration gave a mean control i_{Na}, and was significantly decreased in response to AVP from 0.65 to 0.45 pA in the untreated group. In the CB-treated group, AVP caused i_{Na} to decrease from an averaged 0.58 to 0.45 pA.

Control N_O averaged 16.1 million/cm² at the mean I_{Na} of these CB-untreated experiments. As expected, 30 mU/ml AVP caused significant increases of N_O averaging 244% over the reading for the control, for the untreated group (Table 8). In CB-treated experiments, AVP also caused a significant increase of N_O from mean 12.3 to 21.3 million/cm². Noise analysis results showed that even depolymerization of actin filaments had no significant effect on the modulation of Na^+ channels by AVP (E/C values of N_O and i_{Na} have no significant differences, $p < 0.05$). Accordingly, AVP caused an increase in the Na^+ transport rate mainly by doubling the number of open Na^+ channels (N_O), despite the decrease in single-channel current (i_{Na}). These results provide compelling evidence that AVP increases the apical Na^+ entry by virtue of a change of open channel density, and is consistent with previous conclusions derived from experiments carried out with oxytocin in K^+-depolarized epithelia (Li *et al.*,

1982), and with AVP in non-depolarized frog skin epithelia (Helman *et al.*, 1983). In our experiments, the increases of N_O are accompanied by decreases of i_{Na} leading to a smaller increase of I_{Na} than would be expected from changes of open channel density and the total number of Na^+ channels.

Increases of open channel density may arise by recruitment of channels from closed states into open states of the channel, hence by a change of open the probability of the channel, and/or by an increase of total channel density (open and closed channels). As indicated in Table 8, AVP essentially caused no change in open probability. Similarly, it was observed in the CB-treated experiments, with the mean control value of 0.47 to 0.39 in this group, although here the changes were not significant. Though there was a slight decrease of open probability, it was clear that the increase of open channel density must have occurred by an increase of the total number of channels (N_T).

N_T calculated from the quotient of N_O / β' indicated that control N_T averaged 39.7 (untreated) and 27.3 (CB-treated) milliom/cm², and was significantly increased by AVP to 115.3 (untreated) and 58.2 (CB-treated) million/cm², respectively. N_T was increased by about 200% of control values for both groups, therefore, we concluded that the changes in open channel densities occurred mainly by changes in the total number of channels (N_T) since the channel open probability (β') did not increase.

Our results indicate that disrupting actin microfilaments on isolated frog skin epithelial cells did not alter the regulation of Na^+ channels by AVP. Table 8 has shown that the E/C values of the untreated, and of the CB-treated group have changes which are not significant for all parameters. This means that actin microfilaments may not play a functional role in the hormonal regulation of Na^+ conductive channels via changes in Na^+ channel densities. Whereas, our results with CB-treated tissues support the theory that autoregulatory changes in N_O are regulated by the recruitment of channels from a cytoplasmic pool.

5.2 Immunocytochemical localization of the cytoskeletal network in frog skin granular cells

There has been much interest in the direct effects of the actin cytoskeleton on the regulation of epithelial Na^+ channels. In this regard, Cantiello *et al.* (1991) showed that depolymerization of actin filaments by cytochalasin D increased the Na^+ channel activity in A6 cells. This suggests a direct regulatory role for the cytoskeleton. Because of the apparent contradictions between patch clamp data of Cantiello *et al.* (1991) with cytochalasin D, and our own results of CB on the Na^+ channels, we wished to verify our results, by demonstrating the effects of CB on the actin network in frog skin. While the distribution of the actin network in the toad bladder has been well documented, we could find no description of the actin cytoskeleton in frog skin. Accordingly, we had to modify existing cytochemical techniques to find the best conditions for the optimal demonstration of actin in isolated epithelial cells of *Rana fuscigula*. First at all we present a general description of the histology of the whole frog skin to serve as basis for our further discussions.

5.2.1 General morphology of isolated frog skin epithelium

Figure 5.10A shows a light micrograph of a resin-embedded section of frog skin stained with toluidine blue. The isolated frog skin is a stratified epithelium, which sometimes contains a double layer of cornified cells covering the uppermost layer, the granular cells. Deeper are the spiny cells, and the basal (germinatival) cells. The granular cells are arranged in a layer one or two cells deep beneath the cornified cell layers. The innermost cell layers often showed some evidence of cell damage, presumably due to the enzymatic processing while splitting the skin. While in the intact skin basal cells typically are small and have a columnar shape, the isolated epithelial basal cells often have an irregular shape like the cells of the stratum

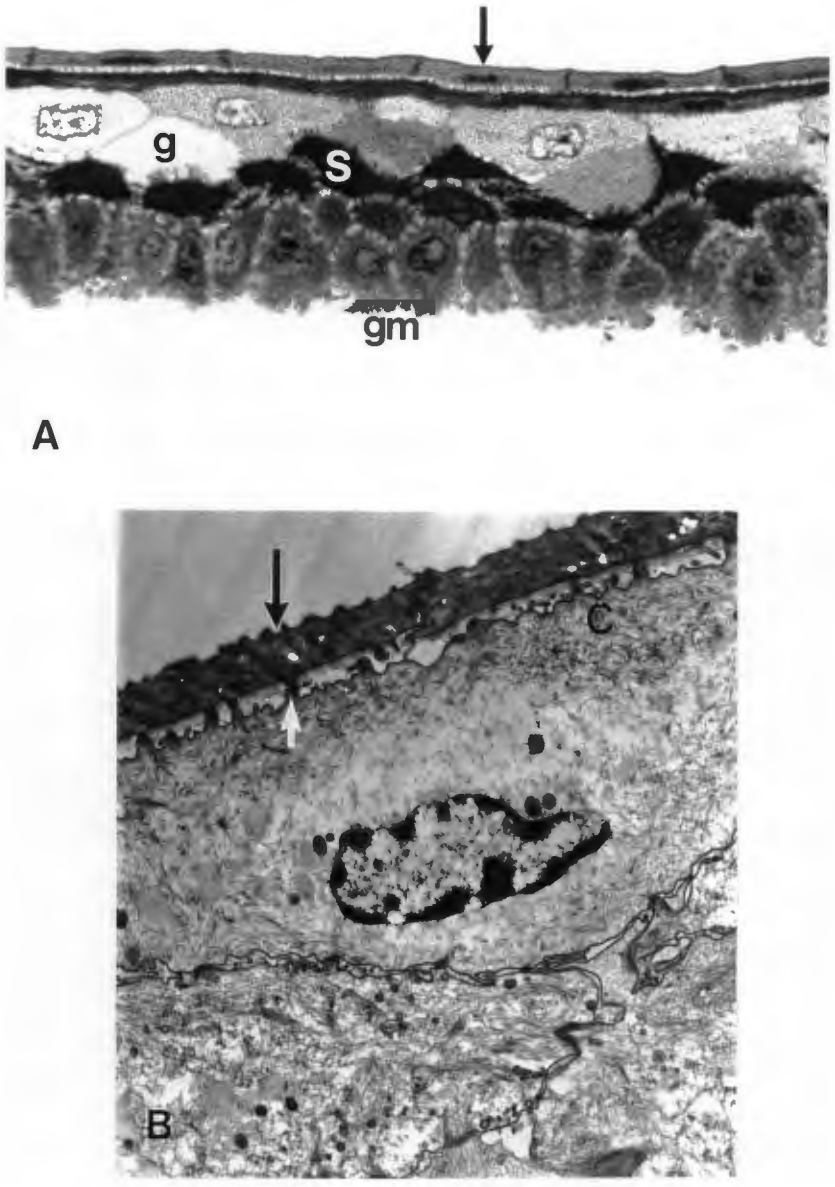

Fig. 5.10 General morphology of isolated frog skin. A: a light micrograph of a resin-embedded section stained with toluidine blue. In this example, the stratum corneum (arrow) consists of a double layer of cornified cells, the uppermost probably in the process of being shed. The stratified epithelium is composed of the outermost granular cells (g), the dark-staining spiny cells (s) and the basal germinatival cells (gm). x 850. B: a low-power electron micrograph of a granular cell beneath the stratum corneum (arrow). Note the density and thickness of the cortical cytoplasm beneath the apical membrane (c). Some intercellular connections (desmosomes) between the apical membrane and the cells comprising the stratum corneum are still maintained (white arrow). x 7150.

spinosum. The intraepithelial portion of glandular ducts was present in some sections, the remainder of the gland was apparently torn off when splitting of the skin. The procedure removed most of the glands, as revealed by scanning E.M. (Richards *et al.*, 1989).

Figure 5.10B shows a transmission electron micrograph of the granular cells which retained some of their connections, through desmosomes, with the cellular remains comprising the stratum corneum. The apical membrane was also thrown into some short folds, resembling microvilli, but not true microvilli since they did not contain a core of actin filaments (see below). The cortical cytoplasm was markedly dense beneath the apical membrane.

5.2.2 Demonstration of the cytoskeleton

5.2.2.1 Demonstration of microtubules

Microtubules in isolated epithelium were visualized with the fluorescence technique described in METHODS. Fig 5.11A shows indirect fluorescence staining of an array of microtubules criss-crossing the isolated frog epithelial cells (Control). It shows that the microtubular system of the supranuclear region is orientated towards the apical membrane, but this is not very clear in the photographs. Fig. 5.11B shows the phase contrast image of the same field for orientation. When frog skin epithelial cells were treated with the tubulin depolymerizing drug, 100 μM colchicinefor 3 hours, the fluorescence of microtubules in the granular cells diminished, but never totally disappeared (Fig. 5.11C). In some cells, a rough network of fluorescent filaments was still present, but it lacked the brightness and sharp aspect of the normal control network. Fluorescence remained quite strong in basal cells. Fig. 5.12 shows a positive control staining on the rat embryonic pancreas.

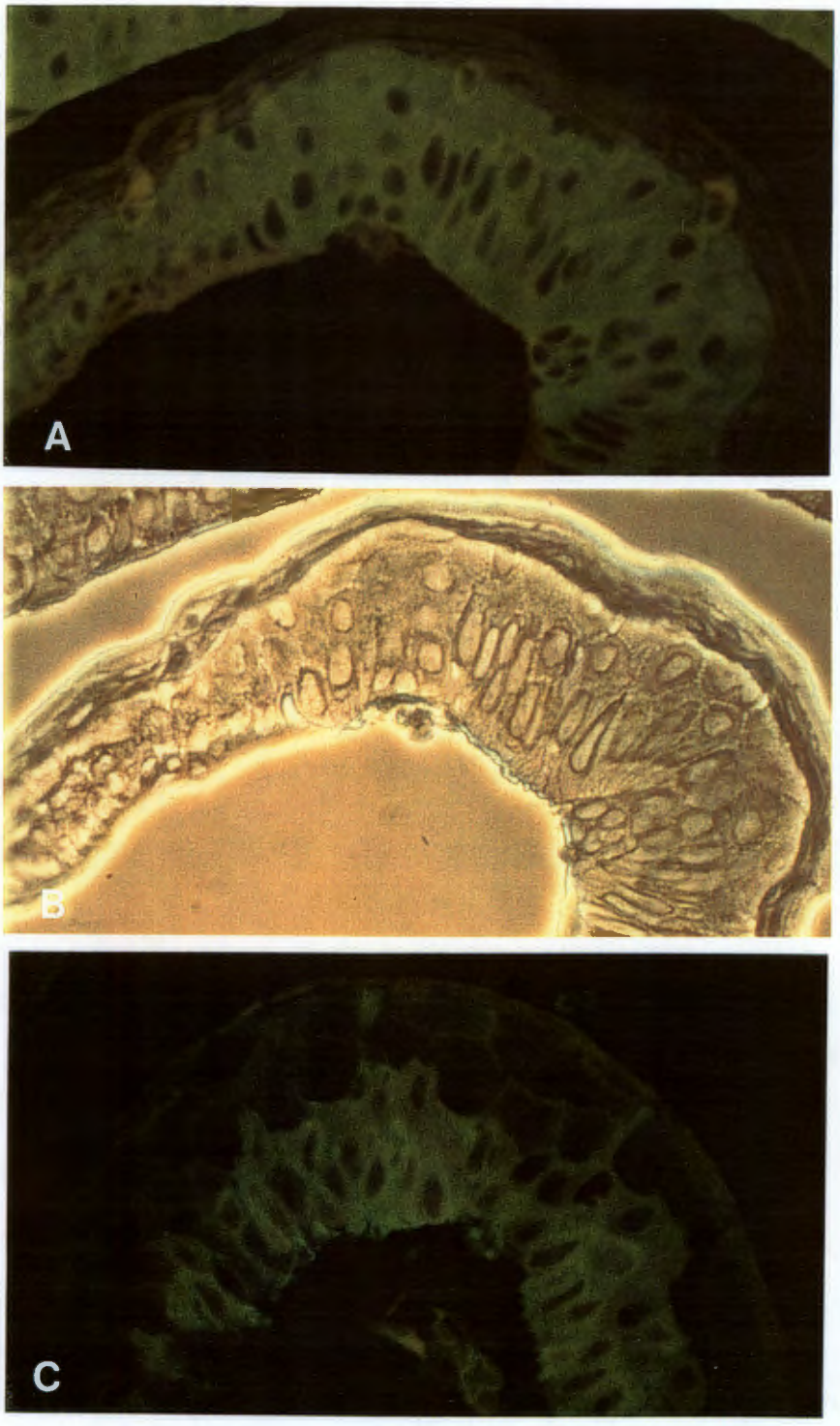

Fig. 5.11 Immunofluorescence of isolated frog skin for tubulin with FITC. **A**: shows the bright staining criss-crossing thus representing the part of the microtubules. The nuclei are the oval dark shadows at the center of the cells. **B**: phase-contrast micrograph of the same field as A showing the morphological aspect of these cells. **C**: 100 µM colchicine effects on the microtubule network. The normal continuity of the microtubules is almost destroyed in the granular cells (g). In the basal germinatival cells, fluorescence remained strong staining. Sections x 1200.

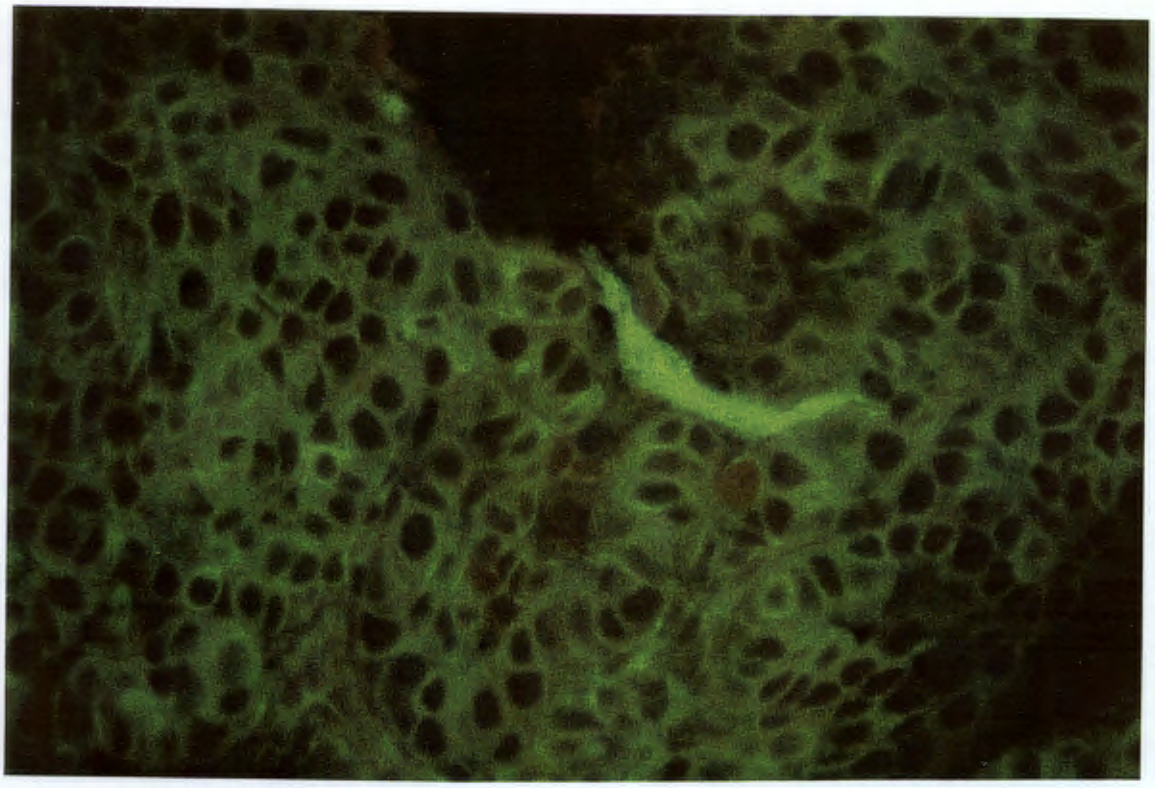

Fig. 5.12 Immunofluorescence staining for tubulin with FITC. Positive staining for tubulin is labelled on the rat embryonic pancreatic cells. Bright fluorescence staining shows that microtubules are distributed in the perinuclear space. The nuclei are the oval dark shadows at the center of the cells. x 800.

5.2.2.2 Demonstration of microfilaments

At first we used the direct immunofluorescent technique to localise microfilaments. With rhodamine-phalloidin staining, brightly fluorescent actin bundles underlie the intact plasma membrane of granular cells, and delineate the cell boundaries (Fig. 5.13A). The fluorescence was slightly diffuse and we could not clearly observe the fibrillar nature of the cytoskeleton. The central cytoplasm of the cells and the nuclei was largely devoid of any fluorescence and no stress fibres were seen. Figure 5.13A shows that a similar distribution was also seen in the spiny cells. In the basal germinatival cells, brightly fluorescent fibres were often observed along the basolateral membrane of the cell. Whether this was the result of the collagenase digestion, or is a feature of the younger germinatival cells, is not clear. Basal cells in the toad bladder similarly stained strongly (Kraehenbuhl *et al.*, 1979), but in the stratum corneum fainter fluorescencing bundles could also be observed along the borders of the cell remains. It was impossible to determine precisely the effects of cytochalasin B on the microfilament network with this technique. Incubation for 2 hours in cytochalasin B reduced the fluorescence of actin around the periphery of, especially, the granular cells. The bundles did appear to be fragmented, presumably indicative of depolymerization of the fibres (Fig. 5.13B). In paired physiological experiments, similar treatment with the drug caused the transepithelial electrical resistance of the tissues to decrease on average by about 50%, this is consistent with its physiological effects (Els and Chou, 1993). Fig. 5.14 shows the positive control for the rhodamine-phalloidin staining on the rat thyroid follicular epithelial cells. No non-specific fluorescence within the cells was revealed.

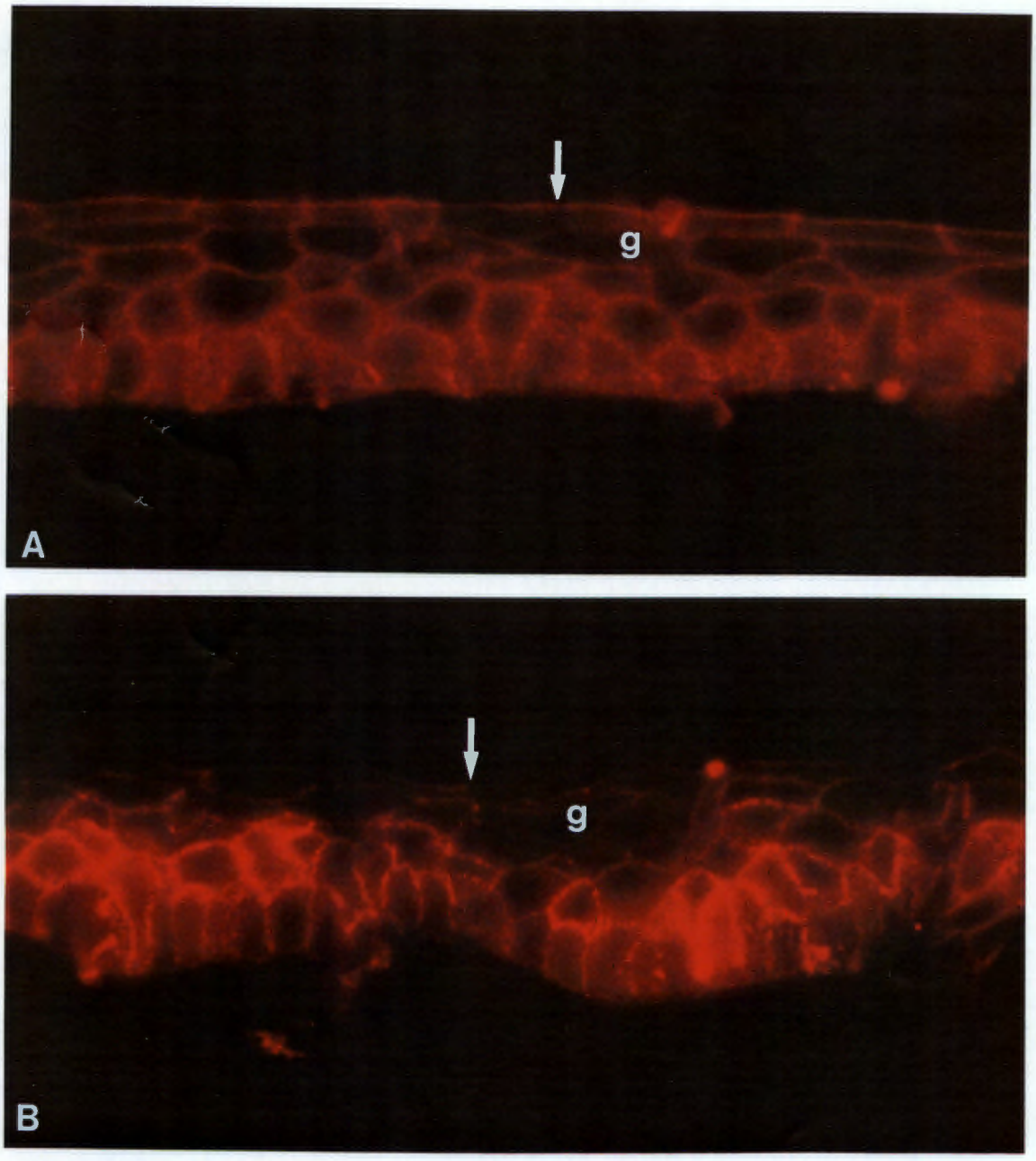

Fig. 5.13 Immunofluorescence of isolated frog skin stained for F-actin with rhodamine-phalloidin. The position of the stratum corneum is indicated by an arrow. Some slight staining is still observed along these cell boundaries. **A**: actin appears as a brightly fluorescent band around the periphery of the granular cell (g). The central areas of the cells remain clear. More diffuse fluorescence appears in the basal germinatival cells. **B**: shows the effects of a two hours treatment with cytochalasin B on the actin network. Most of the fluorescence has disappeared from the granular cells. Both sections x 880.

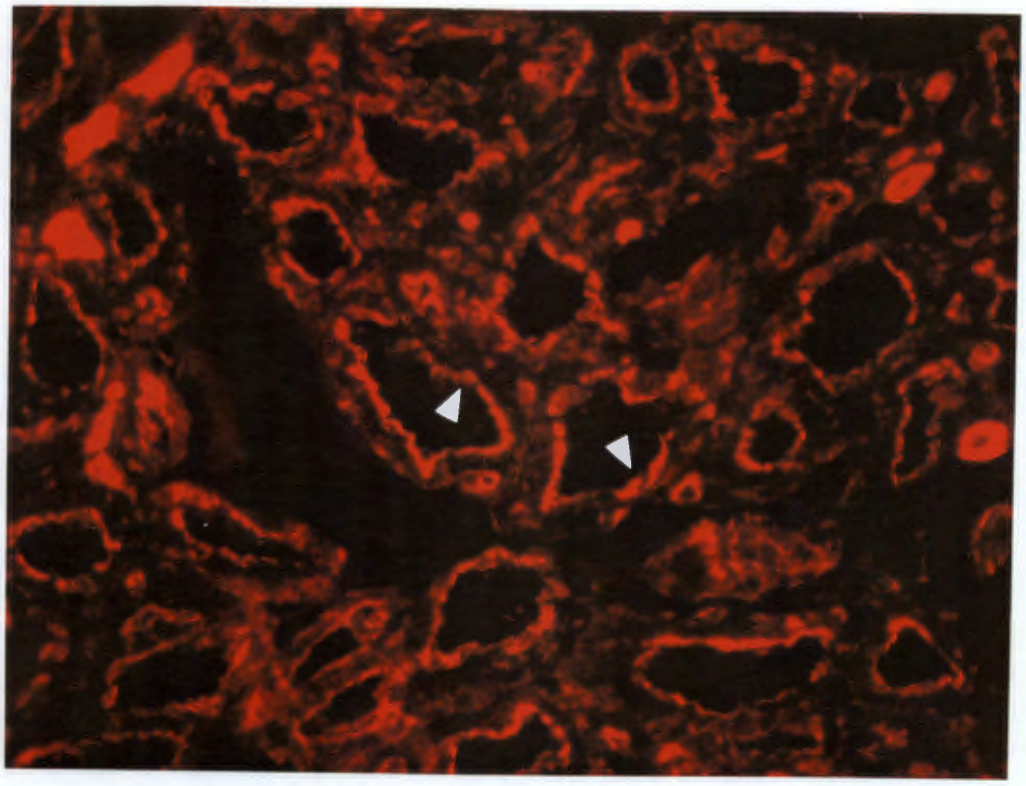

Fig. 5.14 Immunofluorescence of rat thyroid follicular epithelial cells stained for F-actin with rhodamine-phalloidin. Microfilaments bound to rhodamine-phalloidin are mainly distributed in the apical cytoplasm (arrow head). x 320.

5.2.2.3 Immunogold labelling of actin filaments

The resolution of fluorescence microscopy was not sufficient to distinguish the differences between actin filaments, or to determine the effects of depolymerization and AVP on the filaments. Immunogold labelling for actin fibres was performed specifically in the granular cells, since these cells are implicated in the important rate-limiting entry step of transepithelial Na^+ transport in the frog skin (Rick, 1992). The fixation of 1.5% paraformaldehyde and 1% glutaraldehyde mixture provided a good tissue preservation for our experiments, and allowed consistent specific labelling with negligible background staining. While it was expected that a smaller gold particle size would provide a higher density of labelling (Lackie *et al.*, 1985), we found very little apparent difference using either 10 or 15 nm gold particles. Results showed only the size 15 nm gold labelling on the actin filaments.

Figure 5.15A shows a low-power view of immunogold staining of actin fibres in a granular cell. Gold particles, indicative of the presence of actin, were seen along the periphery of the cell. Specifically, the cytoskeleton beneath the apical membrane was markedly more dense than along the basolateral membrane, and was particularly rich in actin, more so than along the basolateral membrane. Actin was also found in the central cytoplasm of the cell. In this area the degree of labelling varied markedly, but mainly a sparse distribution of gold particles was seen. The subapical cytoplasm often contained a number of mucin vesicles (Voûte, 1963) and the gold labels were localised close to the periphery of these vesicles. The origin of a few gold particles, which were sometimes observed within the nucleus (Fig. 5.15A), is unknown. These disappeared with a higher dilution of the primary antibody, and could be the result of non-specific reactions.

Higher magnification shows details of the immunogold labelling on actin filaments making up the cytoskeleton beneath the apical membrane of a granular cell (Fig. 5.15B). The gold labelling was particularly rich in this area, indicating that actin filaments comprise a substantial portion of the cytoskeleton. Bundles of labelled actin filaments lay in an undulating pattern mainly parallel to the apical membrane. We assumed that the apical cytoskeleton also contains other filaments, particularly tonofilaments, but this was not shown with double labelling. Figure 5.15C is a negative control section from the same area in which the primary antibody was omitted from the incubation solution. Virtually no particles were visible, attesting to the specificity of the gold label. Less dense labelling of actin was seen along the basolateral membrane of the cell where it was also associated with fibres extending the intercellular junctions from both basal and lateral interdigitations (Fig. 5.15D). For positive control, Fig. 5.16 shows the electron micrograph of a frog intestinal epithelial cell. Gold particles were labelled specifically on the actin filaments.

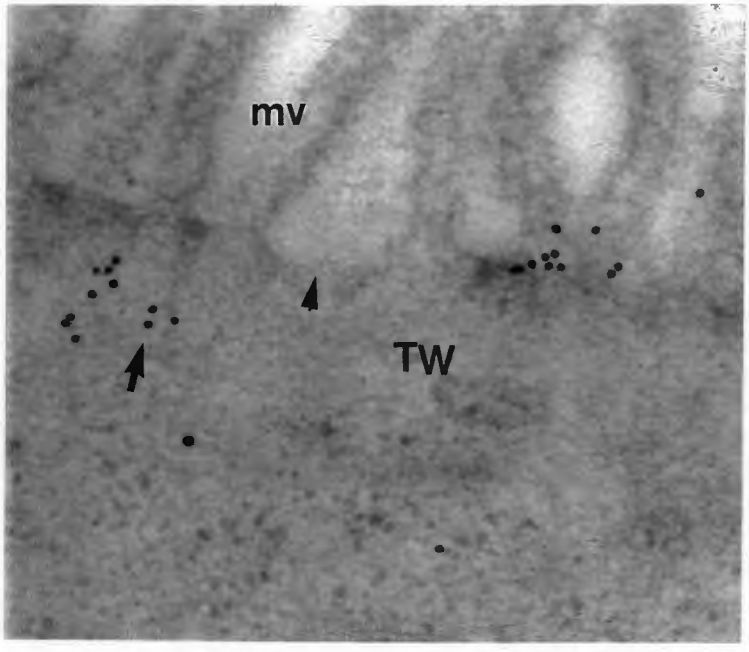

Fig. 5.16 Electron micrograph of a longitudinal section through a frog intestinal epithelial cell, showing the terminal web (TW) beneath the apical membrane (arrow head). Gold particles (arrows) were labelled on the actin filaments. Actin filaments forming the core of microvilli (mv) extend into the terminal web. x 72000.

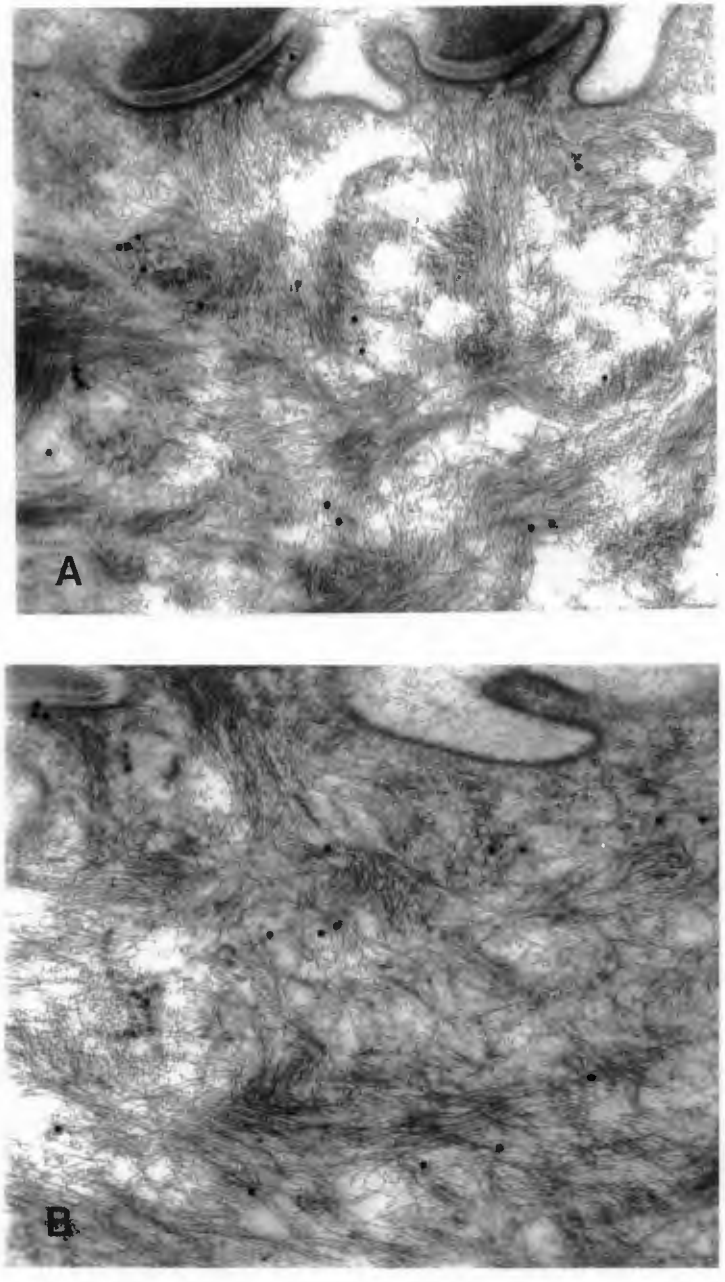

Fig. 5.17 Effects of cytochalasin B and AVP on the actin network beneath the apical membrane. **A**: treated with cytochalasin B for 2 hours and, **B**: with AVP for 30 minutes. By comparison with Fig. 5.15B, there were apparently fewer gold particles in both sections while the networks also seemed to be disarranged. Both sections x 53200.

We also wanted to verify the effects that the 2 hour treatment with CB had on the actin cytoskeleton. Accordingly, we examined, sometimes in paired tissues, the effects of CB in tissues treated similarly to our electrophysiological experiments. These results are illustrated in Fig. 5.17A. In a similar way, we also examined the effects of AVP on the actin network (Fig. 5.17B), since Gao *et al.* (1992) showed that in the toad urinary bladder AVP depolymerized the actin network. These authors demonstrated a relationship between the actin cytoskeleton and the hydrosmotic effect of water flow in response to AVP.

Figure 5.17A and B illustrate respectively the effects of cytochalasin B and AVP on the organization of actin beneath the apical membrane. Comparison of figures 5.17A and 5.17B, shows that both cytochalasin B and AVP disrupt the regular pattern of the cytoskeletal fibres and result in " bunching " of shortened filaments. The effect was more obvious with cytochalasin B than with AVP. Concurrently, the treatments apparently also resulted in a reduction in the density of gold particles.

Chapter 6

Discussion

6.1 Modulation of epithelial Na^+ channels by autoregulatory mechanism

The phenomenon, whereby cells adjust to a reduction in apical Na^+ entry rate by inducing an increase in the number of open channels, was referred to as autoregulation of channel densities by Abramcheck *et al.* (1985). They suggested that autoregulatory changes in channel densities might well be a major factor in regulating Na^+ permeability. We also observed that in isolated frog skin epithelium from Rana fuscigula, changing the rate of Na^+ entry led to regulatory adjustments in Na^+ permeability. Two main hypotheses have been advanced to explain the mechanisms whereby the cells accomplish the modification: change in channel conductance and change in the number of active Na^+ channels.

6.1.1 Regulation of Na^+ channels by luminal Na^+ concentrations

Using current fluctuation analysis on frog skin and rabbit urinary bladder (Van Driessche and Lindemann, 1979; Lewis *et al.*, 1984) found no evidence for single-channel current saturation in response to changes in luminal Na^+ concentrations. These authors concluded that Na^+ permeability was modified primarily by regulating the number of active channels. Not all results are consistent with this idea. Using patch clamp, Palmer and Frindt (1988) did not observe any change in the number of active channels in response to an increase in external Na^+ concentration in rat CCT. The effects of increasing luminal Na^+ up to 100 mM have been described in terms of channel saturation in rat CCT (Palmer and Frindt, 1988). A similar mechanism was

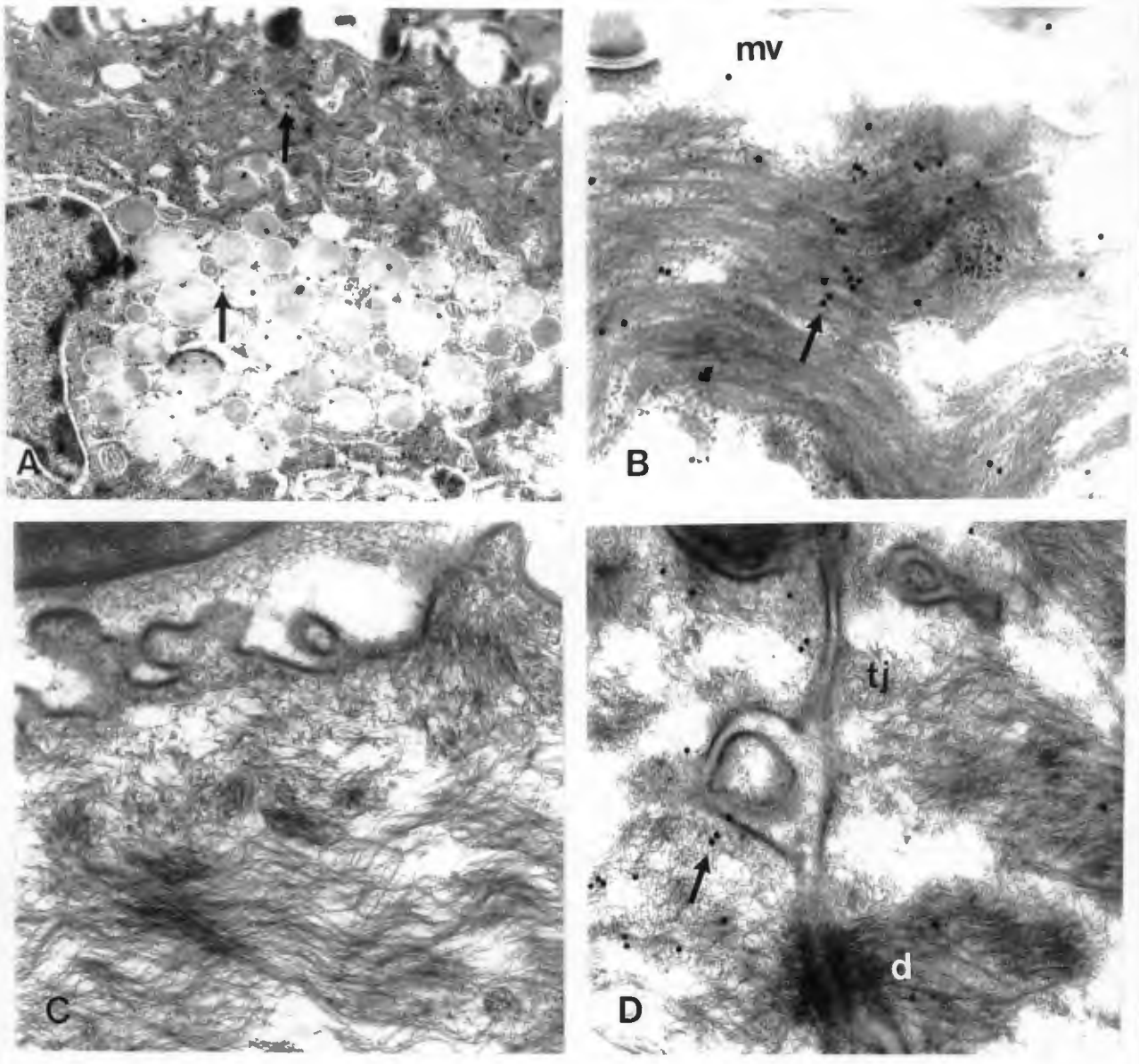

Fig. 5.15 Immunogold staining of actin especially in the apical regions of granular cells can be seen (all electron micrographs are printed with the apical membrane towards the top). **A**: shows the general distribution of actin in a granular cell (actin was labelled with 15 nm gold). Gold particles (arrows) were found mainly along the periphery of the cell with some staining in the supranuclear regions, particularly around the mucin vesicles. Note the dense apical cytoskeleton in comparison to the network along the basolateral membrane, which also contained less of the label. A few gold particles persisted in the stratum corneum. x17800. **B**: heavy labelling of actin fibres beneath the apical membrane (arrow). Most of the fibres run parallel to the membrane, but some may be observed in cross section. Folds in the apical membrane resembled microvilli (mv) and sometimes contained a single gold particle. The image was focused on the granules, hence, the apical membrane is not clearly defined. x 65000. **C**: a control section in which the primary antibody was omitted. The section is devoid of any label. x 53200. **D**: gold label along the lateral cell border (arrow) near a lateral fold and it also shows the tight junction (tj) and desmosome (d). Labelling was less intense. x 53200.

proposed for Na^+ channels reconstituted from A6 cells into planar lipid bilayers (Olans *et al.*, 1984). A number of factors, including differences in species, methods, and conditions have been advanced to explain the contradictions.

We re-evaluated the effects of a reduction in luminal Na^+ concentration on the Na^+ permeability in isolated frog skin with CDPC-induced noise analysis. By avoiding the use of potent Na^+ channel blockers to induce channel fluctuations, we could investigate changes in channel densities under conditions close to spontaneous rates of Na^+ absorption (Helman and Baxendale, 1990). With this approach we also avoided certain problems sometimes associated with the use of potent Na^+ channel blockers, specifically with regard to difficulties in measuring off-rate coefficients and determining autoregulatory changes in channel densities (Helman *et al.*, 1983; Abramcheck *et al.*, 1985; Helman and Kizer, 1990). Our results clearly demonstrated that the reduction in luminal Na^+ concentrations mainly induced an increase in the number of conducting Na^+ channels (Table 3). The procedure, amongst others, decreased the electrochemical driving force across the apical membrane, resulting in approximately a 60% reduction of the mean i_{Na}. Despite the decrease in i_{Na}, the macroscopic transport rate relaxed towards previous levels, mainly as a result of the increase in N_O. Our data were also consistent with recent patch clamp results. Using cell-attached patches on A6 cells, Ling and Eaton (1989) showed that decreasing the Na^+ concentration in the bath to 5 mM activated " new " channels in the patch membranes, and did not change the channel conductance.

The autoregulatory increases in N_O were generated within 2 to 3 minutes of changing to low Na^+ (Fig. 5.5). This time course is consistent with the effects of decreasing luminal Na^+ observed with patch clamp on A6 cells (Ling and Eaton, 1989). The rapid rate at which changes occurred rule out that the channels were recruited by the synthesis of new channels. It is also not known currently how the changes in channel

densities are mediated. Since recent evidence argues against a direct interaction of Na^+ with the membrane channels, it is likely that the changes were mediated via some intracellular mediator (Schultz, 1985; Ling and Eaton, 1989). There is ample evidence suggesting that intracellular Na^+ performs this role (Van Driessche and Erlij, 1983; Abramcheck *et al.*, 1985) either directly or indirectly via changes in, for example, intracellular hydrogen or calcium ions (Palmer and Frindt, 1987).

The underlying mechanisms for autoregulation of channel densities are unknown. Frog skins which had been exposed to 10 or 5 mM Na^+ for 2 or 3 hours contained markedly higher values of N_O and N_T compared to values for skins bathed in the normal Ringer solution (Els and Helman, 1991). It was suggested that in *Rana pipiens*, autoregulatory changes in N_O occurred primarily by changes in N_T. Along similar lines, inhibition of apical Na^+ entry by the use of mucosal Na^+ channel blockers leads to large increases in channel densities and transient return of the I_{SC} towards control levels (Abramcheck *et al.*, 1985; Helman and Baxendale, 1990). Since open probability remained constant during inhibition of Na^+ entry, it was inferred that the autoregulatory changes in N_O occurred via long time-constant changes of N_T. This was clearly not the situation in our experiments. A reduction in the luminal Na^+ concentration induced relatively small changes of N_T, varying between 24% and 81% in 20 and 10 mM Na^+, respectively. These small changes could not alone account for the large increases in N_O. Obviously, other factors, like the increase in open probability are equally important.

Using the patch clamp technique, Palmer and Frindt (1988) found that the open probability of the channels in rat CCD was independent of changes in the luminal Na^+ concentration. Using noise analysis, Helman and Baxendale (1990) also found that a reduction in apical Na^+ entry by Na^+ channel blockers did not change β' in *R. pipiens*. Nevertheless, the latter investigators emphasized the notion that changes of open

probability may still, in some unknown manner, be an important mechanism in the regulation of the rate of the Na^+ entry. In support of this view, but in contrast with the previous observations, our data show very clearly that autoregulatory increases in N_O were accompanied by parallel changes in open probability. Despite large spontaneous variability in open probability amongst tissues, β' increased consistently by about 55-60% when the luminal Na^+ concentration was lowered. In support of our own observations, Ling and Eaton (1989) reported that in cell-attached patches they consistently observed a relative increase in open probability by a reduction in the luminal Na^+ concentration. The conflicting results with the patch clamp may be attributed to differences in experimental conditions. Palmer and Frindt (1988) only changed the Na^+ concentration in the pipette, which directly affected the channels. On the other hand, Ling and Eaton (1989) changed Na^+ concentration in the bathing solution outside the patch pipette. Our results imply that, contrary to previous beliefs, and at least in epithelium from *Rana fuscigula*, changes of channel open probability are an important mechanism in the autoregulation of channel densities in response to a reduction in mucosal Na^+ concentrations.

The reason why autoregulatory changes in open channel densities in *Rana fuscigula* do not occur primarily by changes in N_T is not clear. Species and tissue variability could account for differences in cellular strategies to compensate for a reduction in Na^+ transport rate. The low innate Na^+ transport rates in our tissues were primarily the result of the small number of open channels (P. H. Russel and W. J. Els unpublished data). While mean open probability in this study did not differ markedly from those in other frog skins, values of about 17 million/cm² for N_O and 60 million/cm² for N_T were about 3~4 times less than in other species (see Helman and Kizer, 1990). Since the inherent pool of channels in our frog skins was relatively small it was perhaps not surprising that we only observed small changes N_T in response to a reduction in

luminal Na^+ concentration. This is unlike the situation in *R. pipiens* where a reduction in Na^+ uptake by mucosal amiloride increased Na^+ channel densities by an order of magnitude or more (Abramcheck *et al.*, 1985; Helman and Baxendale, 1990). In fact, cells in tight epithelia are capable of responding to non-hormonal influences by eliciting changes of channel densities comparable to, or greater than, those elicited by hormones (Els and Helman, 1991). In this regard, it was also apparent that the moderate capacity of our tissues to autoregulate the channel densities was reflected in the long time-constant relaxation of the I_{Na}. After 20 minutes in low Na^+ (20 mM) we found that the I_{Na} had recovered on average to within 24% of the original level. At this stage, the transport rate had reached an apparent steady-state. Although they did not do paired experiments, Els and Helman (1991) found that with *Rana pipiens* after 2 hours in 10 or 5 mM Na^+ the average value of I_{Na} was not significantly different from those exposed to 100 mM Na^+.

6.1.2 Effects of disrupting the cytoskeleton on autoregulation of Na^+ channel densities

We studied the role of the cytoskeleton in the regulation of channel densities because we suspected that an increase in N_O might occur via recruitment from subapical membrane storage vesicles containing Na^+ channels (Garty and Edelman, 1983; Lewis *et al.*, 1984). Alternatively, channels may be acquired from a pool of quiescent channels already present in the membrane (Li *et al.*, 1982). In epithelial cells cytoskeletal proteins mediate important membrane functions. The function and composition of the apical membranes may be rapidly modulated by the exocytotic insertion and the endocytotic removal of specific membrane components. Specifically, in the renal collecting duct and urinary bladder, in response to environmental changes, the cytoskeleton mediates the rapid insertion of water channels and proton pumps into their plasma membranes (Stetson and Steinmetz, 1983; Brown, 1989).

Microtubules play a large role in sorting and guiding membrane-bound traffic in certain polarized epithelial cells. Hence, disruption of microtubules with depolymerizing drugs blocks the transfer of proteins bound for the apical membrane in MDCK cells (Parczyk *et al.*, 1989) and markedly interferes with the delivery of water channels to the apical membrane in amphibian urinary bladder (Valenti *et al.*, 1988). In our experiments prior treatment of the tissues for 3 hours with colchicine had negligible effects on the macroscopic Na^+ transport rate and also did not affect the autoregulation of channel densities by a reduction in luminal Na^+ concentration. Apparently, at least within the time frame of our experiments, the integrity of the microtubules is not essential for regulation of apical Na^+ entry. The result is also consistent with previous observations where, in the amphibian urinary bladder, disruption of the microtubules did not interfere with Na^+ transport (Pearl and Taylor, 1985). We cannot rule out the probability that microtubules are involved in the delivery of channels to the apical membrane. Autoregulation might only involve channels already present in, or at, the apical membrane. Parallel immunocytochemical investigations showed that our results could not be attributed to colchicine resistance of microtubules. After 3 hours incubation in colchicine, the microtubules in most of the epithelial granular cells disappeared or were severely altered by the treatment (Fig. 5.11) (Chou and Els, 1991).

It has long been suspected that microfilaments play an important role in the regulation of water and solute transport in tight epithelia. Disruption of the actin cytoskeleton inhibits the ADH-induced increase in water permeability in toad urinary bladder and other tissues (Pearl and Taylor, 1985). Less is known about its role in solute transport but disruption of the cytoskeleton with cytochalasins reduced volume regulation in *Necturus* gall bladder (Foskett and Spring, 1985) and rabbit proximal tubules (Linshaw, 1989), probably by a mechanism which prevented the activation of KCl

transport out of the cell. More recently it was reported that the disruption of microfilaments severely inhibits Na^+ reabsorption in perfused proximal tubules from rats (Kellerman *et al.*, 1990). We could see much larger effects of colchicine and CB on the transport rate when using much higher concentrations. However, at these concentrations the effects on the I_{SC} were so severe that we could not use the tissues for noise analysis. Accordingly, we used submaximal doses of the drugs for the subsequent experiments. Nevertheless, at these concentrations we could still unquestionably demonstrate the effects on the transport rate and on the structure of the filaments (hence the necessity of the structural studies).

Results of the present study showed that microfilaments appear to be involved in the regulation of channel densities in *R. fuscigula*. Treating the tissue with cytochalasin B for 2 hours, markedly decreased the relaxation of I_{Na} in response to a reduction in luminal Na^+ concentration. The data summarized in Table 7 indicates that the lack of recovery could be attributed to the absence of an autoregulatory increase in N_O to compensate for the decrease in Na^+ entry. In particular, treatment with cytochalasin B did not affect the change of β', but prevented an increase of N_T. These results implied that depolymerization of microfilaments did not affect channels already present in the membrane, but apparently prevented the recruitment of new channels which would increase the total number of channels. Although direct proof is lacking, the data suggest that autoregulatory activation of Na^+ channels also occurs by recruitment from the cytoplasmic pool. A similar mechanism has been reported by Lewis *et al.* (1984) whereby, in the urinary bladder, new Na^+ channels could be recruited from intracellular stores in response to physiological signals. Foskett and Spring (1985) also suggested that during volume regulation in the *Necturus* gallbladder, microfilaments allow cytoplasmic vesicles with ion channels to fuse with the cell membrane. The system is in fact, widespread amongst epithelia, enabling them to respond rapidly to

external stimuli by selective exocytosis of intracellular vesicles to the membrane (Brown, 1989). Other hypotheses for the recruitment of Na^+ channels, or interpretations of the results, are equally tenable. Patch clamp investigations have shown a close association between Na^+ channel in A6 cells and cytoskeletal proteins, leaving open the possibility that the cytoskeleton may play an important direct role in modulating transport by influencing the properties of the channels. Prat *et al.* (1991) demonstrated that in both cell-attached and excised membrane patches, disruption of microfilaments with cytochalasin D enhanced Na^+ channel activity.

Accordingly we concluded in summary that, in *R. fuscigula*, autoregulatory changes in Na^+ channel densities induced by a reduction in Na^+ transport load, came about through recruitment of channels from closed states (an increase in open probability) and through an increase of the total channel pool. This is the first demonstration on a paired basis with noise analysis that a decrease in luminal Na^+ concentration activates Na^+ channels by increasing the open probability. The autoregulatory changes in channel densities were moderate, possibly reflecting variance among species or differences in the functional states of the tissues. This leaves the open possibility that the degree of autoregulation would also depend on the size of the epithelial Na^+ channel pool, i. e. the functional state. While we have no definite proof, our results support the possibility that changes in N_T occurred by recruitment from a cytoplasmic pool. Clearly, morphological and other evidence is necessary to determine the cellular mechanism whereby autoregulatory changes in channel densities occur in tight epithelia.

6.2 Role of actin in regulation of epithelial Na^+ channels by AVP

We chose to study the effects of AVP on Na^+ transport because it is a potent stimulator of Na^+ transport in frog skin and its mechanisms of action are well-known. The

addition of AVP caused large increases in channel densities without affecting channel conductance which was similar to the effect caused by a reduction in Na^+ concentration. However, the manner in which AVP brings about the changes in channel densities is unknown and has frustrated investigators for many years. In this regard, it has long been suspected that microfilaments play an important role in the regulation of solute transport in epithelia, particularly as they regulate the delivery of membrane-bound proteins.

In epithelial cells the actin network is generally implicated in a number of physiological actions through interactions with the plasma membrane (Leister and Molitoris, 1993). Regarding its role in regulation of solute transport, it is well documented that actin is involved in the process whereby AVP induces the insertion of aggregates with water channels into apical membranes to increase water permeability (Pearl and Taylor, 1985; Verkman, 1989). However, the role of actin in control of Na^+ transport by AVP is not known. Experiments with patch clamp have demonstrated a possible regulatory role for actin on Na^+ channels (Cantiello *et al.*, 1991). It was of interest, therefore, to study the effects of disrupting the actin cytoskeleton on the modulation of Na^+ channel densities with AVP using fluctuation analysis.

6.2.1 Regulation of epithelial Na^+ channels by AVP

Various studies using fluctuation analysis have demonstrated that AVP increases Na^+ permeability mainly by increasing the Na^+ channel density in the apical membrane. There is little or no change in single channel conductance or in channel open probability (Helman *et al.*, 1983; Els and Helman, 1991). These studies have been confirmed by our results. In *R. fuscigula* AVP caused a 144% increase in N_O, with no significant change in open probability (Table 8). Previous studies have not resolved the question whether this increase in Na^+ channel density results from either the

recruitment of new channels into the apical membrane from an intracellular pool, or through the activation of quiescent channels. Owing to the short time in which changes in N_O occur, it can be ruled out that new channels are synthesized in response to AVP.

Several experiments are consistent with the insertion theory, for example, Garty and Edelman (1983) have shown evidence supporting an insertion mechanism. By prior trypsinization of the apical membrane AVP had no diminishing effect on Na^+ transport in the urinary bladder. This finding indicated that the channels were not present in the membrane and had to be new (non-membrane) channels activated by AVP, which were not accessible to proteolysis before the hormone action. These authors have also suggested that AVP caused the insertion of Na^+ channels in a way similar to the AVP stimulated insertion of water channels. Support for the insertion hypothesis comes from several sources. Warncke and Lindemann (1981) using impedance analysis, found that AVP causes an increase in the apical membrane area. This evidence has supported the hypothesis that AVP induces the recruitment of a cytoplasmic pool of apical Na^+ channels from channel-containing vesicles into the apical membrane. The most convincing evidence for the insertion theory comes from Marunaka and Eaton (1991). These investigators demonstrated that in excised patches on A6 cells, 30 to 40 min pretreatment of AVP had no effect on the channel open probability (P_o), but caused a change in the number of channels. These results showed that AVP increases N_O, and were consistent with our noise analysis data (Table 8). Interestingly, Marunaka and Eaton (1991) also found that when AVP was added to the basolateral solution, there was no increase in the number of channels in cell-attached patches on A6 cells. An explanation could be that vesicles did not or could not fuse with the patch membrane. Not all results support the insertion theory. Prat *et al.* (1993a) reported that under cell-attached patches on A6 cells AVP enhanced the Na^+ channel

activity within 5 minutes. The AVP-induced channel activity was a reflection of an increase in both the average number of channels, and of the channel open probability. These authors also demonstrated that, in the presence of ATP, cAMP-dependent PKA induced Na^+ channel activity in excised inside-out patches with an increase in average channel number and in percent channel open probability. These results are similar to those observed with AVP. In excised inside-out patches, the addition of pertussis toxin completely blocked the AVP- or PKA-induced Na^+ channel activity, whereas incubation of intact cells with the toxin prevented the effect of both AVP and PKA. These data indicate that both AVP and PKA activation appear to be mediated through a G protein pathway thus supporting the conclusion that the AVP-sensitive pool of Na^+ channels is silent, but already present in the apical membrane before either AVP or PKA stimulation (Prat *et al.*, 1993a).

From our results it can be shown that the addition of AVP to the serosal solution caused an increase in the macroscopic Na^+ current (I_{Na}) by about 56%, which was brought about an increase in the number of conducting Na^+ channels. The small increase in N_T in comparison with other species (Helman and Kizer, 1990) or other authors' experiments (Els and Helman, 1991), is attributed to the low I_{SC} in this study (Table 2). This study also reported a significant decrease in the mean i_{Na}. In addition, AVP caused a slight decrease in the β' from 0.45 to 0.40 (not significant). This result is in accordance with a similar study done by Els and Helman (1991), who observed that the changes of β' caused by AVP were not significant. The result of β' is also confirmed by Marunaka and Eaton (1991), who found that AVP caused no change in channel open probability (P_o) on A6 cells patches. Therefore, in our study we concluded that the increase of N_O caused by AVP was due to an increase of N_T (Table 8).

6.2.2 The effect of disrupting actin filaments on the modulation of Na^+ channels by AVP

Experiments carried out on putative water channels clearly showed that disruption of the cytoskeleton reduced the hydro-osmotic effect induced by vasopressin (Bourguet *et al.*, 1988). Verkman (1989) also demonstrated that in renal epithelial cells the actin filaments are involved in the process whereby AVP induces the insertion of aggregates containing water channels into the apical membrane. Much less is known regarding the role of actin in regulation of Na^+ transport.

There is current interest in the role of actin in the modulation of Na^+ channels. Recently, Smith *et al.* (1991) showed that the Na^+ channel is structurally linked to the cytoskeleton by regulating proteins in A6 cells, but the significance of this regarding the regulation of the channel is not fully understood yet. In contrast to the autoregulation experiments, the actin cytoskeleton does not appear to perform a central role in the control of apical membrane Na^+ transport modulated by AVP.

As shown before (Fig. 5.6 and 5.8) treatment with CB for 2 hours markedly decreased the transepithelial membrane resistance. Concurrently, there was a moderate decline in the I_{SC}. In part, the decreases in transepithelial resistance could be the result of a decrease in the resistance of the paracellular pathway. This was described by Madara *et al.* (1986).

Examination of the data presented in Table 8 suggests that disrupting the actin network did not effect the steady-state changes to Na^+ channels brought about by addition of AVP. The differences between changes in untreated and CB-treated tissues were not significant. Accordingly, the macroscopic responses to AVP in untreated and CB-treated tissues appears very similar (Fig. 5.8). At best, the data suggests that the intact actin network is not essential for short-term steady-state response in Na^+

transport by AVP. It is arguable whether this supports the recruitment theory over the activation theory. The data seem to support the view that AVP activates quiescent channels already present in the membrane. Support for this theory comes from work done on A6 cells derived from *Xenopus laevis* renal tubular cells (Oh *et al.*, 1993). Using the biotinylation / immunoprecipitation protocol, Oh *et al.* (1993) showed that AVP causes the direct phosphorylation of the 300-kD subunit of Na^+ channel protein, thus providing evidence supporting the hypothesis that Na^+ channels are directly activated. However, whether these channels are already present in the membrane or in cytoplasmic vesicles is uncertain. On the other hand, results with patch clamp most strongly favours the insertion mechanism (discussed above).

Support for the insertion theory also comes from recent results with membrane electrical impedance analysis. Addition of 2.5 μM forskolin caused a rapid increase in apical membrane capacitance in a time dependent manner. The mean increase in the dc capacitance was about 0.2 $\mu F/cm^2$, from an average of 1.85 $\mu F/cm^2$. The time course of increase of capacitance was parallelled that of Na^+ channel densities increased by forskolin. These results support the idea that frog skin regulates the Na^+ channel densities via cAMP through a mechanism of vesicle fusion with the apical membrane (Awayda and Helman, 1992). Studies with the patch clamp also provided evidence that AVP increases the amiloride-sensitive Na^+ transport (I_{Na}) in intact IMCD cells, but causes no increase in channel activity in cell-attached patches (Light *et al.*, 1988). These results may indicate that when a membrane is dissociated from the underlying cytoskeleton by formation of the patch, the Na^+ channel cannot be inserted.

How does cytochalasin B affect the apical membrane Na^+ channels in response to AVP? The data summarized in Table 8 shows that in response to AVP stimulation, there were no differences in the Na^+ channel properties of CB-untreated and CB-treated groups. This indicates indirectly, that actin microfilaments apparently do

not play a direct role in the instantaneous hormonal regulation of Na^+ conductance via changes in Na^+ channel densities. Taken together, the data support the idea that AVP activates Na^+ channels which are either already present, but are quiescent, in the membrane, or are inactivated by specific phosphorylation reactions which may be important in the regulation of Na^+ reabsorption. The data do not support the view that, new channels are recruited from cytoplasmic stores.

6.3 Immunocytochemical evidence for a possible interaction between the actin network and the Na^+ channel regulatory mechanisms

Electrically tight epithelia like those in the kidney and frog skin, play an important role in water and salt homeostasis. Although the functional role of the cytoskeleton in these cells is still not very clear, apparently an intact actin network is necessary for the functional integrity of the cells (Kellerman *et al.*, 1990; Els and Chou, 1993). Unlike the situation regarding water transporting epithelia (Pearl and Taylor, 1985; Gao *et al.*, 1992), the distribution and role of actin in the epithelial cells, which are responsible for Na^+ reabsorption, has not been thoroughly explored. The apical cytoplasm of renal cells is generally rich in actin regulating proteins (Hartwig *et al.*, 1990), while in A6 cells the apical Na^+ channel is linked to the actin cytoskeleton by proteins that include ankyrin and fodrin (Smith *et al.*, 1991). Important evidence suggests that the cytoskeleton may be directly involved in regulating the activity of the Na^+ channels, thus patch clamp studies show that the addition of cytochalasin B or short actin filaments induces Na^+ channel activity in cell-attached or excised patches of A6 cells (Cantiello *et al.*, 1991).

With immunofluorescence we demonstrated the general arrangement of actin in the granular cells of frog skin. Actin was mainly displayed as a diffuse thin band along the plasma membrane; there was little evidence of actin in the central areas. No difference was seen in the degree of staining between apical and basolateral

membranes. Fluorescence methods showed a similar distribution in the epithelial cells of the toad bladder (Kraehenbuhl *et al.*, 1979; Pearl and Taylor, 1985, Hugon *et al.*, 1989) and A6 cells (Cantiello *et al.*, 1991).

The actin network beneath the apical membrane is of particular significance in Na^+ transporting epithelia. The higher resolution provided by immunogold staining allowed us to demonstrate the fibrous nature of the actin bundles in this area. While some researchers routinely use cold embedding procedures for immunogold labelling, we, followed others (Johnson and Bettica, 1989; Watanabe *et al.*, 1993) who had effectively applied the same procedures on epoxy embedded tissues. We were unable to do a quantitative comparison between the degree of gold labelling in our studies with those of others. However, by visual assessment, we obtained a corresponding degree of labelling to that observed in apical microvilli of A6 cells (Gao *et al.*, 1992). In frog skin, actin was concentrated beneath the apical membrane where it formed part of a dense network of fibres arranged in bundles, mainly parallel to the apical membrane. By comparison, there appeared to be fewer gold particles along the basolateral membranes and in the central cytoplasm (Fig. 5.15A and B). This distribution was consistent with the results from quantitative analysis of gold labelling in A6 cells and the rat collecting duct (Gao *et al.*, 1992; Simon *et al.*, 1993).

Effects of cytochalasin B on actin filaments are complicated, and often unpredictable; in fact, certain investigations have failed to show any depolymerizing effect at all (Morris and Tannenbaum, 1980), hence, it was specially important for our electrophysiological studies to know the effects of cytochalasin B on the actin network. The results from fluorescence studies on effects of CB were not too convincing; however, with immunogold we demonstrated that after 2 hours incubation with cytochalasin B, the regular arrangement of apical actin filaments was fragmented,

but concurred with an apparent decrease in the number of gold particles (Fig. 5.17A). These changes may be consistent with the depolymerization of actin.

Regarding the mechanism of action of AVP, as discussed above, it has been suggested that vesicles containing Na^+ channels are recruited from subapical stores (Garty and Edelman, 1983; Lewis and de Moura, 1984). The actin network could present a barrier to fusion of vesicles and, thus would have to depolymerise to allow the insertion of vesicle. Analogously, it was demonstrated that AVP causes fragmentation of the actin network, allowing water channels to reach and fuse with the apical membrane of the toad bladder epithelium (Handler, 1988). Recently, several studies have confirmed that actin is, in fact, rapidly depolymerized by AVP, which leads to an increase in water flux (Ding *et al.*, 1991; Franki *et al.*, 1992; Gao *et al.*, 1992; Simon *et al.*, 1993). Unfortunately, there is very little evidence for a similar mechanism modulating Na^+ reabsorption. Our results showed that treatment with AVP for 30 minutes caused some fragmentation of the cytoskeleton (Fig. 5.17B). This was also accompanied by an apparent reduction in the number of gold particles similar to that observed by Gao *et al.* (1992) in the toad urinary bladder. Nevertheless, this is not sufficient evidence to support the theory that AVP increases Na^+ transport by vesicle fusion; treatment of a frog skin epithelium with cytochalasin B for 2 hours had little effect on the AVP-stimulated Na^+ transport rate which rather decreased compared to control values (see Table 8 and Fig.5.8). Recently, Oh *et al.* (1993) showed that AVP directly phosphorylated Na^+ channels already present in the membrane. This argues against the insertion theory.

Although the exact mechanisms are still ill-defined, it seems clear from some physiological studies that dynamic interactions of actin with the plasma membrane may be involved in the control of Na^+ channel activity. There is much evidence supporting the insertion theory for regulation of cAMP-dependent changes in channel

densities. Our results do not favour either of the hypotheses, however, it does indicate that, in the event of the insertion theory being correct, in frog skin, this does not occur by means of an actin-dependent mechanism. The cytochemical results from this study substantiate to the important structural basis underlying the mechanisms regulating Na^+ transport in frog skin epithelium.

Chapter 7

Conclusion

We have clearly demonstrated that autoregulatory and hormonally regulated membrane conductance is increased mainly by inducing an increase in the number of active channels, and not by a change in channel conductance.

We were able to demonstrate that in response to a decrease in mucosal Na^+ concentrations, autoregulatory changes in Na^+ channel activity occur by two mechanisms; an increase in β' and changes in N_T. The latter mechanism is dependent on an intact actin network. Disruption of actin by CB diminished the autoregulatory response. This leaves open the idea that increases in the N_T also occurred via an insertion mechanism. Disruption of microfilaments inhibited the autoregulatory increase in N_O in response to a reduction in mucosal Na^+ by blocking changes in N_T, while leaving the response by an increase in open probability unchanged. These conclusions suggest that cytochalasin B did not affect the Na^+ channels already residing in the membrane, but apparently prevented the activation of channels by recruitment from cytoplasmic stores.

In contrast, disruption of microfilaments did not impair the hormonal recruitment of channels. Our results with AVP apparently indicate that autoregulatory and cAMP-mediated changes in N_O occur by distinct mechanisms: autoregulation by recruitment of new channels from a cytoplasmic pool, and possibly AVP-induced activation of quiescent channels already residing in the apical membrane.

Actin filaments are believed to participate in the anchoring and regulation of apical membrane Na^+ channels in Na^+-transporting epithelia. Although recent results support

our theories, we extended our electrophysiological studies to find direct morphological evidence by using immunocytochemical labelling methods. The use of direct rhodamine-phalloidin fluorescence was useful to demonstrate the general distribution of actin around the periphery of the granular cells. Further resolution of the localisation of actin had to be studied by immunogold labelling technique. In frog skin regular bundles of F-actin comprised a substantial portion of the cytoskeleton beneath the apical membrane of granular cells, with markedly less label along the basolateral membrane and in the remaining cytoplasm. Treating cells with cytochalasin B and AVP caused disruption of the apical actin fibres, concurrent with an apparent decrease in gold particles. These signs are indicative of depolymerization of the actin fibres. At present, the significance of this distribution of actin is unknown. The apical polarisation of actin is consistent with a role in regulating the Na^+ permeability of the apical membrane.

The apical membrane Na^+ channel is subjected to multiple regulatory mechanisms, many of which interact with each other. Regulation probably also involves control of distribution between membrane and intracellular pools. Our contrasting results with autoregulatory and cAMP-dependent regulatory mechanisms seemingly equates to differential control by the actin network. We have, at present, no idea which intracellular receptors serve changes in Na^+ entry, or initiate regulatory changes. In addition, there is more than one type of Na^+ channel present in apical membrane of tight epithelia, some of which might not be measured by our methods. Similarly, changes in membrane lipid domains may be an important regulatory mechanism. Details of the complex mechanisms needed to regulate transcellular Na^+ transport will come from contributions in the fields electrophysiology and/or immunocytochemical studies. Advances in electrophysiological methods will provide new, important information and a deeper understanding of Na^+ transport mechanisms in cell biology.

Future work will include studies for the identification of Na^+ channels in cytoplasmic vesicles and the trafficking of putative channels between vesicles and the apical membrane, or between different cytoplasmic pools.

Chapter 8

References

Abramcheck, F. J., Van Driessche, W. and Helman, S. I. (1985) Autoregulation of apical membrane Na+ permeability of tight epithelia. Noise analysis with amiloride and CGS 4270. *Journal of General Physiology* **85**: 555-582.

Alberts, B., Bray, D. and Lewis, J. (1989) The plasma membrane. In: *Molecular Biology of the Cell*. 2nd edition. Garland Publishing Inc. New York. Chapter **6**: 275-280.

Anand-Srivastava, M. B., Vinay, P., Genest, J. and Cantin, M. (1986) Effect of atrial natriuretic factor on adenylate cyclase in various nephron segments. *American Journal of Physiology* **251**: F417-F423.

Armstrong, C. M. (1975) In excitable membranes. *Biophysical Journal* **15**: 932-933.

Asher, C. and Garty, H. (1988) Aldosterone increases the apical Na^+ permeability of toad bladder by two different mechanisms. *Proceedings of the National Academy of Sciences USA* **85**: 7413-7417.

Ausiello, D. A., Skorecki, K. L., Verkman, A. S. and Bonventre, J. V. (1987) Vasopressin signaling in kidney cells. *Kidney International* **31**: 521-529.

Ausiello, D.A., Sorscher, E., Harlin, C. and Benos, D. J. (1989) Subunits of the epithelial Na^+ channel may be G-proteins. *FASEB Journal* **3**: A228.

Ausiello, D. A., Stow, J. L., Cantiello, H. F., de Almeida, J. B. and Benos, D. J. (1992) Purified epithelial Na^+ channel complex contains the pertussis toxin-sensitive G alpha i-3 protein. *The Journal of Biological Chemistry* **267**: 4759-4765.

Awayda, M. S. and Helman, S. I. (1992) Na^+ transport related changes of apical membrane capacitance in the tight epithelium of frog skin. *FASEB Journal* **6**: A1239.

Barbry, P., Chassande, O., Vigne, P., Frelin, C., Ellore, C., Cragoe, E. J., Jr. and Lazdunski, M. (1987) Purification and subunit structure of the [^{3}H]phenamil receptor associated with the renal apical Na^+ channel. *Proceedings of the National Academy of Sciences USA* **84**: 4836-4840.

Barbry, P., Chassande, O., Marsault, R., Lazdunski, M. and Frelin, C. (1990) [^{3}H]phenamil binding protein of the renal epithelium sodium channel. Purification, affinity labeling and functional reconstitution. *Biochemistry* **29**: 1039-1045.

Barthel, L. K. and Raymond, P. A. (1990) Improved method for obtaining 3-µm cryosections for immunocytochemistry. *The Journal of Histochemistry and Cytochemistry* **38** (9): 1383-1388.

Bastl, C. P. and Hayslett, J. (1992) The cellular action of aldosterone in target epithelia. *Kidney International* **42**: 250-264.

Benos, D. J. (1982) Amiloride: a molecular probe of sodium transport in tissues and cells. *American Journal of Physiology* **242**: C131-145.

Benos, D. J., Mandel, L. J. and Simon, S. A. (1980) Cation selectivity and competition at the sodium entry site in frog skin. *Journal of General Physiology* **76**: 223-247.

Benos, D. J., Reyes, J. and Shoemaker, D. G. (1983) Amiloride fluxes across erythrocyte membranes. *Biochimica et Biophysica Acta* **734**: 99-104.

Benos, D. J., Saccomani, G., Brenner, B. M. and Sariban-Sohraby, S. (1986) Purification and characterisation of the amiloride-sensitive sodium channel from A6 cultured cells and bovine renal papilla. *Proceedings of the National Academy of Sciences USA* **83**: 8525-8529.

Benos, D. J., Saccomani, G. and Sariban-Sohraby, S. (1987) The epithelial sodium channel. Subunit number and location of the amiloride binding site. *The Journal of Biological Chemistry* **262**:10613-10618.

Bindels, R. J. M., Schaffer, J. A. and Reif, M. C. (1988) Stimulation of sodium transport by aldosterone and arginine vasotocin in A6 cells. *Biochimica et Biophysica Acta* **972**: 320-330.

Bourguet, J., Hugon, J. S., Valenti, G. and Svelto, M. (1988) ADH-induced water permeability: what role for the microtubular network? *Comparative Biochemical Physiology* **90** (4): 669-672.

Bremec, J. L., Bridges, R. J., Frizzell, R. A. and Benos, D. J. (1987) Cationic selectivity of the amiloride-blockable sodium channel from rat colonic enterocytes. *Federation Proceedings* **46**: 1270.

Brown, A. M. (1991) Ion channels as G protein effectors. *News in Physiological Sciences* **6**: 158-161.

Brown, D. (1989) Membrane recycling and epithelial cell function. *American Journal of Physiology* **256**: F1-F12.

Brown, D., Grosso, A. and DeDousa, R. C. (1983) Correlation between water flow and intramembrane particle aggregates in toad epidermis. *American Journal of Physiology* **245**: 334-342.

Brown, D., Sorscher, E. J., Ausiello, D. A. and Benos, D. J. (1989) Immunocytochemical localization of Na^+ channels in rat kidney medulla. *American Journal of Physiology* **256**: F366-F369.

Brown, K. M. and Dennis, J. E. (1972) Derivative free analogues of the Levenburg-Marquardt and Gauss algorithms for non-linear least squares approximation. *Numerische Mathematik* **18**: 289-297.

Cantiello, H. F. and Ausiello, D. A. (1986) Atrial natriuretic factor and cGMP inhibit amiloride-sensitive Na^+ transport in the cultured renal epithelial cell line, LLC-PK1. *Biochemical and Biophysical Research Communications* **134**: 852-860.

Cantiello, H. F., Patenaude, C. R. and Ausiello, D. A. (1989) G-protein subunit, α_i-3, activates a pertussis-toxin-sensitive Na^+ channel from the epithelial cell line A6. *The Journal of Biological Chemistry* **264**: 20867-20870.

Cantiello, H. F., Patenaude, C. R. and Ausiello, D. A. (1990) G-protein activation of an epithelial Na^+-channel is mediated via phospholipid metabolites. *Journal of the American Society of Nephrology* **1**: 25A.

Cantiello, H. F., Stow, J. L., Prat, A. G. and Ausiello, D. A. (1991) Actin filaments regulate epithelial Na^+ channel activity. *American Journal of Physiology* **261**: C882-C888.

Chen, L., Williams, S. K. and Schaffer, J. A. (1990) Differences in synergistic actions of vasopressin and deoxycorticosterone in rat and rabbit CCD. *American Journal of Physiology* **259**: F147-F156.

Chou, K.-Y. and Els, W. J. (1991) The localization of microtubules and microfilaments in frog skin epithelial cells: an immunological investigation. *Proceedings of the Electron icroscopy Society of Southern Africa* 21: 17-18.

Clausen, C., Lewis, S. A. and Diamond, J. M. (1979) Impedance analysis of a tight epithelium using a distributed resistance model. *Biophysical Journal* **26**: 291-318.

Clausen, C., Reinach, P. S. and Marcus, D. C. (1986) Membrane transport parameters in frog corneal epithelium measured using impedance analysis techniques. *Journal of Membrane Biology* **91**: 213-225.

Cole, K. S. (1972) In: *Membranes, Ions, and Impulses*. University of California Press, Berkeley. p.12.

Cole, K. S. and Cole, R. H. (1941) Dispersion and absorption in dielectrics. *Journal of Chemical Physics* **9**: 341-351.

Coleman, R. A., Harris, H. W. and Wade, J. B. (1987) Visualization of endocytosed markers in freeze-fracture studies of toad urinary bladder. *Journal of Histochemistry and Cytochemistry* **35**: 1405-1414.

Colquhoun, D. and Hawkes, A. G. (1983) The principles of the stochastic interpretation of ion-channel mechanisms. In: *Single Channel Recording*. edited by Sakmann, B. and Neher, E. Plenum press, New York. Chapter **9**: 135-175.

Cooley, J. W., Lewis, P. A. W. and Welch, P. D. (1967) The fast Fourier transform and its applications. *IBM Research* RC **1743**: 15-33.

Cort, J. H., Schück, O., Stribrna, J., Skopkova, J., Jost, K. and Mulder, J. L. (1975) Role of the disulfide bridge and C-terminal tripeptide in the antidiuretic action of vasopressin in man and in the rat. *Kidney International* **8**: 292-297.

Darnell, J., Lodish, H. and Baltimore, D. (1990) Cell-to-cell signaling: hormones and receptors. In: *Molecular Cell Biology*, 2nd edition. Scientific American Books, Inc. New York. Chapter**19**: 709-714.

Dawson, D. C., Van Driessche, W. and Helman, S. I. (1988) Osmotically induced basolateral K^+ conductance in turtle colon: Lidocaine-induced K^+ channel noise. *American Journal of Physiology* **254**: C165-C174.

Das, S., Garepapaghi, M. and Palmer, L. G. (1991) Stimulation by cGMP of apical Na channels and cation channels in toad urinary bladder. *American Journal of Physiology* **262**: C234-C241.

Desmedt, L., Simaels, J. and Van Driessche, W. (1993) Ca^{++}-blockable, poorly selective cation in the apical membrane of amphibian epithelia. UO_2^{++} reveals two channel types. *Journal of General Physiology* **101**: 85-102.

De Wolf, I. and Van Driessche, W. (1986) Voltage-dependent Ba^{++} block of K^{+} channels in apical membrane of frog skin. *American Journal of Physiology* **251**: C696-C706.

Ding, G., Franki, N., Condeelis, J. and Hays, R. M. (1991) Vasopressin depolymerizes F-actin in the toad bladder epithelial cell. *American Journal of Physiology* **260**: C9-C16.

Eaton, D. C. (1981) Intracellular sodium ion activity and sodium transport in rabbit urinary bladder. *Journal of Physiology* **316**: 527-544.

Eaton, D. C. and Hamilton, K. L. (1988) The amiloride-blockable sodium channel of epithelial tissue. In: *Ion Channels*, edited by Narahashi, T. New York: Plenum. **1**: 151-182.

Eaton, D. C. and Marunaka, Y. (1990) Ion channel fluctuations:" Noise" and single channel measurements. In: *Current Topics in Membranes and Transport*, edited by Bronner, F. Acdemic Press, Inc. **37**: 61-114.

Edelman, I. S. (1981) Receptors and effectors in hormone action on the kidney. *American Journal of Physiology* **241**: F333-F339.

Els, W. J. and Mahlangu, A. F. D. (1987) Microelectrode studies on the effects of exogenous cyclic adenosine monophosphate on active sodium transport in frog skin. *Journal of Physiology* **388**:547-563.

Els, W. J. and Helman, S. I. (1989) Regulation of sodium channel densities by vasopressin signalling. *Cellular Signalling* **1**(6): 533-539.

Els, W. J. and Helman, S. I. (1991) Activation of epithelial Na channels by hormonal and autoregulatory mechanisms of action. *Journal of General Physiology* **98**: 1197-1220.

Els, W. J. and Chou, K.-Y. (1993) Sodium-dependent regulation of epithelial sodium channel densities in frog skin; a role for the cytoskeleton. *Journal of Physiology* 462: 447-464.

Fisher, R. S., Erlij, D. and Helman, S. I. (1980) Intracellular voltage of isolated epithelia of frog skin. Apical and basolateral cell punctures. *Journal of General Physiology* **76**: 447-453.

Foskett, J. K. and Spring, K. R. (1985) Involement of calcium and the cytoskeleton in gallbladder epithelial cell volume regulation. *American Journal of Physiology* **248**: C27-C36.

Franki, N., Ding, G., Gao, Y. and Hays, R. M. (1992) Effect of cytochalasin D on the actin cytoskeleton of the toad bladder epithelial cell. *American Journal of Physiology* **263**: C995-C1000.

French, A. S. (1992) Mechanosensitive ion channels. *Annual Review of Physiology* **54**: 135-152.

Frindt, G., Silver, R. B., Windhager, E. E. and Palmer, L. G. (1993) Feedback regulation of Na channels in rat CCT. 2. Effects of inhibition of Na entry. *American Journal of Physiology* **264**: F565-F574.

Frings, S. and Lindemann, B. (1988) Odorant response of isolated olfactory receptor cells is blocked by amiloride. *Journal of Membrane Biology* **105**: 233-243.

Frings, S., Purves, R. D. and MacKnight, A. D. C. (1988) Single-channel recordings from the apical membrane of the toad urinary bladder epithelial cell. *Journal of Membrane Biology* **106**:157-172.

Fuchs, W., Larsen, E. H. and Lindemann, B. (1977) Current-voltage curve of sodium channels and concentration dependence of sodium permeability in frog skin. *Journal of Physiology* **267**: 137-166.

Gao, Y., Franki, N., Macaluso, F. and Hays, M. (1992) Vasopressin decreases immunogold labeling of apical actin in the toad bladder granular cell. *American Journal of Physiology* **263**: C908-C912.

Gardner, P., Ogden, D. C. and Colquhoun, D. (1984) Conductance of single ion channels opened by nicotinic agonists are indistinguishable. *Nature* **309**: 160-162.

Garty, H. (1986) Mechanisms of aldosterone action in tight epithelia. *Journal of Membrane Biology* **90**: 193-205.

Garty, H. and Edelman, I. S. (1983) Amiloride-sensitive trypsinization of apical sodium channels. Analysis of hormonal regulation of sodium transport in toad bladder. *Journal of General Physiology* **81**: 785-803.

Garty, H. and Benos, D. J. (1988) Characteristics and regulatory mechanisms of the amiloride-blockable Na^+ channels. *Physiological Reviews* **68**: 309-373.

Garty, H., Yeger, O., Yanovsky, A. and Asher, C. (1989) Guanosine nucleotide-dependent activation of the amiloride-blockable Na^+ channel. *American Journal of Physiology* **256**: F965-F969.

Gogelein, H. and Greger, R. (1986) Na^+ selective channels in the apical membrane of the rabbit late proximal tubules (pars recta). *Pflügers Archiv European Journal of Physiology* **406**: 198-203.

Granitzer, M., Leal, T., Nagel, W. and Crabbe, J. (1991) Apical and basolateral conductance in cultured A6 cells. *Pflügers Archiv European Journal of Physiology* **417**: 463-468.

Gumbiner, B. (1987) Structure, biochemistry, and assembly of epithelial tight junctions. *American Journal of Physiology* **253**: C749-C758.

Hamill, O. P., Lane, J. W. and McBride, D. W. Jr. (1992) Amiloride: a molecular probe for mechnosensitive channels. *Trends in Pharmacological Science* **13**: 373-376.

Hamill, O. P., Marty, A., Neher, E., Sakmann, B. and Sigworth, F. J. (1981) Improved patch-clamp techniques for high-resolution current recording from cells and cell-free membrane patches. *Pflügers Archiv European Journal of Physiology* **91**: 85-100.

Hamilton, K. L. and Eaton, D. C. (1985) Single-channel recordings from amiloride-sensitive epithelial sodium channel. *American Journal of Physiology* **249**: C200-C207.

Hamilton, K. L. and Eaton, D. C. (1986) Regulation of single sodium channels in renal tissue: a role in sodium homeostasis. *Federation Proceedings* **45**(12):2713-2717.

Handler, J. S., Preston, A. S. and Orloff, J. (1972) Effect of ADH, aldosterone, ouabain and amiloride on toad bladder epithelial cells. *American Journal of Physiology* **222**: 1071-1074.

Handler, J. S. (1988) Antidiuretic hormone moves membranes. *American Journal of Physiology* **255**: F375-F382.

Harris, H. Jr. and Handler, J. S. (1988) The role of membrane turnover in water permeability: response to antidiuretic hormone. *Journal of Membrane Biology* **103**: 207-216.

Hartwig, J. H., Brown, D., Ausiello, D. A., Stossel, T. P. and Orci, L. (1990) Polarization of gelsolin and actin binding protein in kidney epithelial cells. *Journal of Histochemistry and Cytochemistry* **38**: 1145-1153.

Harvey, B. J. and Kernan, R. P. (1984) Sodium-selective microelectrode study of apical permeability in frog skin: effect of sodium, amiloride and ouabain. *Journal of Physiology* **356**: 359-374.

Helman, S. I. (1979) Electrochemical potentials in frog skin: inferences for electrical and mechanistic models. *Federation Proceedings* **38**(13): 2743-2750.

Helman, S. I. and Miller, D. A. (1971) In vitro techniques for avoiding edge damage in studies of frog skin. *Science* **173**: 146-148.

Helman, S. I. and Fisher, R. S. (1977) Microelectrode studies of the active Na transport pathway of frog skin, *Journal of General Physiology* **69**: 571-604.

Helman, S. I. and Baxendale, L. M. (1990) Blocker-related changes of channel density: Analysis of a three-state model for apical Na channels of frog skin. *Journal of General Physiology* **95**:647-678.

Helman, S. I. and Kizer, N. L. (1990) Apical sodium ion channels of tight epithelia as viewed from the perspective of noise analysis. In: *Current Topics in Membrane and Transport*, edited by Bronner, F. Academic Press, Inc. **37**: 117-155.

Helman, S. I. and Van Driessche, W. (1990) Channels and noise in epithelial tissues. In: *Current Topics in Membranes and Transport*, edited by Bronner, F. Acdemic Press, Inc. Volume **37**.

Helman, S. I., Nagel, W. and Fisher, R. S. (1979) Ouabain on active transepithelial sodium transport in frog skin. Studies with microelectrodes. *Journal of General Physiology* **74**: 105-127.

Helman, S. I., Cox, T. C. and Van Driessche, W. (1983) Hormonal control of apical membrane Na transport in epithelia. Studies with fluctuation analysis. *Journal of General Physiology* **82**: 201-220.

Helman, S. I., Koeppen, B. M., Beyenbach, K. W. and Baxendale, L. M. (1985) Patch clamp studies of apical membranes of renal cortical collecting ducts. *Pflügers Archiv European Journal of Physiology* **405**(Suppl. 1): S71-76.

Holmgren, K., Magnusson, N., Franki, N. and Hays, R. M. (1992) ADH-induced depolymerization of F-actin in the toad bladder granular cell: a confocal microscope study. *American Journal of Physiology* **262**: C672-677.

Horisberger, J.-D., Canessa, C. and Rossier, B. C. (1993) The epithelial sodium channel: recent developments. *Cellular Physiology and Biochemistry* **3**: 283-294.

Hoshiko, T. and Van Driessche, W. (1986) Effect of sodium on amiloride- and triamterene-induced current fluctuations in isolated frog skin. *Journal of General Physiology* **87**: 425-442.

Hugon, J. S., Ibarra, C., Valenti, G. and Bourguet, J. (1989) Microtubules and actin microfilaments in the amphibian bladder granular cells. *Biology of the Cell* **66**: 77-84.

Johnson, A. B. and Bettica, A. (1989) On-grid immunogold labeling of glial intermediate filaments in epoxy-embedded tissue. *American Journal of Anatomy* **185**: 335-341.

Johnson, G. D., Davison, R. S., Mcnamee, K. C., Russell, G., Goodwin, D., and Holborow, E. J. (1982) Fading of immunofluorescence during microscopy: a study of the phenomenon and its remedy. *Journal of Immunology Methods* **55**: 231-42.

Jorgensen, F. and Ohmori, H. (1988) Amiloride blocks the mechanoelectrical transduction channel of hair cells of the chick. *Journal of Physiology* **403**: 577-588.

Kellerman, P. S., Clark, R. A. F., Hoilein, C. A., Linas, S. L. and Molitoris, B. A. (1990) Role of microfilaments in maintenance of proximal tubule structural and functional integrity. *American Journal of Physiology* **259**: F279-F285.

Kemendy, A. E., Kleyman, T. R. and Eaton, D. C. (1992) Aldosterone alters the open probability of amiloride-blockable sodium channels in A6 epithelia. *American Journal of Physiology* **263**: C825-C837.

Kleyman, T. R. and Cragoe, E. J., Jr. (1988) Amiloride and its analogs as tools in the study of ion transport. *Journal of Membrane Biology* **105**: 1-21.

Kleyman, T. R., Cragoe, E. J., Jr. and Kraehenbühl, J.-P. (1989) The cellular pool of Na^+ channels in the amphibian cell line A6 is not altered by mineralocorticoids. Analysis using a new photoactive amiloride analog in combination with anti-amiloride antibodies. *The Journal of Biological Chemistry* **264**: 11995-12000.

Kleyman, T. R., Kraehenbuhl, J.-P. and Ernst, S. A. (1991) Characterisation and cellular localisation of the epithelial Na^+ channel. Studies using an anti-Na^+ channel antibody raised by an antiidiotypic route. *The Journal of Biological Chemistry* **266**: 3907-3915.

Kleyman, T. R., Yulo, T., Ashbaugh, C., Landry, D., Cragoe, E. J., Jr., Karlin, A. and Al-Awqatio, Q. (1986) Photoaffinity labelling of the epithelial sodium channel. *The Journal of Biological Chemistry* **261**: 2839-2843.

Koefoed-Johnsen, V. and Ussing, H. H. (1958) The nature of the frog skin potential. *Acta Physiologica Scandinavica* **42**: 298-308.

Kraehenbuhl, J. P., Pfeiffer, J., Rossier, M. and Rossier, B. C. (1979) Microfilament-rich cells in toad bladder epithelium. *Journal of Membrane Biology* **48**: 167-180.

Krattenmacher, R., Fischer, H., Van Driessche, W. and Clauss, W. (1988) Noise analysis of cAMP-stimulated Na current in frog colon. *Pflügers Archiv European Journal of Physiology* **412**: 568-573.

Krause, W. J. and Cutts, J. H. (1986) Epithelium. *Concise text of Histology*, 2nd edition. Waverly Press Inc. USA Chapter **2**: 30-33.

Krogh, A. (1937) Osmotic regulation in the frog (*R. esculenta*) by active absorption of chloride ions. *Skandinavisches Archiv fur Physiologie* **76** : 60-74.

Kubat, B., Lorenzen, M. and Reale, E. (1989) Vasopressin-induced intramembrane particle aggregates. A dose-response relationship in the isolated collecting of the rabbit kidney. *Biology of the Cell* **66**: 59-63.

Kurihara, H., Uchida, K. and Fujita, H. (1990) Distribution of microtubules and microfilaments in thyroid follicular epithelial cells of normal, TSH-treated, aged, and hypophysectomized rats. *Histochemistry* **93**:335-345.

Lackie, P. M., Hennessy, R. J., Hacker, G. W. and Polak, J. M. (1985) Investigation of immunogold-silver staining by electron microscopy. *Histochemistry* **83**: 545-550.

Lane, J. W., Levine, C., Levine, K. and Hamill, O. P. (1990) Amiloride directly blocks the mechanosensitive cation channel in *Xenopus* oocytes. *Biophysical Journal* **57**: 317a.

Lane, J. W., McBride, D. W. Jr. and Hamill, O. P. (1991) Amiloride block of the mechanosensitive cation channel in *Xenopus* oocytes. *Journal of Physiology* **441**: 347-366.

Lauger, P. (1980) Kinetic properties of ion carriers and channels. *Journal of Membrane Biology* **57**: 163-178.

Leister, J. and Molitoris, B. A. (1993) Disease processes in epithelia: the role of the actin cytoskeleton and altered surface membrane polarity. *Biochimica et Biophysica Acta* **1225**: 1-13.

Lester, D. S., Asher, C. and Garty, H. (1988) Characterization of cAMP-induced activation of epithelial sodium channels. *American Journal of Physiology* **254**: C802-808.

Lewis, S. A. and de Moura, J. L. C. (1982) Incorporation of cytoplasmic vesicles into apical membrane of mammalian urinary bladder epithelium. *Nature* **297**: 685-688.

Lewis, S. A. and Wills, N. K. (1983) Apical membrane permeability and kinetic properties of the sodium pump in rabbit urinary bladder. *Journal of Physiology* **341**: 169-184.

Lewis, S. A. and de Moura, J. L. C. (1984) Apical membrane area of rabbit urinary bladder increases by fusion of intracellular vesicles: an electrophysiological study. *Journal of Membrane Biology* **82**: 123-136.

Lewis, S. A. and Hanrahan, J. W. (1985) Apical and basolateral membrane ionic channels in rabbit urinary bladder epithelium. *Pflügers Archiv European Journal of Physiology* **405** (Suppl. 1): S83-S88.

Lewis, S. A. and Alles, W. P. (1986) Urinary kallikrein: a physiological regulator of epithelial Na absorption. *Proceedings of the National Academy of Sciences USA* **83**: 5345-5348.

Lewis, S. A., Eaton, D. A. and Diamond, J. M. (1976) The mechanism of Na^+ transport by rabbit urinary bladder. *Journal of Membrane Biology* **28**: 41-70.

Lewis, S. A., Ifshin, M. S., Loo, D. D. F. and Diamond, J. M. (1984) Studies of sodium channels in rabbit urinary bladder by noise analysis. *Journal of Membrane Biology* **80**:135-151.

Li, J. H.-Y., Cragoe, E. J. Jr. and Lindemann, B. (1985) Structure-activity relationship of amiloride analogs as blockers of epithelial Na^+ channels. I. Pyrazine-ring modifications. *Journal of Membrane Biology* **83**: 45-56.

Li, J. H.-Y., Palmer, L. G., Edelman, I. S. and Lindemann, B. (1982) The role of sodium-channel density in the natriferic response of the toad urinary bladder to an antidiuretic hormone. *Journal of Membrane Biology* **64**: 77-89.

Light, D. B., McCann, F. V., Keller, T. M. and Stanton, B. A. (1988) Amiloride-sensitive cation channel in apical membrane of inner medullary collecting duct. *American Journal of Physiology* **255**: F278-F286.

Light, D. B., Schwiebert, E. M., Karlson, K. H. and Stanton, B. A. (1989a) Atrial natriuretic peptide inhibits a cation channel in renal inner medullary collecting duct cells. *Science* **243**: 383-385.

Light, D B., Ausiello, D. A. and Stanton, B. A. (1989b) Guanine nucleotide-binding protein α_i-3 directly activates a cation channel in rat renal inner medullary collecting duct cells. *Journal of Clinical Investigation (New York NY)* **84**: 352-356.

Lindemann, B. (1984) Fluctuation analysis of sodium channels in epithelia. *Annual Review of Physiology* **46**: 497-515.

Lindemann, B. and Van Driessche, W. (1977) Sodium-specific membrane channels of frog skin are pores: current fluctuations reveal high turnover. *Science* **195**: 292-294.

Lindemann, B. and Van Driessche, W. (1978) The mechanism of Na uptake through Na-selective channels in the epithelium of frog skin. In: *Membrane Transport Processes*, edited by Hoffman, J. F. Raven Press, New York. **1**: 155-178.

Ling, B. N. and Eaton, D. C. (1989) Effects of luminal Na^+ on single Na^+ channels in A6 cells, a regulatory role for protein kinase C. *American Journal of Physiology* **256**: F1094-F1103.

Ling, B. N., Hinton, C. F. and Eaton, D. C. (1991) Amiloride-sensitive sodium channels in rabbit cortical collecting tubule primary cultures. *American Journal of Physiology* **261**: F933-F944.

Linshaw, M. A. (1989) Volume control of isolated rabbit proximal tubules. *Seminars in Nephrology* **9**: 83-90.

Linshaw, M. A., Macalister, T. J., Welling, L. W., Bauman, C. A., Hebert, G. Z., Downey, G. P., Koo, E. W. Y. and Gotlieb, A. I. (1991) Role of the cytoskeleton in isotonic cell volume control of rabbit proximal tubules. *American Journal of Physiology* **261**: F60-F69.

Lipton, P. (1972) Effect of changes in osmolarity on sodium transport across isolated toad bladder. *American Journal of Physiology* **222**: 821-828.

Loo, D. D. F., Lewis, S. A., Ifshin, M. S. and Diamond, J. M. (1983) Turnover, membrane insertion, and degradation of sodium channels in rabbit urinary bladder. *Science* **221**: 1288-1290.

Loris, L., Krouse, M. E., Hagiwara, G., Bell, C. L. and Wine, J. J. (1989) Patch-clamp study of cultured human sweat duct cells: amiloride-blockable Na^+ channel. *Pflügers Archiv European Journal of Physiology* **414**: 369-372.

Luft, J. H. (1973) Embedding media - old and new. In: *Advanced Techniques in Biological Electron Microscopy,* edited by J. K. Koehler. Spring-Verlag, New York. (E.M. Unit).

Lux, H. D. and Brown, A. M. (1984) Patch and whole cell calcium currents recorded simultaneously in snail neurons. *Journal of General Physiology* **83**: 727-750.

Maack, T., Camargo, M. J. F., Kleinert, H. D., Laragh, J. H. and Atlas, S. (1985) Atrial natriuretic factor: structure and functional properties. *Kidney International* **27**: 607-615.

Madara, J. L., Banenberg, D. and Carlson, S. (1986) Effects of cytochalasin D on occluding junctions of intestinal absorptive cells: further evidence that the cytoskeleton may influence paracellular permeability and junctional charge selectivity. *Journal of Cell Biology* **102**: 2125-2136.

Mar, H. and Wight, T. N. (1988) Colloidal gold immunostaining on deplasticized ultra-thin sections. *The Journal of Histochemistry and Cytochemistry* **36** (11): 1387-1395.

Margineanu, D. G. and Van Driessche, W. (1990) Effects of millimolar concentrations of glutaraldehyde on the electrical properties of frog skin. *Journal of Physiology* **427**: 567-581.

Marunaka, Y. and Eaton, D. C. (1991) Effects of vasopressin and cAMP on single amiloride-blockable Na channels. *American Journal of Physiology* **260**: C1071-1084.

McNeil, H. and Nelson, W. J. (1992) Shaping an epithelial cell: the role of cell adhesion molecules in the reorganisation of the membrane cytoskeleton. In: *Epithelial Organisation and Development,* edited by Tom P. Fleming. 1st edition. Published by Chapman and Hall, London. Chapter **2**: pp.53-55.

Mills, J. W., Thurau, K., Dörge, A. and Rick, R. (1985) Electron microprobe analysis of intracellular electrolytes in resting and isoproterenol-stimulated glands of frog skin. *Journal of Membrane Biology* **86**: 211-220.

Minuth, W. W., Steckelings, U. and Gross, P. (1987) Complex physiological and biochemical action of aldosterone in toad urinary bladder and mammalian renal collecting duct cells. *Renal Physiology* **10**: 297-310.

Mohrmann, M., Cantiello, H. F. and Ausiello, D. A. (1987) Inhibition of epithelial Na^+ transport by atriopeptin, protein kinase C, and pertussis toxin. *American Journal of Physiology* **253**: F372-F376.

Morris, A. and Tannenbaum, J. (1980) Cytochalasin D does not produce net depolymerization of actin filaments in HEp-2 cells. *Nature* **287**: 637-639.

Morris, C. E. (1990) Mechanosensitive ion channels. *Journal of Membrane Biology* **113**: 93-107.

Muller, J., Kachadorian, W. A. and DiScala, V. A. (1980) Evidence that ADH-stimulated intramembrane particle aggregates are transferred from cytoplasmic to luminal membrane in toad bladder epithelial cells. *Journal of Cell Biology* **85**: 83-95.

Neher, E. and Sakmann, B. (1976) Single-channel currents recorded from membrane of denervated frog muscle fibres. *Nature* **260**: 779-802.

Neher, E. and Stevens, C. F. (1977) Conductance fluctuations and ionic pores in membranes. *Annual Review of Biophysics and Bioengineering* **6**: 345-381.

Neher, E. and Marty, A. (1982) Discrete changes of cell membrane capacitance observed under conditions of enhanced secretion in bovine adrenal chromaffin cells. *Proceedings of the National Academy of Sciences USA* **79**: 6712-6716.

Neher, E., Sakmann, B. and Steinbach, J. H. (1978) The extracellular patch clamp: a method for resolving currents through individual open channels in biological membranes. *Pflügers Archiv European Journal of Physiology* **375**: 219-228.

Noniguchi, H., Sands, J. M. and Knepper, M. A. (1989) ANF inhibits Nacl and fluid absorption in cortical collecting tubule of rat kidney. *American Journal of Physiology* **256**: F179-F186.

Oh, Y. and Benos, D. J. (1993) Single-channel characteristics of a purified bovine renal amiloride-sensitive Na^+ channel in planar lipid bilayers. *American Journal of Physiology* **264**: C1489-C1499.

Oh, Y., Smith, P. R., Bradford, A. N., Keeton, D. and Benos, D. A. (1993) Regulation by phosphorylation of purified epithelial Na^+ channels in planar lipid bilayers. *American Journal of Physiology* **265**: C85-C91.

Olans, L., Sariban-Sohraby, S. and Benos, D. J. (1984) Saturation Behavior of single, amiloride-sensitive Na^+ channels in plannar lipid bilayers. *Biophysical Journal* **46**: 831-835.

Omachi, R. S., Robbie, D. E., Handler, J. S. and Orloff, J. (1974) Effects of ADH and other agents on cyclic AMP accumulation in the toad bladder epithelium. *American Journal of Physiology* 226: 1152-1157.

Orloff, J. and Handler, J. S. (1962) The similarity of effects of vasopressin, adenosine-3,5 monophosphate (cAMP) and theophylline on the toad bladder. *Journal of Clinical Investigation* **41**: 702-709.

Palmer, L. G. (1982a) Ion selectivity of the apical membrane Na channel in the toad urinary bladder. *Journal of Membrane Biology* **67**: 91-98.

Palmer, L. G. (1982b) Na^+ transport and flux ratio through apical Na^+ channels in toad bladder. *Nature* **297**: 688-690.

Palmer, L. G. (1987) Ion selectivity of epithelial Na channels. *Journal of Membrane Biology* **96**: 97-106.

Palmer, L. G. (1990) Epithelial Na channels: the nature of the conducting pore. *Renal Physiology and Biochemistry* **13**: 51-58.

Palmer, L. G. (1992) Epithelial Na channels, function and diversity. *Annual Review of Physiology* **54**: 51-66.

Palmer, L. G. and Frindt, G. (1986a) Epithelial sodium channel: characterisation by using the patch-clamp technique. *Federation Proceedings* **45**: 2708-2712.

Palmer, L. G. and Frindt, G. (1986b) Amiloride-sensitive Na channels from the apical membrane of the rat cortical collecting tubule. *Proceedings of the National Academy of Sciences USA* **83**: 2767-2770.

Palmer, L. G. and Frindt, G. (1987) Effects of cell Ca and pH on Na channels from rat cortical collecting tubule. *American Journal of Physiology* **253**: F333-339.

Palmer, L. G. and Frindt, G. (1988) Conductance and gating of epithelial Na channels from rat cortical collecting tubule. Effects of luminal Na and Li. *Journal of General Physiology* **92**: 121-138.

Palmer, L. G., Edelman, I. S. and Lindemann, B. (1980) Current-voltage analysis of apical sodium transport in toad urinary bladder: effects of inhibitors of transport and metabolism. *Journal of Membrane Biology* **57**: 59-71.

Palmer, L. G., Li, J. H., Lindemann, B. and Edelman, I. S. (1982) Aldosterone control of the density of sodium channels in the toad urinary bladder. *Journal of Membrane Biology* **64**: 91-102.

Palmer, L. G., Frindt, G., Silver, R. and Strieter, J. (1989) Feedback regulation of epithelial sodium channels. In: *Current Topics in Membrane and Transport* **34**: 45-60.

Palmer, L. G., Cortésy-Theulaz, I., Gaeggler, H.-P., Kraehenbuhl, J.-P. and Rossier, B. C. (1990) Expression of epithelial Na channels in *Xenopus* oocytes. *Journal of General Physiology* **96**: 23-46.

Parczyk, K., Haase, W. and Kondor-Koch, C. (1989) Microtubules are involved in the insertion of proteins at the apical cell surface of the polarized epithelial cell, Madin-Darby canine kidney. *The Journal of Biological Chemistry* **264**: 16837-16846.

Pearl, M. and Taylor, A. (1985) Role of the cytoskeleton in the control of transcellular water flow by vasopressin in amphibian urinary bladder. *Biology of the Cell* **55**: 163-172.

Perkins, F. M. and Handler, J. S. (1981) Transport properties of toad kidney epithelia in culture. *American Journal of Physiology* **241**: C154-C159.

Petersen, O. H. and Petersen, C. C. H. (1986) The patch-clamp technique: Recording ionic currents through single pores in the cell membrane. *News in Physiological Sciences* **1**: 5-8.

Prat, A. G., Ausiello, D. A. and Cantiello, H. F. (1991) Actin filament organization controls Na^+ channels in A6 epithelial cells. *FASEB Journal* **5**: A690.

Prat, A. G., Ausiello, D. A. and Cantiello, H. F. (1993a) Vasopressin and protein kinase A activate G-protein-sensitive epithelial Na^+ channels. *American Journal of Physiology* **265**: C218-223.

Prat, A. G., Bertorello, A. M., Ausiello, D. A. and Cantiello, H. F. (1993b) Activation of epithelial Na^+ channels by protein kinase A requires actin filaments. *American Journal of Physiology* **265**: C224-C233.

Richards, P. D. G., Dando, B. and Els, W. J. (1989) Morphological aspects of two preparations of frog skin epithelium used in studies on sodium transport. *Electron Microscopy Society of Southern Africa Proceedings* **19**: 139-140.

Rick, R., Dörge, A., von Arnim, E. and Thurau, K. (1978) Electron microprobe analysis of frog skin epithelium: evidence for a syncytial sodium transport compartment. *Journal of Membrane Biology* **39**: 313-331.

Rick, R., Spancken, G. and Dörge, A. (1988) Differential effects of aldosterone and ADH on intracellular electrolytes in the toad urinary bladder epithelium. *Journal of Membrane Biology* **101**: 275-282.

Rick, R. (1992) Intracellular ion concentration in the isolated frog skin epithelium: evidence for different types of mitochondria-rich cells. *Journal of Membrane Biology* **127**: 227-236.

Robinson, H. P. C., Sahara, Y. and Kawai, N. (1991) Nonstationary fluctuation analysis and direct resolution of single channel currents at postsynaptic sites. *Biophysical Journal* **59**: 295-304.

Rossier, B. C., Verrey, F. and Kraehenbuhl, J.-P. (1989) Transepithelial sodium transport and its control by aldosterone: a molecular approach. In: *Current Topics in Membrane and Transport*, edited by Schultz, S. G., Academic Press, New York. **34**: 167-183.

Ruknundin, A., Song, M. J. and Sachs, F. (1991) The ultrastructure of patch-clamped membranes: A study using high voltage electron microscopy. *The Journal of Cell Biology* **112**: 125-134.

Sariban-Sohraby, S. and Benos, D. J. (1986a) The amiloride-sensitive sodium channel. *American Journal of Physiology* **250**: C175-190.

Sariban-Sohraby, S. and Benos, D. J. (1986b) Detergent solubilization, functional reconstitution, and partial purification of epithelial amiloride-binding protein. *Biochemistry* **25**: 4639-4646.

Sariban-Sohraby, S. and Fisher, R. S. (1992) Single channel activity by the amiloride binding subunit of the epithelial Na^+ channel. *American Journal of Physiology* **263**: C1111-C1117.

Sariban-Sohraby, S., Burg, M. B., Wiesmann, W. P., Chianh, P. K. and Johnson, J. P. (1984a) Methylation increases sodium transport into A6 apical membrane vesicles: possible mode of aldosterone action. *Science* **225**: 745-746.

Sariban-Sohraby, S., Latorre, R., Burg, M., Olans, L. and Benos, D. (1984b) Amiloride-sensitive epithelial Na^+ channels reconstituted into planar bilayer membranes. *Nature* **308**: 80-82.

Sariban-Sohraby, S., Sorscher, E. J., Brenner, B. M. and Benos, D. J. (1988) Phosphorylation of a single subunit of the epithelial Na^+ channel protein following vasopressin treatment of A6 cells. *The Journal of Biological Chemistry* **263**: 13875-13879.

Sauer, M., Dörge, A., Thurau, K. and Beck, F.-X. (1989) Effect of ouabain on electrolyte concentrations in principle and intercalated cells of the isolated perfused cortical collecting duct. *Pflügers Archiv European Journal of Physiology* **314**: 651-655.

Schafer, J. A. and Hawk, C. T. (1992) Regulation of Na^+ channels in the cortical collecting duct by AVP and mineralocorticoids. *Kidney International* **41**: 255-268.

Schultz, S. G. (1981) Homocellular regulatory mechanisms in sodium-transporting epithelia: avoidance of extinction by "flush-through". *American Journal of Physiology* **241**: F579-F590.

Schultz, S. G. (1985) Regulatory mechanisms in sodium-absorbing epithelia. In: *The Kidney: Physiology and Pathophysiology*, edited by Seldin, D. W. and Giebisch, G.. Raven Press, New York. Chapter **10**: 189-198.

Schultz, S. G. (1989) Intracellular sodium activities and basolateral membrane potassium conductances of sodium-absorbing epithelial cells. In: *Current Topics in Membranes and Transport*, edited by Schultz, S. G., San Diego, CA: Academic. **34**: 21-44.

Schwartz, G. J. and Burg, M B. (1978) Mineralocorticoid effects on cation transport by cortical collecting tubules in vitro. *American Journal of Physiology* **235**: F576-F585.

Sigworth, F. J. and Neher, E. (1980) Single Na-channel currents observed in cultured rat muscle cells. *Nature* **287**: 447-449.

Sigworth, F. J. (1986) The patch clamp is more useful than anyone had expected. *Federation Proceedings* **45** (12): 2673-2677.

Simon, H., Gao, Y., Franki, N. and Hays, R. M. (1993) Vasopressin depolymerizes apical F-actin in rat inner medullary collecting duct. *American Journal of Physiology* **265**: C757-C762.

Simons, K. (1987) Membrane traffic in an epithelial cell line derived from the dog kidney. *Kidney International* **32** (Suppl. 23): S201-207.

Simons, K. and Fuller, F. D. (1985) Cell surface polarity in epithelia. *Annual Review of Cell Biology* **1**: 243-288.

Smith, P. R. and Benos, D. J. (1991) Epithelial Na^+ channels. *Annual Review of Physiology* **53**: 509-530.

Smith, P. R., Saccomani, G., Joe, E. H., Angelides, K. J. and Benos, D. J. (1991) Amiloride-sensitive sodium channel is linked to the cytoskeleton in renal epithelial cells. *Proceedings of the National Academy of Sciences USA* **88**: 6971-6975.

Sorscher, E. J., Accavitti, M. A., Keeton, D., Steadman, E., Frizzell, R. A. and Benos, D. J. (1988) Antibodies against purified epithelial sodium channel protein from bovine renal papilla. *American Journal of Physiology* **255**: C835-C843.

Spooner, P. M. and Edelman, I. S. (1975) Further studies on the effect of aldosterone on electrical resistance of toad bladder. *Biochimica et Biophysica Acta* **406**: 304-314.

Stetson, D. L. and Steinmetz, P. R. (1983) Role of membrane fusion in CO_2 stimulation of proton secretion by turtle bladder. *American Journal of Physiology* **245**: C113-C120.

Stoddard, J. S. and Helman, S. I. (1985) Dependence of intracellular Na^+ concentration on apical and basolateral membrane Na^+ influx in frog skin. *American Journal of Physiology* **249**: F662-F671.

Sugimoto, K., Fujii, S., Kaiho, M. and Nakamura, I. (1990) Stress fibers in the mesenteric mesothelial cells of the large intestine of the bullfrog, *Rana catesbeiana*. *Cell and Tissue Research* **261**:509-516.

Szerlip, H. M., Weisberg, L., Clayman, M., Neilson, E., Wade, J. B. and Cox, M. (1989) Aldosterone-induced proteins: purification and localization of GP65, 70. *American Journal of Physiology* **256**: C865-C872.

Thomas, S. R., Suzuki, Y., Thompson, S. M. and Schultz, S. G. (1983) Electrophysiology of *Necturus* urinary bladder. I. "Instantaneous" current-voltage

relations in the presence of varying mucosal sodium concentrations. *Journal of Membrane Biology* **73**: 157-175.

Thurman, C. L. and Higgins, J. T., Jr. (1982) Amiloride stimulation of sodium transport in the presence of calcium and a divalent cation chelator. *Biochimica et Biophysica Acta* **689**: 561-566.

Tokuyasu, K. T. (1973) A technique for ultracryotomy of cell suspensions and tissue. *Journal of Cell Biology* **57**: 551-565.

Tousson, A., Alley, C. D., Sorscher, E. J., Brinkley, B. R. and Benos, D. J. (1989) Immunochemical localization of amiloride-sensitive Na^+ channels in sodium transporting epithelia. *Journal of Cell Science* **93**: 349-62.

Turnheim, K. (1991) Intrinsic regulation of apical sodium entry in epithelia. *Physiological Reviews* **71**(2): 429-445.

Turnheim, K., Frizzell, R. A. and Schultz, S. G. (1978) Interaction between cell sodium and the amiloride-sensitive sodium entry step in rabbit colon. *Journal of Membrane Biology* 39: 233-256.

Turnheim, K., Thompson, S. M. and Schultz, S. G. (1983) Relationship between intracellular sodium and active sodium transport in rabbit colon: current-voltage relations of the apical sodium entry mechanism in the presence of varying luminal sodium concentrations. *Journal of Membrane Biology* **76**: 299-309.

Ussing, H. H. (1949) The active ion transport through the isolated frog skin in the light of tracer studies. *Acta Physiologica Scandinavica* **17**: 1-37.

Ussing, H. H. (1982) Volume regulation of frog skin epithelium. *Acta Physiologica Scandinavica* **114**: 363-369.

Ussing, H. H. and Zerahn, K. (1951) Active transport of sodium as the source of electric current in the short-circuited isolated frog skin. *Acta Physiologica Scandinavica* **23**: 110-127.

Ussing, H. H. and Windhager, E. (1964) Nature of shunt-path and active sodium transport path through frog skin epithelium. *Acta Physiologica Scandinavica* **61**: 484-504.

Ussing, H. H., Erlij, D. and Lassen, V. (1974) Transport pathways in biological membranes. *Annual Review of Physiology* **36**: 17-49.

Valenti, G., Hugon, J. S. and Bourguet, J. (1988) To what extent is microtubular network involved in antidiuretic response? *American Journal of Physiology* **255**: F1098-F1106.

Van Deynse, N. and Van Driessche, W. (1992) Effects of serosal hypotonicity and anion substitutions on apical and basolateral K^+ conductances. *Cellular Physiology and Biochemistry* **2**: 37-48.

Van Driessche, W. (1986) Lidocaine blockage of basolateral potassium channel in the amphibian urinary bladder. *Journal of Physiology* **381**: 575-593.

Van Driessche, W. and Lindemann, B. (1978) Low-noise amplification of voltage and current fluctuations arising in epithelia. *Reviews of Scientific Instrument* **49**: 52-57.

Van Driessche, W. and Lindemann, B. (1979) Concentration dependence of current through single sodium-selective pores in frog skin. *Nature* **282**: 519-520.

Van Driessche, W. and Zeiske, W. (1980) Ba^{++}-induced conductance fluctuations of spontaneously fluctuating K^+ channels in the apical membrane of frog skin (*Rana temporaria*). *Journal of Membrane Biology* **56**: 31-42.

Van Driessche, W. and Gullentops, K. (1982) Conductance fluctuation analysis in epithelia. In: *Techniques in the life sciences. Techniques in Cellular Physiology* edited by Baker, P. F., Elsevier/North-Holland Scientific Publishers, Amsterdam. **2**: 1-13.

Van Driessche, W. and Erlij, D. (1983) Noise analysis of inward and outward currents across the apical border of oubain-treated frog skin. *Pflügers Archiv European Journal of Physiology* **398**: 179-188.

Van Driessche, W. and Zeiske, W. (1985) Ionic channels in epithelial cell membranes. *Physiological Reviews* **65**(4): 833-903.

Van Meer, G. and Simons, K. (1986) The function of tight junctions in maintaining differences in lipid composition between the apical and basolateral cell surface domains of MDCK cells. *EMBO Journal* **1**: 847-852.

Verkman, A. S. (1989) Mechanisms and regulation of water permeability in renal epithelia. *American Journal of Physiology* **257**: C837-C850.

Verrey, F., Schaerer, E., Zoerkler, P., Paccolat, M. P., Geering, K., Kraehenbuhl, J.-P. and Rossier, B. C. (1987) Regulation by aldosterone of Na^+-K^+-ATPase, mRNA,

protein synthesis, and sodium transport in cultured kidney cells. *Journal of Cell Biology* **104**: 1231-1237.

Verrier, B., Champigny, G., Barbry, P., Gerard, C., Mauchamp, J. and Lazdunski, M. (1989) Identification and properties of a novel type of Na^+-permeable amiloride-sensitive channel in thyroid cells. *European Journal of Biochemistry* **183**: 499-505.

Viale, G., Dell'orto, P., Braidotti, P. and Goggi, G. (1985) Ultrastructural localisation of intracellular immunogold staining (ABC) methods. *The Journal of Histochemistry and Cytochemistry* **33**(5): 400-406.

Vigne, P., Champigny, G., Marsault, R., Barbry, P., Frelin, C. and Lazdunski, M. (1989) A new type of amiloride-sensitive cationic channel in endothelial cells of brain microvessels. *The Journal of Biological Chemistry* **264**: 7663-7668.

Voûte, C. L. (1963) An electron microscopic study of the skin of the frog (*Rana pipiens*). *Journal of Ultrastructural Research* **9**: 497-510.

Voûte, C. L. and Ussing, H. H. (1968) Some morphological aspects of active sodium transport. *Journal of Cell Biology* **36**: 625-638.

Wade, J. B. (1989) Dynamics of apical membrane responses to ADH in amohibian bladder. *American Journal of Physiology* **257**: R998-1003.

Warncke, J. and Lindemann, B. (1981) Effect of ADH on the capacitance of epithelial membranes. In: *Physiology of Non-excitable Cells*, edited by Salanki, J. Tihany, Hungary: Pergamon. **3**: 129-133.

Watanabe, T., Jeziorwski, T., Wuttke, W. and Grube, D. (1993) Secretory granules and grains in hyperstimulated male rat gonadotropes. *Journal of Histochemistry and Cytochemistry* **41**: 1801-1812.

Wiesmann, W. P., Johnson, J. P., Miura, G. A. and Chiang, P. K. (1985) Aldosterone-stimulated transmethylations are linked to sodium transport. *American Journal of Physiology* **248**: F43-F47.

Wills, N. K. and Clausen, C. (1987) Transport-dependent alterations of membrane properties of mammalian colon measured using impedance analysis. *Journal of Membrane Biology* **95**: 21-35.

Wills, N. K. and Zweifach, A. (1987) Recent advances in the characterisation of epithelial ionic channels. *Biochimica et Biophysica Acta* **906**: 1-32.

Wills, N. K., Millinoff, L. P. and Crowe, W. E. (1991) Na^+ channel activity in cultured renal (A6) epithelium: regulation by solution osmolarity. *Journal of Membrane Biology* **121**: 79-90.

Wills, N. K., Purcell, R. K. and Clausen, C. (1992) Na^+ transport and impedance properties of cultured renal (A6 and 2F3) epithelia. *Journal of Membrane Biology* **125**: 273-285.

Wills, N. K., Purcell, R. K., Clausen, C. and Millinoff, L. P. (1993) Effects of aldosterone on the impedance properties of cultured renal amphibian epithelia. *Journal of Membrane Biology* **133**: 17-27.

Zeiske, W. and Van Driessche, W. (1984) The sensitivity of apical Na^+ permeability in frog skin to hypertonic stress. *Pflügers Archiv European Journal of Physiology* **400**: 130-139.

Zweifach, A. and Lewis, S. A. (1988) Characterisation of a partially degraded Na^+ channel from urinary tract epithelium. *Journal of Membrane Biology* **101**: 49-56.

Appendix

Buffers and Solutions

A. Electrophysiology

1. Agar Bridges:

5 M NaCl:

NaCl	29.22 g
Distilled water	100.00 ml

4% Agar:

Agar	2.00 g
5 M NaCl	50.00 ml

This solution was autoclaved for 15 minutes at 121 °C.

2. Collagenase:

Final concentration = 50 I.U./ml Ringer.

3. 6-chloro-3,5-diamino-pyrazine-2-carboxamide (CDPC):

50 µM CDPC:

CDPC	2.814 mg
Ringer solution	300.0 ml

This solution was stirred for 20 minutes and always made fresh.

[CDPC] (µM)	50 µM CDPC (ml)	Ringer solution (ml)
10	20	80
20	40	60
30	60	40
40	80	20
50	100	0
Total volume	300	200

4. Amiloride:

10^{-2} Amiloride:

Amiloride	30.165 mg
Distilled water	10.0 ml

This solution was stored at 4 °C.

10^{-4} Amiloride:

10^{-2} Amiloride	1.0 ml
Distilled water	99.0 ml

This solution was always made fresh.

5. 110 mM Na (Cl / HCO_3) Ringer solution:

NaCl	6.43 g
$KHCO_3$	240.29 mg
$CaCl_2$	294.04 mg
Distilled water	to 1000.0 ml

This solution was adjusted to pH 8.1.

6. 20 mM Na (Cl / HCO_3) Ringer solution:

NaCl	1.17 g
Tetramethylammonium chloride	9.87 g
$KHCO_3$	240.29 mg
$CaCl_2$	294.04 mg

This solution was adjusted to pH 8.1.

7. 10 mM Na (Cl / HCO_3) Ringer solution:

NaCl	0.58 g
Tetramethylammonium chloride	10.96 g
$KHCO_3$	240.29 mg
$CaCl_2$	294.04 mg

This solution was adjusted to pH 8.1.

8. 10 μg/ml cytochalasin B:

2mg cytochalasin B dissolve in 1ml DMSO, then keep the stock solution at -20 °C. Take the stock solution to dilute in 200 ml Ringer solution, then the final concentration is 10 μg/ml.

9. 100 μM Colchicine:

Colchicine	39.94 mg
Ringer solution	to 1000.0 ml

This solution was made fresh every time.

10. 30 mU/ml Arginine-vasopressin (AVP):

AVP(Grade V)(Stock solution = 11.1 I.U./ml)	1.351 ml
Ringer solution	to 500.0 ml

This solution was made fresh every time.

B. Cytochemistry

1. 0.1M Phosphate Buffer Saline (PBS):

NaCl	8.01 g
KCl	0.20 g
KH_2PO_4	0.21 g
Na_2HPO_4	1.14 g
Distilled water	to 1000.0 ml

This solution was stored at 4 °C, and adjusted to pH 7.6.

2. 0.01M Phosphate Buffer Saline:

0.1M PBS	50.0 ml
Distilled water	to 500.0 ml

This solution was made fresh every time, and adjusted to pH 7.6.

3. 3% Paraformaldehyde fixative:

Paraformaldehyde	0.75 g
0.1 M PBS or Ringer solution	to 25 ml

This fixative was heated for 10-15 minutes, then adjusted to pH 7.6 by 1 M NaOH. **Do not overheat!**

4. 1.5% paraformaldehyde + 1% Glutaldehyde mixture fixative:

(1) 1.5 g Paraformaldehyde was dissolved in 100 ml 0.1 M PBS to make 1.5% Paraformaldehyde and pH was adjusted to 7.6.

(2) 4 ml 25% Glutaldehyde was added to 96 ml 1.5% Paraformaldehyde, then adjusted pH to 7.6.

This fixative was made fresh every time.

5. 1% Bovine Serum Albumin (BSA):

BSA	100.0 mg
0.01 M PBS	to 10.0 ml

6. 0.05% Tween 20:

Tween 20	5 µl
0.01 M PBS	to 10 ml

This buffer solution was made fresh every time.

7. 2% Uranyl Acetate:

Uranyl Acetate	1 g
Distilled water	50 ml

This solution was stored at 4 °C.

8. Lead Citrate:

Solution A.	Trisodium citrate ($Na_3C_6H_5O_7.H_2O$)	37.79 g
	Distilled water	100.0 ml
Solution B.	Lead nitrate ($Pb(NO_3)_2$)	33.10 g
	Distilled water	100.0 ml
Solution C.	1N Sodium Hydroxide (NaOH)	4.00 g
	Distilled water	100.0 ml

To make stain solution:

16 ml H_2O+3 ml Solution A.+2 ml Solution B.+4 ml Solution C
This solution was stored at 4 °C and was filtered before used.

9. Formulation of Epon/Araldite:

Epoxy resin (Araldite CY212)	5.62g
Agar 100 resin	7.75g
DDSA (dodecyl succinic anhydride) flexibiliser	15.00g
DMP-30 accelerator	0.71g